Tunable and cell-responsive 3D poly(ethylene glycol) microenvironments for the development of tissue models

THÈSE No 7155 (2016)

PRÉSENTÉE LE 21 JUIN 2016

À LA FACULTÉ DES SIENCES DE LA VIE
CHAIRE MERCK-SERONO EN TECHNOLOGIES D'ADMINISTRATION DE MÉDICAMENTS
PROGRAMME DOCTORAL EN BIOTECHNOLOGIE ET GÉNIE BIOLOGIQUE

ÉCOLE POLYTECHNIQUE FÉDÉRALE DE LAUSANNE

POUR L'OBTENTION DU GRADE DE DOCTEUR ÈS SCIENCES

PAR

Stéphanie Elisabeth METZGER

acceptée sur proposition du jury :

Prof. Dominique Pioletti, président du jury
Prof. Jeffrey A. Hubbell, Dr Martin Ehrbar, directeurs de thèse
Prof. Matthias Lütolf, rapporteur
Prof. Nuria Hernandez, rapporteur
PD Dr Arnaud Scherberich, rapporteur

ÉCOLE POLYTECHNIQUE
FÉDÉRALE DE LAUSANNE

Suisse
2016

Acknowledgements

I would like to thank the following persons who have contributed to my PhD thesis and who have given me the much needed support and encouragement during my life as a PhD student:

Dr Martin Ehrbar for accepting me in his laboratory as a graduate student. It has been an enriching and enjoyable experience working in your group. Thank you for your precious help and guidance, for inspiring me in my work, trusting me and giving me the opportunity to increase my scientific knowledge.

Prof. Jeffrey A. Hubbell for helping me find this PhD position and accepting to be my thesis director. Thank you for your support, the helpful feedback and motivating discussions.

My thesis committee members, **Prof. Dominique Pioletti**, **Prof. Matthias Lütolf**, **Prof. Nuria Hernandez** and **PD Dr Arnaud Scherberich** for accepting and sharing your time to evaluate my thesis.

All current and former members of the Ehrbar Lab for their support and the wonderful working environment. Many thanks to **Dr Philipp Lienemann** for sharing his knowledge and helping me in all my projects, **Dr Algirdas Ziogas** for showing me the ropes and teaching me important methods for my research, **Dr Vincent Milleret**, **Dr Anna-Sofia Kiveliö**, **Yannick Devaud**, **Panagiota Papageorgiou** and **Queralt Vallmajó-Martin** for the nice discussions, the laughs, and the amazing atmosphere in the lab, as well as **Dr Ana Sala**, **Epameinondas Gousopoulos** and **Dr Michela Perrini** for sharing these moments of my PhD life with me. Very special thanks go to my wonderful friends **Ulrich Blache**, for the music and the hikes, for being able to read my mind and for always helping me back up when I was down, as well as **Venkat Ramakrishnan** and **Jeffrey Marschall** who have truly become family and with whom I hope to continue travelling the world for many years to come. I am also very grateful to **Aida Kurmanaviciene**, without whom I wouldn't have achieved all this work, and **Esther Kleiner** for all her help and the beautiful histologies. I also thank **Yvonne Eisenegger** and **Corina von Arx** for their precious help with administration and for always having a bright smile on their face.

Prof. Roland Zimmermann and the members of the Clinic of Obstetrics at USZ for supporting our research.

Sonja Bodmer and **Carol Bonzon**, who have always been so lovely helping me with EPFL administrative work and answering all my many emails and questions.

Prof. Franz Weber and all the members of his laboratory at USZ, especially **Dr Chafik Ghayor**, **Yvonne Bloemhard**, **Nisarat Roungsawasdi** and **Barbara Siegenthaler** for always welcoming me with a smile, and for their help and support with my experiments, as well as sharing of numerous instruments and materials.

Prof. Wilfried Weber, **Dr Maria Karlsson**, **Dr Konrad Müller** and **Dr Erik Christens** from the University of Freiburg for their help with cloning and for the many fruitful collaborations.

Prof. Ivan Martin and **Chiara Stüedle** from the University Hospital Basel for providing us with well characterized mesenchymal cells and the joint efforts in interesting projects.

Prof. Valentin Djonov, **Dr Ruslan Hlushchuk** and **Werner Graber** from the University of Bern. Many thanks for hosting me in your laboratory, giving me the necessary materials, support and advice for successful experiments and for the intensive work done for the acquisition of the TEM images.

Prof. Urara Hasegawa, **Dr André van der Vlies**, and **Masaki Moriyama** from the Osaka University for the very nice discussions and a great collaboration.

Raphael Reuten from the University of Cologne, who provided many engineered proteins and gave me the opportunity to work on a very interesting project.

Dr Edmondo Benetti and **Ella Dehghani** from the ETHZ for their enthusiasm and great ideas for our shared project.

Dr Remo Largo from the USZ/Limmattal Hospital for long hours spent helping me with my experiments and for his precise and perfectionist working methods for which I have great appreciation and admiration.

Flora Nicholls and the staff from the Animal Facility at USZ for providing advice and help with animal experimentation.

Dr Martin Stauber from b-cube AG for providing me with valuable micro-computed tomography data.

Dr Andrea Negro from the Laboratory of Stem Cell Bioengineering at EPFL for providing materials and precious help.

All my friends, who have shared these intense moments of my life and allowed me to take my mind off of work. Special thanks go to **Viviane**, who somehow remained my friend despite the little amount of time I was able to spend with her. I also thank **Matt**, **Chris** and **Dom**, who have been part of my life for so many years and have unknowingly helped me go through the good and the bad times by providing a safe haven for my mind.

My family, who have inspired and supported me in this adventure. I would like especially to thank **my parents** for helping me pursue my dreams since I was little, for encouraging me during my thesis, and for their love and affection. I also thank all my newly acquired family members for all their love and support.

Jo, the love of my life, without whom I would not be standing where I am right now. Thank you for the many late night hours spent in the lab keeping me company, bringing me food, cheering me up with Chuck Norris jokes and listening to me curse like a sailor. Thank you as well for teaching me the secret ways of statistics, I learnt more in a few hours with you than with all the classes I had taken so far. You have always been there for me, sharing the wonderful and happy moments but also the difficult and stressful times. For you, I would go through all of it again.

Abstract

The recapitulation of tissue organization and function *in vitro* is one of the main objectives of tissue engineering. The increasing need for tissue replacements in order to overcome donor organ shortages and to provide better tissue models for research has placed the engineering of tissue constructs in the spotlight.

In order to reproduce natural tissue as closely as possible, three-dimensional (3D) structure and architecture of normal tissue must be examined. Indeed, proper tissue function strongly depends on the spatial assembly and interactions between key components such as cells, growth factors, signaling cues and extracellular matrix (ECM). The ECM in particular is of utmost importance in the design of engineered tissues, since it not only provides support but also actively interacts with cells and growth factors to regulate tissue function. The field of tissue engineering has thus pushed towards the development of novel biocompatible and biodegradable materials that are capable of both supporting and interacting with cells. Furthermore, such biomaterials are expected to allow the positioning of different cell types and the localization of biological factors, as well as having controlled adhesive properties and stiffness.

Yet, despite the constant improvement on biomaterial design, technological advances and the increasing knowledge gained on tissue functions, the synthesis of artificial tissues and organs still remains a goal that lies far ahead. Current achievements in research have enabled the generation of engineered constructs with either controlled positioning of cells or patterning of growth factors. But the combination of both aspects in a reproducible and high-throughput strategy still remains a task at hand, especially for the complex 3D architectures found in normal tissue. Another limitation of tissue engineering is the current inability to recreate stable vascularization in tissue constructs. Vascularization is a compulsory aspect of engineering artificial tissues, since survival of any clinical-sized constructs depends on the availability of oxygen and nutrients, which are mainly provided by blood circulation *in vivo*. Such a shortcoming is directly linked to the necessity of establishing new strategies for the localized control of cellular function in 3D-arranged microenvironments. Indeed, vascularization is a complex and well-orchestrated phenomenon that requires various processes, such as cell migration and differentiation under the control of specific guidance and signaling cues.

To this end, a platform for the synthesis of tunable tissue constructs was developed in this thesis work. Taking advantage of the enzymatically cross-linked poly(ethylene glycol) hydrogel platform, which is biocompatible and highly customizable, a strategy for the controlled incorporation of bioactive factors via peptide linkers was developed. The successful localized immobilization of growth factors and their ability to differentiate cells in a 3D-controlled manner was demonstrated by the osteogenic differentiation of mesenchymal cells by tethered bone morphogenice

protein-2. Furthermore, using the same model, the release dynamics of the immobilized growth factors were investigated and a cell-dependant release strategy was devised by designing a proteolytically degradable peptide linker. The availability of immobilization strategies that are cell-responsive and that can mimic ECM properties is a desirable feature that can also contribute to the improvement of growth factor dose-response relationship. Additionally, selected factors modulating angiogenesis were evaluated for their potential role and use in the design of tissue constructs. Pro-angiogenic, anti-angiogenic effects and influence on cell migration were assessed *in vitro* and using the highly vascularized chicken chorioallantoic membrane. Preliminary experiments support the hypothesis that the selected growth factors could be used for establishing pre-vascular structures in engineered constructs.

Summing up, this thesis presents new tools for the development of engineered tissue constructs. It shows the successful differentiation of cells in spatially controlled manner, as well as evaluates potential growth factors for the regulation of vascular development *in vitro*. Due to the versatile nature of these biomimetic scaffolds, it is expected that this strategy will be employed for the development of various types of tissues and will allow the progression towards more complex 3D tissue architectures.

Keywords: 3D microenvironments, biomimetic matrices, poly(ethylene glycol), growth factor delivery, proteolytic release, cell differentiation, protein positioning, bone morphogenetic protein-2, netrin, ephrins

Résumé

L'ingénierie des tissues possède parmi ses objectifs principaux la génération de substituts tissulaires *in vitro* capables de reproduire l'organisation et la fonction des tissus normaux. Ce domaine de la recherche a notamment gagné en intérêt dû à l'augmentation de la demande en greffes d'organe ainsi qu'au besoin croissant de modèles de tissus pour la recherche.

Il est important d'examiner et comprendre la structure tridimensionnelle (3D) ainsi que l'architecture de tissus normaux, afin de pouvoir fabriquer des tissus artificiels fonctionnels. En effet, les fonctions essentielles d'un tissu dépendent principalement de la répartition spatiale et des interactions entre divers facteurs clés, dont notamment les cellules, les facteurs de croissance, des signaux moléculaires et la matrice extracellulaire (MEC). La MEC mérite une considération particulière dans le développement de tissus synthétiques car en plus d'assurer le soutien structurel du tissu, elle interagit activement avec les cellules et facteurs de croissance afin de réguler la fonction des tissus. Le domaine de l'ingénierie tissulaire a donc fortement évolué en direction du développement de nouveaux matériaux biocompatibles et biodégradables capables d'interagir avec les cellules et de leur apporter un soutien structurel. En outre, il est également souhaitable que ce genre de biomatériaux puissent permettre le positionnement de différents types cellulaires et la localisation de facteurs biologiques, tout en garantissant un contrôle sur leurs propriétés adhésives et leur rigidité.

Pourtant, la fabrication de tissus et organes artificiels reste un objectif lointain, malgré les avancées technologiques et l'augmentation des connaissances acquises sur le fonctionnement des tissus. L'état actuel de la recherche permet la génération de tissus synthétiques offrant des possibilités pour le positionnement précis des cellules ou pour la création de motifs de facteurs de croissance. Cependant la combinaison de ces deux aspects pour la synthèse de matrices à haut rendement et de manière reproductible reste une tâche à effectuer, en particulier pour la reproduction d'architectures 3D complexes présentes dans les tissus normaux. Une autre limite de l'ingénierie tissulaire est l'incapacité de recréer un réseau vasculaire stable dans les tissus artificiels. Le processus de vascularisation est en effet un aspect crucial lors de la fabrication de tissus artificiels qui ont une pertinence clinique, puisque la survie du tissu dépend de l'oxygénation et l'acheminement de nutriments normalement prodigués par la circulation sanguine *in vivo*. Une telle lacune est directement liée au besoin impératif d'établir de nouvelles stratégies permettant un contrôle localisé des fonctions cellulaires dans leur microenvironnement 3D. La vascularisation est en effet un phénomène complexe qui requiert la coordination de plusieurs processus, dont la migration et la différentiation de cellules sous le contrôle d'une grande variété de facteurs et signaux biologiques spécifiques.

Afin de répondre à ce besoin, une plateforme modulable pour la fabrication de tissus synthétiques a été développée dans ce travail de thèse. Le système de gélification enzymatique d'hydrogels en poly(éthylène glycol) qui est biocompatible et facilement adaptable a été utilisé à son avantage pour le développement d'une stratégie permettant l'immobilisation de facteurs bioactifs par des peptides de liaison. Ce système a été utilisé pour démontrer l'incorporation contrôlée de facteurs de croissances dans un hydrogel permettant la différentiation localisée de cellules en 3D par le biais de cellules mésenchymateuses différenciées osteogénétiquement en présence de protéine morphogénétique osseuse-2. De plus, la libération de facteurs de croissance par ce type de matrice a été examinée afin de développer une stratégie utilisant des peptides de liaison sensibles aux protéases, permettant ainsi la libération de facteurs en réponse à l'activité cellulaire. En effet, il est fortement désirable d'avoir accès à des moyens d'immobilisation qui réagissent à l'activité cellulaire afin d'avoir des conditions proches de la MEC naturelle et afin d'améliorer le rapport dose-réponse des facteurs de croissance immobilisés. Finalement, la dernière partie de ce travail de thèse s'est intéressée aux effets angiogéniques de certains facteurs de croissance et à leur rôle potentiel dans la fabrication de tissus synthétiques. Les effets pro- et anti-angiogéniques de ces facteurs ainsi que leur influence sur la migration cellulaire ont été examinés *in vitro* et sur la membrane chorioallantoique du poulet. Ces expériences préliminaires indiquent fortement que les facteurs sélectionnés pourraient être utilisés pour la formation de structures pré-vasculaires dans les tissus artificiels.

En bref, ce travail de thèse a permis le développement de nouveaux outils pour la fabrication de tissus synthétiques. Des cellules ont pu être différenciées de manière locale et contrôlée et de potentiels facteurs de croissances ont été évalués pour leur rôle dans la formation de vaisseaux sanguins *in vitro*. La stratégie présentée ici constitue un fondement important pour la génération de différents types de tissus artificiels et la progression vers des architectures cellulaires 3D plus complexes grâce à ses propriétés modulables.

Mots-clés : microenvironnements 3D, matrices biomimétiques, poly(éthylène glycol), facteurs de croissances, clivage protéolytique, différentiation cellulaire, positionnement de protéines, protéine morphogénétique osseuse-2, ephrines, netrines

Contents

Acknowledgements ..... **i**

Abstract ..... **iii**

Résumé ..... **v**

Contents ..... **vii**

Chapter 1 Introduction **1**

1.1 Tissue engineering 1

1.1.1 Engineered tissues for transplantation 1

1.1.2 In vitro tissue-engineered 3D models 2

1.2 The extracellular matrix 3

1.2.1 Main components of the ECM 4

1.2.2 Cell-ECM interactions and remodeling 5

1.2.3 Role of the ECM in would healing 6

1.3 Growth factors interactions with the ECM 7

1.4 Approaches to recreate the ECM 8

1.4.1 Poly(ethylene glycol) as a biopolymer for engineering scaffolds 9

1.4.2 Enzymatically cross-linked PEG hydrogel platform 9

1.5 Vascularization and tissue engineering models 10

1.5.1 Regulation of angiogenesis 11

1.5.2 The role of the extracellular matrix in angiogenesis 12

1.5.3 Angiogenic growth factors 12

1.6 Motivation and objectives 13

1.7 References 14

Chapter 2 Modular poly(ethylene glycol) matrices for controlled 3D-localized cell differentiation **19**

2.1 Introduction 19

2.2 Results and Discussion 21

2.2.1 Design of streptavidin/biotin-based growth factor-presenting TG-PEG hydrogels 21

2.2.2 Production and characterization of streptavidin-modified TG-PEG hydrogels 22

2.2.3 Biotinylation of BMP-2 23

2.2.4 Binding and release of rhBMP-2-biotin from Gln-streptavidin hydrogels 26

2.2.5 Osteogenic differentiation of C2C12 cells on hydrogels with immobilized BMP-2 27

2.2.6 Localized 3D osteogenic differentiation of mesenchymal stem cells 28

2.3 Conclusion 32
2.4 Experimental Section 32
2.5 References 37
Chapter 3 Engineered poly(ethylene glycol) matrices for cell-dependent proteolytic release of growth factors 39
3.1 Introduction 39
3.2 Results and Discussion 41
3.2.1 Design of a proteolytically degradable streptavidin peptide linker 41
3.2.2 Production and characterization of the degradable streptavidin linker 42
3.2.3 Binding of biotinylated proteins to streptavidin hydrogels 44
3.2.4 Release of rhBMP-2-biotin from streptavidin hydrogels 46
3.2.5 Osteogenic differentiation of cells in streptavidin hydrogels 47
3.2.6 Degradable linkers for the immobilization and release of growth factors 51
3.3 Conclusion 52
3.4 Experimental Section 53
3.5 References 56
Chapter 4 Evaluation of growth factors modulating angiogenesis 59
4.1 Introduction 59
4.1.1 Objective 61
4.2 Results and discussion 61
4.2.1 Anti-angiogenic effect of netrin-4 on the chicken CAM 61
4.2.2 Effects of ephrins and VEGF on the chicken CAM 63
4.2.3 Casting of the CAM with polyurethane for µCT quantification 65
4.2.4 Effects of ephrins cell migration 66
4.3 Conclusion 69
4.4 Experimental Section 70
4.5 References 72
Chapter 5 Conclusion 75
5.1 Achieved results 75
5.1.1 Streptavidin linker for the controlled and localized immobilization of growth factors 75
5.1.2 MMP-sensitive streptavidin linker for cell-dependent release of immobilized growth factors 76
5.1.3 Growth factors modulating angiogenesis 76
5.2 Future developments 78
5.3 References 80
Bibliography 83
Curriculum Vitae 91
List of publications 93

Chapter 1 *Introduction*

1.1 Tissue engineering

Tissue engineering is an interdisciplinary engineering field, which aims to provide adequate and functional substitutes for tissues and organs. One of the great expectations from this field is the ability to respond to the current limitations in organ transplantation, due to the shortage of organ donors, the occurrence of immunological incompatibility and the required long-term use of immunosuppressive drugs.[1-3] A further aspect of developing engineered tissues is the providing of suitable *in vitro* tissue or organ models. These models would provide valuable and more precise information than current 2D cell culture models, allowing better understanding of tissue functions, diseases and more accurate assessment of new treatments and drugs.[3]

1.1.1 Engineered tissues for transplantation

In recent years, technological advances have allowed breakthrough progress in tissue engineering. Many efforts made in the development of novel manufacturing techniques, new biomaterials and better understanding of biological and cellular processes have shown that tissue engineering could meet the demands of organ transplantation, as well as answer some of its limitations.[4] Indeed, bioengineered organs such as the bladder[5], trachea[6], urethra[7] or pulmonary artery[8] have already been successfully transplanted into human patients. Yet, one of the many challenges remains in the ability to recreate the complexity of certain tissues and organs. As the previous examples of successfully transplanted engineered tissues show, flat, tubular and hollow structures can already be assembled in a satisfying and functional manner. But organs such as the liver, the heart or the kidney have a much higher complexity, which is why the regeneration of such tissues is usually a more difficult task. Recapitulation of such complex architectures requires technologies that are able to combine multiple cell types, gradients or localized supply of growth factors, vascularization, as well as 3D structural arrangements, but they must also be compatible with high-throughput manufacturing. To this end, employed strategies often involve the use of either acellular matrices, which will necessitate new tissue growth from the host, or matrices that contain cells originating from a donor tissue, which can be of autogeneic, allogeneic or xenogeneic source.[1] In both cases, the presence of a structural and biological environment that closely mimics the properties of the native organs is of utmost importance in order to support and direct the cells for tissue formation. Options to provide this environment encompass two main strategies: (1) organs

from allogeneic or xenogeneic origin can be completely decellularized, leaving only the extracellular matrix and the vascular architecture behind, ready to be repopulated by autologous cells, or (2) synthetic scaffolds can be created to mimic the mechanical, biological and architectural properties of the extracellular matrix in order to provide the necessary cell support.[9, 10] In both strategies, the extracellular matrix plays an important role and in order to recapitulate it, engineered scaffolds must be dynamic and hierarchically organized, but also provide the required growth factors and cues to regulate cellular functions.

1.1.2 *In vitro* tissue-engineered 3D models

Although two-dimensional cell culture models are still commonly used in research and provide a vast amount of knowledge on various cell and tissue functions, it has become clear in the last two decades that the cellular microenvironment has an important influence on the properties, functions and behavior of cells and tissues.[11, 12] Thus, the transition to 3D cell culture models is an important step in the development of physiologically relevant tissue models. In addition to gaining better insights on normal tissue functions, 3D tissue models also contribute to the development of better injury or disease modeling strategies and drug screening platforms. And in some cases, the availability of relevant 3D tissue models could reduce the use of animal models by providing high-throughput, less expensive, and more tightly controlled systems.

In order for such 3D tissue models to be successful, the natural cellular microenvironment has to be mimicked closely. Complex cell-cell and cell-extracellular matrix interactions, mechanical forces, as well as the presentation of signaling factors thus need to be recapitulated *in vitro*. But despite what could seem a difficult task, several engineered 3D tissue models have been created and used to reproduce biological functions or study diseases *in vitro*. Examples include engineered cardiac[13], liver[14, 15], kidney[16] and bone tissues[17, 18], as well as cancer models[19, 20].

Bone tissue engineering is of particular interest, since in the following chapters of this thesis, osteogenic differentiation has been used as a model to evaluate our new tissue engineering strategies. Bone tissue can be divided into two types of structures: (1) trabecular bone, which is porous and provides support for the bone marrow, and (2) cortical bone, which is the compact bone that surrounds the marrow region and provides mechanical strength. Both types of bone are subject to maturation, differentiation and resorption via cellular interactions involving osteocytes, osteoblasts, osteoclasts and their extracellular matrix.[21] Healthy bone is maintained via remodeling, where osteoblasts are mainly responsible for new bone formation, and osteoclasts resorb old bone tissue. The outer layer covering the surface of cortical bone is known as the periosteum and contains mainly blood vessels as well as osteoblasts and progenitor cells activated during bone repair. Although bone has regenerative properties, large bone defects cannot be fully healed by the body and require external intervention, often in the form of bone grafts. Bone tissue engineering has thus become popular and many advances have been made, especially regarding cell sources, scaffold design and identification of key growth factors that regulate bone formation and vascularization.[21-23] Better understanding of the bone extracellular matrix and its remodeling has especially contributed to the development of new scaffold biomaterials. Bone matrix is highly mineralized with calcium and phosphate in the form of

hydroxyapatite crystals distributed across the collagen fibers, which confer mechanical strength and resistance to impact.[21] Thus, ideal scaffolds for bone tissue engineering have to provide a certain rigidity for the support of cells, as well as being porous and having osteoinductive properties.

Regardless of the type of tissue, it becomes evident that the extracellular matrix plays a crucial role in the maintenance of healthy tissue. Understanding its functions and interactions with cells and signaling factors is therefore an important key factor in the establishment of tissue-engineered constructs.

1.2 The extracellular matrix

The extracellular matrix (ECM) is the scaffold that surrounds and supports cells in living tissues, but also influences their behavior via physical and chemical mechanisms (**Figure 1.1**). Distinction is made between the interstitial connective tissue matrix, which surrounds cells and provides support to tissues in general, and the basement membrane, which is a specialized type of ECM that separates epithelium from stroma and is usually more compact than the interstitial matrix.[24]

The cells within each tissue regulate the establishment and maintenance of the ECM. Its composition and remodeling rely on tightly controlled processes and are essential during development, wound healing and normal tissue homeostasis.[25] The main components of the ECM are collagens, elastin, fibrin, laminins, fibronectin, and proteoglycans (some of which are highlighted in the following section) and the overall composition varies according to each type of tissue and can be influenced by binding and releasing of growth factors.[24, 26]

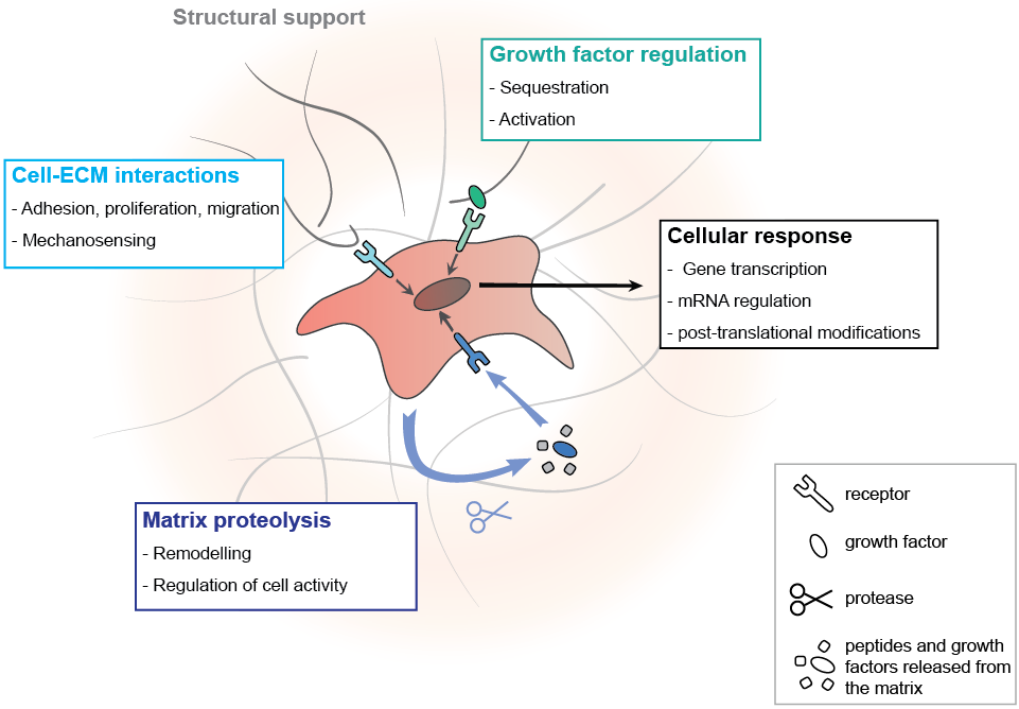

Figure 1.1. Functions of the ECM.

The ECM provides structural support to cells, but it also actively interacts with them. The ECM can thus participate in the regulation of cell activity, which in return can regulate ECM homeostasis.[1]

1.2.1 Main components of the ECM

Collagens are one of the most abundant proteins of the ECM and are predominantly synthesized by fibroblasts, but in some cases also by epithelial cells. They are secreted by cells as procollagens, which have extra domains that need to be cleaved outside the cells by specific proteinases before being able to assemble into collagen fibrils, and then fibers. Organization and alignment of collagens can be influenced by matrix tension exerted by fibroblasts. Together collagen type I, II and III constitute around 90% of all collagens in the body and are very common in connective tissue. The basement membrane usually contains collagen type IV.[27, 28]

Elastin is another ECM protein, which often associates with collagens. Elastin is mainly responsible for the elastic properties of tissues such as arteries, skin and tendons. Elastin is secreted by various cells as a precursor that forms into elastic fibers by associating with other ECM components. Together, the balance between elastic fibers and collagen fibers determine the mechanical properties of the ECM. [27-29]

[1] *Adapted from:* D Hubmacher and S Apte, **The biology of the extracellular matrix: novel insights**, *Curr Opin Rheumatol*, 2013 Jan, 25(1): 65–70.

Cellular fibronectin is another type of fibrous ECM protein and is secreted by many cell types including fibroblasts, endothelial cells and chondrocytes. It helps organize the ECM by binding to other ECM components and offering cell-binding sites, mostly via the Arg-Gly-Asp (RGD) motif that interacts with cell-surface integrins.[27, 28, 30]

Proteoglycans are another important component of the ECM and are composed of glycosaminoglycans chains covalently attached to a core protein (except for hyaluronic acid). They are hydrophilic and contribute in the hydrogel-like nature of the ECM and its resistance to high compressive forces. In addition to interacting to both cell-surface receptors and other ECM components, proteoglycans can also bind to a variety of growth factors, thus sequestering them to specific parts of the ECM.[27, 29]

1.2.2 Cell-ECM interactions and remodeling

The ECM provides a structural support and a dynamic microenvironment for the cells, by presenting various tethered or soluble signaling cues such as growth factors to guide cellular process (e.g. morphogenesis, proliferation, differentiation, migration). Furthermore, many sequences of the ECM can be recognized by cell-surface receptors such as integrins. Integrins are transmembrane receptors that bind among other target sequences to the RGD motif, which was first discovered in fibronectin but is also present in various other ECM components. They are the main receptors involved in the formation of focal adhesions and are essential for cell migration, due to their interaction with the actin cytoskeleton.[31, 32] Integrins are thus important for cell attachment to the ECM, but can also trigger signaling cascades leading to gene expression with varying outcomes involved in cell survival, apoptosis, growth or receptor phosphorylation, depending on ECM composition.[33]

In addition to influencing cells, the ECM is also highly responsive to cell behavior. Indeed the ECM is constantly being remodeled by the cells through proteolytic degradation and by deposition of new ECM components, which in turn can again have an effect on cell behavior. This means that the cells and their surrounding ECM are constantly influencing each other in a reciprocal manner.[33, 34]

ECM remodeling happens throughout cellular processes such as development, healing or homeostasis and is a tightly controlled feature of the ECM. In order to be proteolytically degraded, most proteins composing the ECM possess cleavage sites for enzymes secreted by the cells, such as matrix-metalloproteinases (MMPs), plasmin or cathepsin.[34] MMPs are on the major type of enzymes involved in matrix degradation. They are zinc- and calcium-dependent endopeptidases that take part in the digestion of collagens, proteoglycans, and other glycoproteins and can be distributed into five families according to their substrate specificity. Amongst them are collagenases (MMP-1 and MMP-8), which principally degrade type I, II and III collagens, and gelatinases (MMP-2 and MMP-9, which can digest type IV and VII collagens.[35] The expression and activity of MMPs is regulated at different levels including gene transcription, proenzyme activation and endogenous inhibition. One example of such inhibitors are tissue inhibitors of metalloproteinases (TIMPs), which together with MMPs play a very important role in maintaining the balance of the cellular microenvironment.[34, 36, 37]

1.2.3 Role of the ECM in would healing

The synthesis and deposition of the ECM components is also a key factor in the process of wound healing. The repair of an injured tissue depends strongly on the interactions between platelets, cells (such as neutrophils, monocytes, fibroblasts), growth factors and ECM.[38-40]

First the ECM serves as structural support for repair processes in areas that have been injured, by providing a temporary matrix. For instance, platelets undergo adhesion and aggregation upon contact with collagen from damaged blood vessels. This is the start of a cascade of events that include activation of thrombin, polymerization of fibrinogen and lead to the formation of a blood clot, which will serve as a temporary matrix facilitating the interactions between signaling cues and recruited cells.[41-43]

Then, the ECM also actively participates in signal transduction and actively regulates biological processes by facilitating cell adhesion and migration. The ECM regulates interaction among cells, between cells and ECM, and between various ECM components. For example, during the inflammatory phase of wound healing, monocytes will migrate from blood vessels to the ECM where they differentiate into macrophages under the influence of fibrin and fibronectin fragments originating from the degradation of the temporary wound matrix. In turn, macrophages secrete proteinases that will degrade the ECM but release factors that will stimulate the synthesis of new matrix. Thus, the temporary matrix that consists mainly of fibrin and fibronectin is slowly replaced by granulation tissue, composed of collagen and enriched with proteoglycans and other glycoproteins, which contributes to the restoration of normal tissue function.[38, 44, 45]

In the final phases of wound healing, the granulation tissue is replaced by scar tissue. This involves the remodeling of the ECM, where both the composition and the spatial organization are rearranged to increase the tensile strength. This shows that the ECM plays a fundamental role in tissue repair and understanding the mechanisms by which ECM components influence the different phases of wound healing can be an important advantage for the development of therapeutic strategies.[43, 46, 47]

All these aspects show that the ECM provides far more than only mechanical and structural support. Not only does it contribute to establishing a spatial context for signaling events between cells, growth factors and other signaling molecules and proteins, but it also actively participates in all these biological processes, including wound healing.

1.3 Growth factors interactions with the ECM

As mentioned previously, growth factors are important key players of the ECM. Indeed, many growth factors can bind to ECM proteins such as fibronectin, collagen and proteoglycans, either directly or in combination with heparin and heparan sulfate.[48, 49] Moreover, binding of growth factors is often facilitated by the presence of conserved binding motifs present in the sequence of ECM proteins, such as the FN III 12–14 repeats in fibronectin,[50] or the heparin-binding domain of fibrinogen.[51] This creates a reservoir of growth factors that can be either bound by cell-surface receptors directly in their tethered form or in their soluble form when the surrounding ECM is degraded.[52] The immobilization to the ECM also has for effect the protection and stabilization of the growth factor active conformation. Thus the ECM plays an essential role not only in the spatial localization, but also on the activity and stability of the growth factors.[34, 53] In turn, growth factors can also regulate the composition of the ECM by either inducing the deposition of more ECM components by cells or by stimulating the production of proteases, which break down the ECM.[32, 39, 52]

Several growth factors are good examples of the indispensable interactions taking place in the ECM. For instance, basic fibroblast growth factor (FGF-2), which can stimulate the growth of fibroblasts and endothelial cells, is often bound by heparan sulfate, a glycosaminoglycan present in the ECM. This interaction has been shown to participate not only in the preservation of the growth factor bioactivity, but also stabilizes its binding to the FGF receptor.[54, 55]

Vascular endothelial growth factor (VEGF) is another example for growth factor-ECM binding and interactions. Amongst the most abundant isoforms of this growth factor, $VEGF_{165}$, $VEGF_{189}$ and $VEGF_{206}$ contain a heparin-binding region, whereas $VEGF_{121}$ lacks this binding domain. This has for consequence that $VEGF_{121}$ produced by cells can be freely released, whereas $VEGF_{165}$, $VEGF_{189}$ and $VEGF_{206}$ are partially sequestered by the ECM due to their affinity for heparan sulfate. This can constitute a reservoir of growth factor that will be slowly released over time by heparanases or can be released more rapidly by specific proteases such as plasmin.[56, 57] Furthermore, VEGF also strongly interacts with integrins, which are cell-surface receptors that allow cells to attach to the ECM. Indeed, crosstalk between VEGF receptors and integrins has been shown in research and is essential for VEGF-induced angiogenesis during development and during wound healing, showing that cell attachment to the ECM is often required for the induction of an efficient cell response to growth factors.[58, 59]

Examples of growth factors that can influence the composition of the ECM are platelet-derived growth factor (PDGF) that can induce the production of collagen, and transforming growth factor beta (TGF-β) that also increases collagen production, as well as fibronectin and hyaluronic acid in certain cell lines.[39, 60, 61] Additionally TGF-β also influences the ECM composition by decreasing the production of proteases and increasing the production of protease inhibitors.[62]

A final example of growth factor, which interacts strongly with the ECM, is bone morphogenetic protein-2 (BMP-2), a factor mainly known for its role in bone and cartilage formation. Indeed BMP-2 binding to ECM components such as collagen is thought to preserve its bioactivity as well as enhance its interaction with BMP receptors.[32, 63, 64]

Furthermore, BMP-2 has also been shown to stimulate collagen and proteoglycan production, and plays an important role cartilage ECM remodeling.[65]

These examples of growth factor-ECM interactions, which are only a few amongst others, clearly show that the ECM represents a complex system and all these properties need to be taken into consideration when trying to develop ECM-mimicking platforms for tissue engineering.

1.4 Approaches to recreate the ECM

As previously stated, tissue engineering strategies often involve combinations of biomaterial scaffolds, cells and signaling molecules for the repair of damage tissues or the development of tissue models. With advances in biomaterial science and increasing understanding of the natural ECM, scaffolds are constantly evolving and improving at mimicking natural properties of the ECM. Some of the biomaterials used as scaffolds include naturally derived polymers, such as collagen or hyaluronic acid, but many synthetic materials have also been developed to be able to provide an environment compatible with cell growth. The key advantage of using naturally occurring materials is that they have the intrinsic ability to support cell attachment, proliferation and differentiation, in addition to being enzymatically degradable. But due to their nature, there is often a great variability in their different properties, such as degradation kinetics or mechanical strength or batch-to-batch inconsistencies and sometimes immunogenic responses upon implantation.[9, 66] As a result, many synthetic materials are continuously being developed and improved in order to recapitulate structural and biological functions of the ECM, while increasing biocompatibility and control over material variability. Some important features that need to be considered for the development of synthetic matrices include topography, mechanical strength and physiochemical cues, which can all have an effect on cell behavior, as well as the three-dimensionality of the matrix, which has an effect on localization, diffusion and transport of signaling cues and proteins.[66] Amongst the various material strategies that have evolved to answer the need of biomaterial scaffold, hydrogels are an appealing solution due to their similarity to the ECM viscoelastic properties, their biocompatibility and ease of processing. Furthermore, many cross-linking methods for the formation of such hydrogel scaffolds, such as Michael-type addition, photopolymerization or enzymatic cross-linking, are mild enough processes to allow the viable encapsulation of cells.[67]

Although hydrogels can be composed of naturally occurring ECM components (such as collagen, fibrin or hyaluronic acid), many synthetic hydrogel strategies have emerged and evolved. Benefitting of important breakthroughs in polymer chemistry, 3D patterning techniques and biomimetic design, hydrogels based on synthetic polymers have become highly reproducible and allow precise tuning of mechanical properties, while remaining easy to process and manufacture.[68, 69]

1.4.1 Poly(ethylene glycol) as a biopolymer for engineering scaffolds

An example of synthetic biomaterial used for the formation of hydrogels is poly(ethylene glycol) (PEG). PEG is a very important polymer for biomedical applications because it is biocompatible, non-immunogenic and resistant to protein adsorption.[70, 71] It is therefore widely used for surface modification, drug delivery and tissue engineering. But because PEG is biologically inert, it has to be modified in order to support important cellular processes. One concept that has been explored to synthesize cell-compatible PEG hydrogels relies on the incorporation of ECM-derived peptides into the PEG scaffold in order to mimic the functions of the natural ECM.[72, 73]

1.4.2 Enzymatically cross-linked PEG hydrogel platform

Amongst the variations of this concept, one system in particular utilizes star-shaped PEG macromeres containing MMP-sensitive domains in their backbone as well as Factor XIII (FXIII) transglutaminase (TG) substrate sequences to obtain enzymatically cross-linked hydrogels, in which bioactive peptides also containing FXIII substrate sequences can be simultaneously incorporated (**Figure 1.2**).[74, 75] FXIII is the enzyme normally responsible for the cross-linking of fibrin, therefore the incorporation of FXIII substrate sequences in the backbone of this PEG-based hydrogel platform allows for a site-specific coupling of the hydrogel components in presence of FXIII. Furthermore, the enzymatic reaction is used for the covalent incorporation of an adhesion ligand composed of the fibronectin-derived integrin-binding RGD motif. And because the PEG backbone contains a protease-sensitive sequence (degraded mostly by MMP-1 and MMP-2, but also collagenases and plasmin),[74, 76] the obtained hydrogels are proteolytically degradable and can thus be remodeled by cells. This platform, hereafter referred to as TG-PEG hydrogel platform, has been successfully used to sustain 3D culture of various cell types *in vitro*.[77-80]

Furthermore, these hydrogel scaffolds are also highly tunable and the enzymatic cross-linking reaction can be used to incorporated several bioactive molecules, especially growth factors. Indeed, growth factors can be indirectly immobilized via affinity linkers that are cross-linked to the hydrogel backbone. One such linker is the Gln-ZZ linker that consists of a FXIII substrate sequence (Gln) followed by two repeats of the synthetic protein A analogue (Z).[81] Due to the high affinity of the ZZ domain for the fragment crystallizable (Fc) region of antibodies, proteins that have been engineered to contain an Fc-tag can be stably immobilized in PEG hydrogels, while remaining biologically active.

Such tools represent an interesting approach on the development of ECM-mimicking scaffold for tissue engineering, because they allow for a great flexibility regarding the incorporation of growth factors and other bioactive signals. As such, they could be used to answer one of the current limitations of hydrogels, which is the absence of spatiotemporal heterogeneity, which is often present in the natural ECM and important for certain cell interactions. Although many efforts still need to be made in regard of evolution and change of the cellular microenvironment over time for the design ECM-mimicking scaffolds, many alternatives already exist regarding the

spatial arrangement and structure of hydrogels. Several patterning techniques such as photopatterning or bio-printing have been developed to increase control over the three-dimensional structure and localization of biological cues.[66]

Since the above described PEG-based hydrogel platform could be potentially compatible with bio-printing techniques[82], the development of various affinity linker is of great interest for the localized immobilization and release of growth factors in synthetic scaffolds. Different sets of linkers could be combined to assemble modular microenvironment and allow the highly controlled immobilization of biological factors, but each linker could also be designed in order to have cell-responsive or cell-specific features.

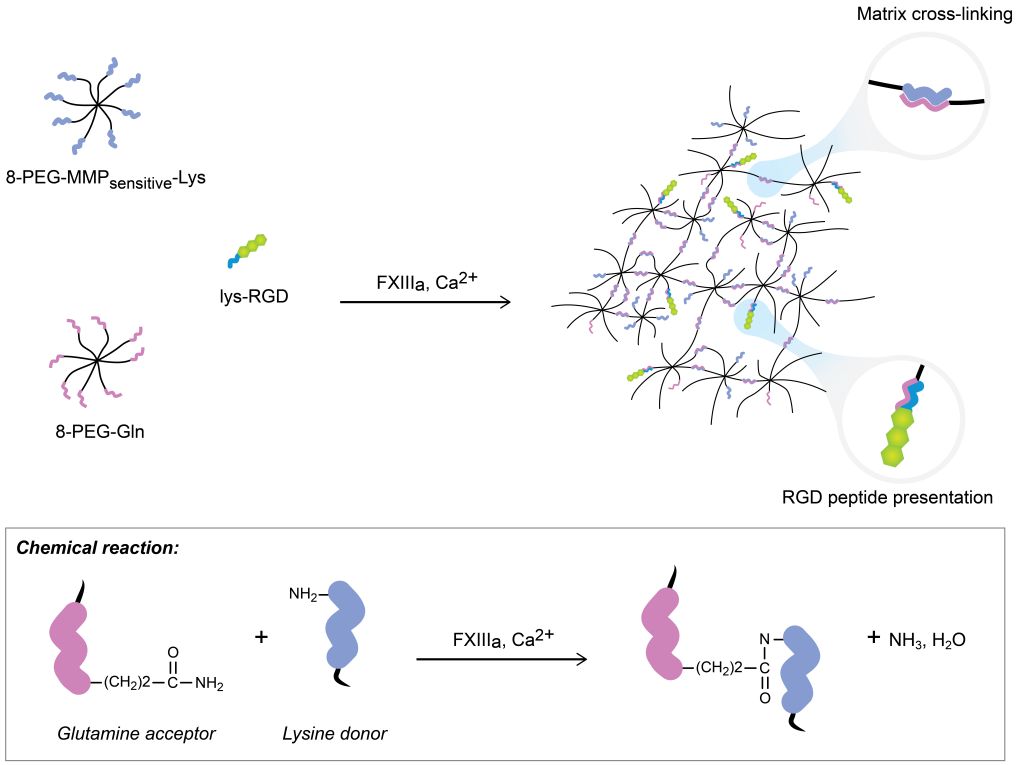

Figure 1.2. TG-PEG hydrogel system.

Two PEG macromeres, possessing either a glutamine acceptor substrate (8-PEG-Gln) or a matrix metalloproteinase-degradable lysine donor substrate (8-PEG-MMPsensitive-Lys) containing MMP-sensitive domains in their backbone, can be enzymatically cross-linked by activated Factor XIII (FXIII) transglutaminase (TG) to form hydrogels. The enzymatic reaction allows the simultaneous covalent incorporation of an RGD motif for cell adhesion into the scaffold.

1.5 Vascularization and tissue engineering models

Another aspect of tissue engineering addressed in this thesis is the limitation due to the difficulty of obtaining vascularized constructs. Indeed, appropriate vascularization is necessary to provide nutrient perfusion and mass transport across tissues and thus needs to be replicated in engineered constructs. Vascularization is particularly

important for oxygen transport and thus for cell survival. The ability of oxygen to diffuse across a tissue is a key factor that will limit the size of any construct. It also plays an important role for the spatial integrity of the constructs, since unwanted oxygen gradients can potentially produce variation in cells numbers and phenotypes.[83]

Many approaches seek to establish pre-vascularized networks in the constructs, which would allow anastomosis to the host vasculature upon implantation. Common methods include the modular assembly of smaller cellular units to created vascular networks and the functionalization of scaffolds with angiogenic factors.[83, 84] To that purpose, many different techniques for the immobilization of growth factors, such as the incorporation of growth factor binding domains to the scaffolds, creation of fusion proteins, or the simple coating or loading of the scaffolds, can be used. As with many tissue engineering approaches, one important constraint for immobilization of such molecules is that their delivery has to be tightly controlled in a spatial and temporal manner, which emphasizes again the need for a modular platform for the incorporation of growth factors.[85]

1.5.1 Regulation of angiogenesis

Angiogenesis is generally defined as the formation of new blood vessels from existing ones. It is an important biological process that takes places in physiological conditions, but also in several types of diseases such as cancer. Angiogenesis is a tightly orchestrated system that involves many signaling factors and depends on complex interactions between endothelial cells (ECs), pericytes and other surrounding cells, and their association with the ECM via integrins, and also with the basement membrane.[86] Typically, the cells of adult mature vasculature remain in a quiescent state. The ECs line the interior of blood vessels forming tight cell-cell junctions to ensure smooth blood flow, limit vascular leaks and minimize blood coagulation. The ECs also interact with the underlying lamina, anchoring the cells to the basement membrane. Scattered across the exterior of capillaries and venules are pericytes, which are in contact with neighboring ECs. Interactions between pericytes and endothelial cells are critical for the stabilization and support of the capillary structures. This combination of strong junctions, support, anchorage, and low proliferation allows for the formation of very resistant mature vascular structure. However this state can be changed upon induction of angiogenesis, which can be prompted by a variety of angiogenic factors that include growth factors, polysaccharides and lipids. This is mainly a local process that occurs in a series of steps starting with the binding of growth factors and cell signaling, followed by genetic and behavioral changes in vascular cells, leading to the remodeling of the cellular environment and invasion of newly formed blood vessels, and finally reaching a maturation stage, where cells ultimately return to a quiescent state. At each of these steps, interactions between cells and the ECM are important in determining the outcome of the angiogenic process.[87]

1.5.2 The role of the extracellular matrix in angiogenesis

The ECM plays a central role during various aspects of angiogenic processes. Indeed, adhesion of ECs to the ECM has been shown to be critical for the proper activation of angiogenic signaling pathways (e.g. via crosstalk with integrins), as well as having an anti-apoptotic effect on ECs,[88, 89] and is thus necessary to enable EC proliferation.[90] Furthermore, ECs also need to adhere to the ECM for migration, which is required for the sprouting and formation of new blood vessels. Research has shown evidences that although EC migration is mainly initiated by signaling factors, migration and morphogenesis later strongly depend on ECM configuration.[88, 91] The ECM also allows cells to communicate over longer distances via tension. ECs can exert mechanical forces on the ECM, which can then be transduced to cells further away, thus creating a guidance pathway for the formation of higher architectures.[92] Angiogenesis also includes the degradation and remodeling of the microenvironment of ECs via protease like MMPs. Upon degradation and release, these ECM components themselves such as collagens, fibronectins and laminins can regulate and guide EC migration and new ECM deposition.[93, 94] Finally, as mentioned in **Section 1.3**, the ECM provides a reservoir for growth factors and cytokines and thus contributes to the modulation and presentation of angiogenic growth factors in order to regulate the formation of new blood vessels.[95]

1.5.3 Angiogenic growth factors

The main growth factors involved in angiogenesis include members of the VEGF, TGF, PDGF and FGF family, as well angiopoietins, tumor necrosis factor-α (TNF-α), and interleukins.[86] The work of this thesis is mainly focused on the pro-angiogenic effects of VEGF, as well as subsidiary factors taking part in angiogenesis, namely ephrins and their Eph receptors,[86, 96] and netrins, which have be shown to act during placental angiogenesis have also been used in therapeutic angiogenesis.[97, 98]

1.5.3.1 Vascular endothelial growth factors

VEGF-A is probably the most studied and best understood member of the VEGF family. VEGF-A interacts with its corresponding receptors, VEGFR-1 and VEGFR-2 (expressed on vascular ECs), as well as neuropilin receptors NP-1 and NP-2 (expressed on neurons but also by the vascular endothelium). It is widely described as an inducer of EC proliferation, sprouting and tube formation and can be linked to vasodilatation and vessel leakiness. Amongst its different isoforms, the heparin-binding $VEGF_{165}$ is the most characterized and is widely used in research to induce angiogenesis.[99-101]

1.5.3.2 Ephrins and Eph receptors

Ephrin ligands and Eph receptors can be linked to many biological processes, such as embryonic development, axonal guidance, or carcinogenesis. But in the past years, more and more research has shown that ephrins and Eph receptors play an essential role in angiogenesis, especially regarding the guidance of cell migration. Eph receptors are a unique family of receptor tyrosine kinases (RTKs) in that they can bind cell surface-bound ligands and activate bi-

directional signaling pathways. Interactions between ephrins and Eph receptors thus necessitate cell-cell contact and can prompt various cellular responses including, adhesion, repulsion or boundary formation. It is also recognized that the signaling outcome can be influenced by the clustering of Eph receptor-ephrin.[102, 103] The ephrin ligands can be attached to the cell membrane through either a GPI anchor or a transmembrane domain and are divided accordingly in classes A and B respectively. The receptors are distributed into EphA and EphB classes as well, depending on which type of ephrin their preferentially bind.[104-106] Amongst the various ephrins and receptors, ephrin-B2 and EphB4 have attracted the most interest. Expression of ephrin-B2 is predominant in arterial ECs, whereas its receptor EphB4 is mostly specific to venous ECs, and so they have been used efficiently as specific markers of arterial or venous blood vessels.[96, 107]

1.5.3.3 Netrin-4

Netrins are a family of proteins related to laminins, which have been initially identified as guidance cues for axonal migration. Since then, netrins have been found to participate in many other biological processes, including angiogenesis. Netrin-4 has been widely studied and reported to bind to certain integrins and laminins and to regulate endothelial cell migration. But it is still unclear whether it has pro-angiogenic or anti-angiogenic role, since reports in literature tend to contain opposing conclusions.[108-110] Nevertheless, many *in vitro* studies have shown that netrin-4 can inhibit endothelial proliferation and tube-like formation, specifically for human vein endothelial cells (HUVECs) and could thus be an interesting anti-angiogenic candidate.[97, 111-113]

1.6 Motivation and objectives

Considering the all the above-mentioned aspects of tissue engineering, the main focus of this thesis is to develop news tools for the recapitulation of the ECM and the microenvironment of cells. In order to do so, we have based our strategy on the pre-existing TG-PEG hydrogel platform described earlier, which is well characterized and has been used to cultivate cells successfully. We have mainly sought to understand and develop new ways of immobilizing growth factors, in a manner that resembles the interactions between cells, ECM and bound growth factors more closely. As we already possessed the protein A-based “Gln-ZZ” linker able to bind Fc-tagged proteins, we wanted to develop additional TG-PEG compatible linkers in order to have immobilization possibilities for more types of growth factors. Importantly, we wanted to develop tools that allowed flexibility regarding the selection of target growth factors. The streptavidin-biotin interaction was thus an ideal candidate due to the strong affinity and the relatively easy biotinylation process for proteins.

In **Chapter 2** of this thesis, we synthesized and characterized a peptide linker that allows the versatile immobilization of biotinylated growth factors. The peptide is composed of a FXIII domain for the covalent incorporation into the TG-PEG hydrogel backbone and of a streptavidin domain able to bind biotinylated proteins. This

binding strategy was used efficiently to immobilize biotinylated BMP-2 and induce the 3D spatially controlled osteogenic differentiation in mesenchymal stem cells, which to our knowledge had not been achieved yet.

In **Chapter 3** we developed a degradable streptavidin-linker containing domains that can be cleaved by cell proteases in order to increase the release of the immobilized growth factor in a cell-dependant manner. By synthesizing a streptavidin linker containing MMP-sensitive sites, we were able to improve the dose-response relationship of the immobilized growth factor.

Another aspect of tissue engineering was studied in **Chapter 4**, where we investigated the effects of netrin-4 and ephrins on blood vessel development. The objective was to evaluate these growth factors as potential cues for the regulation of angiogenesis and thus as tools for the establishment of pre-vascular structures in TG-PEG tissue constructs. This was achieved by studying the effects of the selected proteins on the developing vasculature of the chicken allantoic membrane. Furthermore we investigated the effects of ephrins on endothelial cell migration.

The overall work of this thesis thus presents new tools for the creation of tunable cellular microenvironment. **Chapter 5** summarizes the main findings and discusses future directions and outlooks of this research.

1.7 References

[1] A. Atala, *Rejuvenation Res,* 2004, *7*, 15.

[2] Y. Ikada, *J R Soc Interface,* 2006, *3*, 589.

[3] C. M. Magin, D. L. Alge, and K. S. Anseth, *Biomed Mater,* 2016, *11*, 022001.

[4] S. Baiguera, L. Urbani, and C. Del Gaudio, *Biomed Res Int,* 2014, *2014*, 398069.

[5] A. Atala, S. B. Bauer, S. Soker, J. J. Yoo, and A. B. Retik, *Lancet,* 2006, *367*, 1241.

[6] P. Jungebluth, E. Alici, S. Baiguera, K. Le Blanc, P. Blomberg, B. Bozoky, C. Crowley, O. Einarsson, T. Gudbjartsson, S. Le Guyader, G. Henriksson, O. Hermanson, J. E. Juto, B. Leidner, T. Lilja, J. Liska, T. Luedde, V. Lundin, G. Moll, B. Nilsson, C. Roderburg, S. Stromblad, T. Sutlu, A. I. Teixeira, E. Watz, A. Seifalian, and P. Macchiarini, *Lancet,* 2011, *378*, 1997.

[7] A. Raya-Rivera, D. R. Esquiliano, J. J. Yoo, E. Lopez-Bayghen, S. Soker, and A. Atala, *Lancet,* 2011, *377*, 1175.

[8] T. Shin'oka, Y. Imai, and Y. Ikada, *N Engl J Med,* 2001, *344*, 532.

[9] A. Atala, F. K. Kasper, and A. G. Mikos, *Sci Transl Med,* 2012, *4*, 160rv12.

[10] A. Peloso, A. Dhal, J. P. Zambon, P. Li, G. Orlando, A. Atala, and S. Soker, *Stem Cell Res Ther,* 2015, *6*, 107.

[11] V. van Duinen, S. J. Trietsch, J. Joore, P. Vulto, and T. Hankemeier, *Curr Opin Biotechnol,* 2015, *35*, 118.

[12] N. T. Elliott, and F. Yuan, *J Pharm Sci,* 2011, *100*, 59.

[13] T. Kofidis, P. Akhyari, J. Boublik, P. Theodorou, U. Martin, A. Ruhparwar, S. Fischer, T. Eschenhagen, H. P. Kubis, T. Kraft, R. Leyh, and A. Haverich, *J Thorac Cardiovasc Surg,* 2002, *124*, 63.

[14] R. J. Thomas, R. Bhandari, D. A. Barrett, A. J. Bennett, J. R. Fry, D. Powe, B. J. Thomson, and K. M. Shakesheff, *Cells Tissues Organs,* 2005, *181*, 67.

[15] J. P. Miranda, S. B. Leite, U. Muller-Vieira, A. Rodrigues, M. J. Carrondo, and P. M. Alves, *Tissue Eng Part C Methods,* 2009, *15*, 157.

[16] T. M. DesRochers, L. Suter, A. Roth, and D. L. Kaplan, *PLoS One,* 2013, *8*, e59219.

[17] Y. S. Torisawa, C. S. Spina, T. Mammoto, A. Mammoto, J. C. Weaver, T. Tat, J. J. Collins, and D. E. Ingber, *Nat Methods,* 2014, *11*, 663.

[18] Q. Sun, Y. Gu, W. Zhang, L. Dziopa, J. Zilberberg, and W. Lee, *Bone Res,* 2015, *3*, 15026.

[19] J. S. Jeon, I. K. Zervantonakis, S. Chung, R. D. Kamm, and J. L. Charest, *PLoS One,* 2013, *8*, e56910.

[20] S. Bersini, J. S. Jeon, G. Dubini, C. Arrigoni, S. Chung, J. L. Charest, M. Moretti, and R. D. Kamm, *Biomaterials,* 2014, *35*, 2454.

[21] C. L. M. Bao, E. Y. Teo, M. S. K. Chong, Y. Liu, M. Choolani, and J. K. Y. Chan, 'Advances in Bone Tissue Engineering', in *Regenerative Medicine and Tissue Engineering*, ed. by P. J. A. Andrades InTech, 2013.

[22] S. Bose, S. Vahabzadeh, and A. Bandyopadhyay, *Materials Today,* 2013, *16*, 496.

[23] M. Mravic, B. Peault, and A. W. James, *Biomed Res Int,* 2014.

[24] C. Bonnans, J. Chou, and Z. Werb, *Nat Rev Mol Cell Biol,* 2014, *15*, 786.

[25] T. R. Cox, and J. T. Erler, *Dis Model Mech,* 2011, *4*, 165.

[26] W. P. Daley, S. B. Peters, and M. Larsen, *J Cell Sci,* 2008, *121*, 255.

[27] C. Frantz, K. M. Stewart, and V. M. Weaver, *J Cell Sci,* 2010, *123*, 4195.

[28] J. D. Humphrey, E. R. Dufresne, and M. A. Schwartz, *Nat Rev Mol Cell Biol,* 2014, *15*, 802.

[29] T. Rozario, and D. W. DeSimone, *Dev Biol,* 2010, *341*, 126.

[30] W. S. To, and K. S. Midwood, *Fibrogenesis Tissue Repair,* 2011, *4*, 21.

[31] S. K. Mitra, D. A. Hanson, and D. D. Schlaepfer, *Nat Rev Mol Cell Biol,* 2005, *6*, 56.

[32] S. H. Kim, J. Turnbull, and S. Guimond, *J Endocrinol,* 2011, *209*, 139.

[33] E. S. Place, N. D. Evans, and M. M. Stevens, *Nat Mater,* 2009, *8*, 457.

[34] J. Zhu, *Biomaterials,* 2010, *31*, 4639.

[35] S. Amano, N. Akutsu, Y. Matsunaga, T. Nishiyama, M. F. Champliaud, R. E. Burgeson, and E. Adachi, *Exp Cell Res,* 2001, *271*, 249.

[36] K. Brew, D. Dinakarpandian, and H. Nagase, *Biochim Biophys Acta,* 2000, *1477*, 267.

[37] I. M. Clark, T. E. Swingler, C. L. Sampieri, and D. R. Edwards, *Int J Biochem Cell Biol,* 2008, *40*, 1362.

[38] P. Olczyk, L. Mencner, and K. Komosinska-Vassev, *Biomed Res Int,* 2014, *2014*, 747584.

[39] G. S. Schultz, and A. Wysocki, *Wound. Rep. Reg.,* 2009, *17*, 153.

[40] G. S. Schultz, J. M. Davidson, R. S. Kirsner, P. Bornstein, and I. M. Herman, *Wound. Rep. Reg.,* 2011, *19*, 134.

[41] R. F. Diegelmann, and M. C. Evans, *Front Biosci,* 2004, *9*, 283.

[42] Y. S. Wu, and S. N. Chen, *Front Pharmacol,* 2014, *5*, 1.

[43] J. M. Reinke, and H. Sorg, *Eur Surg Res,* 2012, *49*, 35.

[44] S. Guo, and L. A. Dipietro, *J Dent Res,* 2010, *89*, 219.

[45] J. M. Shah, E. Omar, D. R. Pai, and S. Sood, *Indian J Plast Surg,* 2012, *45*, 220.

[46] K. S. Midwood, L. V. Williams, and J. E. Schwarzbauer, *Int J Biochem Cell Biol,* 2004, *36*, 1031.

[47] G. C. Gurtner, S. Werner, Y. Barrandon, and M. T. Longaker, *Nature,* 2008, *453*, 314.

[48] M. F. Brizzi, G. Tarone, and P. Defilippi, *Curr Opin Cell Biol,* 2012, *24*, 645.

[49] K. Forsten-Williams, C. L. Chu, M. Fannon, J. A. Buczek-Thomas, and M. A. Nugent, *Ann Biomed Eng,* 2008, *36*, 2134.

[50] M. M. Martino, and J. A. Hubbell, *FASEB J,* 2010, *24*, 4711.

[51] M. M. Martino, P. S. Briquez, A. Ranga, M. P. Lutolf, and J. A. Hubbell, *Proc Natl Acad Sci U S A,* 2013, *110*, 4563.

[52] R. O. Hynes, *Science,* 2009, *326*, 1216.

[53] F. Gattazzo, A. Urciuolo, and P. Bonaldo, *Biochim Biophys Acta,* 2014, *1840*, 2506.

[54] J. Schlessinger, A. N. Plotnikov, O. A. Ibrahimi, A. V. Eliseenkova, B. K. Yeh, A. Yayon, R. J. Linhardt, and M. Mohammadi, *Mol Cell,* 2000, *6*, 743.

[55] M. Mohammadi, S. K. Olsen, and R. Goetz, *Curr Opin Struct Biol,* 2005, *15*, 506.

[56] N. Ortega, F. E. L'Faqihi, and J. Plouet, *Biol Cell,* 1998, *90*, 381.

[57] C. J. Robinson, and S. E. Stringer, *J Cell Sci,* 2001, *114*, 853.

[58] G. H. Mahabeleshwar, W. Feng, K. Reddy, E. F. Plow, and T. V. Byzova, *Circ Res,* 2007, *101*, 570.

[59] P. R. Somanath, N. L. Malinin, and T. V. Byzova, *Angiogenesis,* 2009, *12*, 177.

[60] P. Lijnen, and V. Petrov, *Methods Find Exp Clin Pharmacol,* 2002, *24*, 333.

[61] X. Pan, Z. Chen, R. Huang, Y. Yao, and G. Ma, *PLoS One,* 2013, *8*, e60335.

[62] T. A. Wilgus, *Adv Wound Care (New Rochelle),* 2012, *1*, 249.

[63] A. L. Sieron, N. Louneva, and A. Fertala, *Cytokine,* 2002, *18*, 214.

[64] M. Kisiel, A. S. Klar, M. Ventura, J. Buijs, M. K. Mafina, S. M. Cool, and J. Hilborn, *PLoS One,* 2013, *8*, e78551.

[65] E. N. Blaney Davidson, E. L. Vitters, P. L. van Lent, F. A. van de Loo, W. B. van den Berg, and P. M. van der Kraan, *Arthritis Res Ther,* 2007, *9*, R102.

[66] R. J. Wade, and J. A. Burdick, *Materials Today,* 2012, *15*, 454.

[67] W. E. Hennink, and C. F. van Nostrum, *Adv Drug Deliv Rev,* 2002, *54*, 13.

[68] J. L. Drury, and D. J. Mooney, *Biomaterials,* 2003, *24*, 4337.

[69] D. Seliktar, *Science,* 2012, *336*, 1124.

[70] J. H. Lee, H. B. Lee, and J. D. Andrade, *Progress in Polymer Science,* 1995, *20*, 1043.

[71] J. K. Tessmar, and A. M. Gopferich, *Macromolecular Bioscience,* 2007, *7*, 23.

[72] M. P. Lutolf, J. L. Lauer-Fields, H. G. Schmoekel, A. T. Metters, F. E. Weber, G. B. Fields, and J. A. Hubbell, *Proceedings of the National Academy of Sciences of the United States of America,* 2003, *100*, 5413.

[73] M. P. Lutolf, and J. A. Hubbell, *Nat. Biotechnol.,* 2005, *23*, 47.

[74] M. Ehrbar, S. C. Rizzi, R. G. Schoenmakers, B. S. Miguel, J. A. Hubbell, F. E. Weber, and M. P. Lutolf, *Biomacromolecules,* 2007, *8*, 3000.

[75] M. Ehrbar, S. C. Rizzi, R. Hlushchuk, V. Djonov, A. H. Zisch, J. A. Hubbell, F. E. Weber, and M. P. Lutolf, *Biomaterials,* 2007, *28*, 3856.

[76] K. B. Fonseca, P. L. Granja, and C. C. Barrias, *Progress in Polymer Science,* 2014, *39*, 2010.

[77] A. Sala, P. Hanseler, A. Ranga, M. P. Lutolf, J. Voros, M. Ehrbar, and F. E. Weber, *Integr. Biol. (Camb),* 2011, *3*, 1102.

[78] P. S. Lienemann, Y. R. Devaud, R. Reuten, B. R. Simona, M. Karlsson, W. Weber, M. Koch, M. P. Lutolf, V. Milleret, and M. Ehrbar, *Integr Biol (Camb),* 2015, *7*, 101.

[79] S. Metzger, P. S. Lienemann, C. Ghayor, W. Weber, I. Martin, F. E. Weber, and M. Ehrbar, *Adv Healthc Mater,* 2015, *4*, 550.

[80] U. Blache, S. Metzger, Q. Vallmajo-Martin, I. Martin, V. Djonov, and M. Ehrbar, *Adv Healthc Mater,* 2015.

[81] P. S. Lienemann, M. Karlsson, A. Sala, H. M. Wischhusen, F. E. Weber, R. Zimmermann, W. Weber, M. P. Lutolf, and M. Ehrbar, *Adv Healthc Mater,* 2013, *2*, 292.

[82] K. Pataky, T. Braschler, A. Negro, P. Renaud, M. P. Lutolf, and J. Brugger, *Adv Mater,* 2012, *24*, 391.

[83] M. Lovett, K. Lee, A. Edwards, and D. L. Kaplan, *Tissue Eng Part B Rev,* 2009, *15*, 353.

[84] M. W. Laschke, and M. D. Menger, *Eur Surg Res,* 2012, *48*, 85.

[85] F. A. Auger, L. Gibot, and D. Lacroix, *Annu Rev Biomed Eng,* 2013, *15*, 177.

[86] Z. K. Otrock, R. A. Mahfouz, J. A. Makarem, and A. I. Shamseddine, *Blood Cells Mol Dis,* 2007, *39*, 212.

[87] D. A. Cheresh, and D. G. Stupack, *Oncogene,* 2008, *27*, 6285.

[88] D. R. Senger, C. A. Perruzzi, M. Streit, V. E. Koteliansky, A. R. de Fougerolles, and M. Detmar, *Am J Pathol,* 2002, *160*, 195.

[89] F. Aoudjit, and K. Vuori, *J Cell Biol,* 2001, *152*, 633.

[90] D. R. Senger, and G. E. Davis, *Cold Spring Harb Perspect Biol,* 2011, *3*, a005090.

[91] V. W. van Hinsbergh, A. Collen, and P. Koolwijk, *Ann N Y Acad Sci,* 2001, *936*, 426.

[92] G. E. Davis, and D. R. Senger, *Circ Res,* 2005, *97*, 1093.

[93] L. Lamalice, F. Le Boeuf, and J. Huot, *Circ Res,* 2007, *100*, 782.

[94] S. Kim, M. Harris, and J. A. Varner, *J Biol Chem,* 2000, *275*, 33920.

[95] S. A. Eming, and J. A. Hubbell, *Exp Dermatol,* 2011, *20*, 605.

[96] M. Potente, H. Gerhardt, and P. Carmeliet, *Cell,* 2011, *146*, 873.

[97] M. Dakouane-Giudicelli, N. Alfaidy, and P. de Mazancourt, *Biomed Res Int,* 2014, *2014*, 901941.

[98] B. D. Wilson, M. Ii, K. W. Park, A. Suli, L. K. Sorensen, F. Larrieu-Lahargue, L. D. Urness, W. Suh, J. Asai, G. A. Kock, T. Thorne, M. Silver, K. R. Thomas, C. B. Chien, D. W. Losordo, and D. Y. Li, *Science,* 2006, *313*, 640.

[99] N. Ferrara, H. P. Gerber, and J. LeCouter, *Nat Med,* 2003, *9*, 669.

[100] H. Takahashi, and M. Shibuya, *Clin Sci (Lond),* 2005, *109*, 227.

[101] M. N. Nakatsu, R. C. Sainson, S. Perez-del-Pulgar, J. N. Aoto, M. Aitkenhead, K. L. Taylor, P. M. Carpenter, and C. C. Hughes, *Lab Invest,* 2003, *83*, 1873.

[102] S. H. Wimmer-Kleikamp, P. W. Janes, A. Squire, P. I. Bastiaens, and M. Lackmann, *J Cell Biol,* 2004, *164*, 661.

[103] J. P. Himanen, L. Yermekbayeva, P. W. Janes, J. R. Walker, K. Xu, L. Atapattu, K. R. Rajashankar, A. Mensinga, M. Lackmann, D. B. Nikolov, and S. Dhe-Paganon, *Proc Natl Acad Sci U S A,* 2010, *107*, 10860.

[104] N. Cheng, D. M. Brantley, and J. Chen, *Cytokine Growth Factor Rev,* 2002, *13*, 75.

[105] E. B. Pasquale, *Nat Rev Mol Cell Biol,* 2005, *6*, 462.

[106] S. Kuijper, C. J. Turner, and R. H. Adams, *Trends Cardiovasc Med,* 2007, *17*, 145.

[107] B. Mosch, B. Reissenweber, C. Neuber, and J. Pietzsch, *J Oncol,* 2010, *2010*, 135285.

[108] E. Lejmi, L. Leconte, S. Pedron-Mazoyer, S. Ropert, W. Raoul, S. Lavalette, I. Bouras, J. G. Feron, M. Maitre-Boube, F. Assayag, C. Feumi, M. Alemany, T. X. Jie, T. Merkulova, M. F. Poupon, M. M. Ruchoux, G. Tobelem, F. Sennlaub, and J. Plouet, *Proc Natl Acad Sci U S A,* 2008, *105*, 12491.

[109] E. Lambert, M. M. Coissieux, V. Laudet, and P. Mehlen, *J Biol Chem,* 2012, *287*, 3987.

[110] E. Lejmi, I. Bouras, S. Camelo, M. Roumieux, N. Minet, C. Lere-Dean, T. Merkulova-Rainon, G. Autret, C. Vayssettes, O. Clement, J. Plouet, and L. Leconte, *Vasc Cell,* 2014, *6*, 1.

[111] Y. Han, Y. Shao, T. Liu, Y. L. Qu, W. Li, and Z. Liu, *PLoS One,* 2015, *10*, e0122951.

[112] M. Dakouane-Giudicelli, S. Brouillet, W. Traboulsi, A. Torre, G. Vallat, S. Si Nacer, M. Vallee, J. J. Feige, N. Alfaidy, and P. de Mazancourt, *Placenta,* 2015, *36*, 1260.

[113] M. Nacht, T. B. St Martin, A. Byrne, K. W. Klinger, B. A. Teicher, S. L. Madden, and Y. Jiang, *Exp Cell Res,* 2009, *315*, 784.

Chapter 2 *Modular poly(ethylene glycol) matrices for controlled 3D-localized cell differentiation*

Adapted from:

S Metzger, PS Lienemann, C Ghayor, W Weber, I Martin, F E Weber, M Ehrbar, **Modular poly(ethylene glycol) matrices for the controlled 3D-localized osteogenic differentiation of mesenchymal stem cells**, *Adv Healthc Mater*, 2015 Mar 11;4(4):550-8

2.1 Introduction

Living tissues are composed of hierarchically organized three-dimensional (3D) cellular structures, which interact with and are supported by the components of the extracellular matrix (ECM). Tissue formation depends on morphogenetic processes that are tightly regulated by the dynamic presentation of spatially confined soluble or immobilized cell-instructive cues. These tightly orchestrated signaling events are only partially understood and cannot be easily recapitulated *in vitro* due to technical limitations. However, it is hypothesized that structured 3D assembly of tissue progenitor cells within cell-type specific cell-instructive matrices is sufficient as a starting point to initiate late morphogenetic processes, leading to at least partially physiological relevant tissue mimetics.[114] For the creation of such constructs, the positioning of multiple cell types and the local immobilization of biological cues in provisional ECM with defined degradability, stiffness and adhesive properties is essential. Increasing precision for localized 3D positioning of cells and biomaterials is expected to coincide with ever improving manufacturing techniques, such as printing, molding or microfluidics.[115-117]

In order to take advantage of such novel techniques, great strides have been made towards the rational design of biomimetic matrices, which can be tuned towards specific applications and can even be locally and dynamically modified in a user-defined fashion.[118, 119] The binding and immobilization of various bioactive molecules by affinity or covalent interactions have been established. These strategies based on chemical or genetic engineering rely on the incorporation of naturally occurring growth factor-binding sites (such as collagen, laminin, fibronectin, heparin) into matrices, the fusion of growth factors to matrix-binding domains or enzyme recognition sequences, and the modification of matrices and growth factors with the respective high-affinity molecular binding partners (dissociation constants ranging from 10^{-7}-10^{-15} M) such as barnase-barstar, streptavidin-biotin, or protein A-Fc fragment.[81, 120-125]

Although very elegant strategies for the antibiotic-, small molecule-, and light-controlled release or localized presentation of cell-instructive signals has become available, the site-specific 3D differentiation of tissue progenitor cells using therapeutically relevant growth factors has so far not been addressed.[126-128] Bone marrow-derived mesenchymal stem/progenitor cells (BM-MSCs) are a clinically relevant cell source,[129, 130] which also due to their relatively good availability, their high proliferative potential, and their ability to readily differentiate towards the osteogenic lineage have been widely used for the generation of tissue-engineered bone. BM-MSCs in combination with endothelial cells have recently been employed to generate transplantable vascularized constructs.[131] Additionally, the sequential differentiation of MSCs in 3D porous scaffolds by osteoinductive medium and seeding of endothelial cells has been described to enable the generation of pre-vascularized constructs, which anastomose with the host vasculature and form mineralized bone.[132] Thus, the 3D structured assembly of BM-MSCs and endothelial cells (from healthy or diseased individuals) and the localized osteogenic differentiation of BM-MSCs in presence of endothelial cells hold great promise for the *in vitro* generation of bone tissue mimetics.

We have previously described a fibrin-mimicking polyethylene glycol (PEG)-based hydrogel system (TG-PEG) for the modular and flexible design of biomimetic matrices.[75] In this system, 8-arm star-shaped PEG precursors, possessing either a glutamine acceptor substrate (8-PEG-Gln) or a matrix metalloproteinase-degradable lysine donor substrate (8-PEG-$MMP_{sensitive}$-Lys), are cross-linked by the thrombin-activated transglutaminase (TG) Factor XIII ($FXIII_a$) to form hydrogels. Noteworthy is that any peptide or protein containing either substrate sequence can be added on demand to the reaction mixture and will be covalently linked to the forming hydrogel.[74, 75] When formulated in presence of Gln-RGD and with adequate mechanical properties (94 ± 25 to 482 ± 77 Pa) these hydrogels were shown to be excellent substrates for the 3D culture of osteogenic cells *in vitro*.[133] By 3D-positioning of osteogenic (osteoblasts and osteocytes) and endothelial cells within such hydrogels, a first step towards the formation of bone-like structures could be achieved.[77] However, in order to obtain structured and fully differentiated bone constructs *in vitro*, the specific provision of multiple osteogenic or endothelial cues to the individual bone or blood vessel forming cell types would be needed.

As a stepping stone towards the *in vitro* formation of physiologically relevant bone constructs, consisting of multiple cell types such as differentiated osteoblasts and blood vessels, we here aimed at the localized 3D differentiation of BM-MSCs by stable, specific, and orthogonal matrix-immobilization of bone morphogenetic protein-2 (BMP-2). BMP-2 is one of the most potent bone-inducing factors and has been known to direct the differentiation of MSCs towards bone.[134] Since genetic engineering strategies such as fusion with an Fc domain or the Gln sequence largely compromised BMP-2 function and was not compatible with enzymatic immobilization (own unpublished observations) we established a streptavidin-biotin based strategy. Optimal conditions for the biotinylation of recombinant human BMP-2 (rhBMP-2) without compromising its bioactivity were determined. A Gln-streptavidin linker peptide (consisting of a FXIII-substrate and a streptavidin sequence) that is covalently integrated in the forming TG-PEG hydrogels (**Figure 2.1**A) was designed and recombinantly expressed. Streptavidin-modified hydrogels were shown to capture biotinylated proteins and present them in an active form. Finally, 3D patterned TG-PEG hydrogels were designed to prove that BMP-2 presenting hydrogels can promote the osteogenic differentiation of the C2C12 myogenic cell line and human BM-MSCs within locally predefined areas (**Figure 2.1**B).

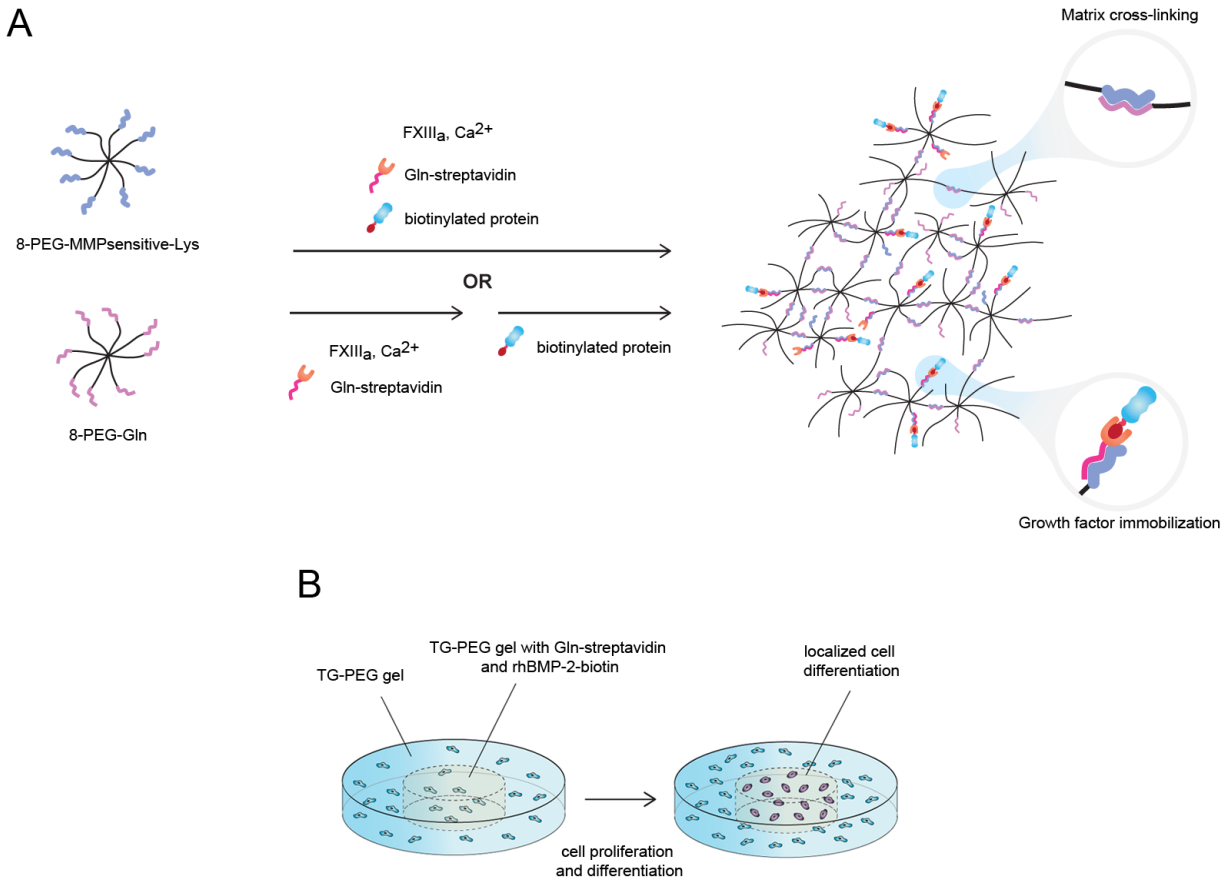

Figure 2.1. Scheme of the Gln-streptavidin linker incorporation and localized differentiation strategy.

(A) Streptavidin-modified TG-PEG hydrogels are formed by the cross-linking of 8-PEG-$MMP_{sensitive}$-Lys and 8-PEG-Gln components via FXIIIa and the addition of Gln-streptavidin linker in the polymerization reaction. Biotinylated proteins can be either immobilized during hydrogel formation or captured subsequently. (B) Mesenchymal cells are cultured for up to 9 days in a TG-PEG hydrogel construct with rhBMP-2-biotin locally immobilized in the center via Gln-streptavidin. The cells exposed to the immobilized BMP-2 environment differentiate towards to osteogenic lineage.

2.2 Results and Discussion

2.2.1 Design of streptavidin/biotin-based growth factor-presenting TG-PEG hydrogels

For the production of streptavidin-modified hydrogels, a recombinant peptide consisting of the glutamine acceptor substrate Gln fused to the N-terminus of monomeric streptavidin was designed. The resulting Gln-streptavidin linker can be covalently incorporated in FXIIIa-formed TG-PEG hydrogels when added during the cross-linking reaction. The localized capturing of biotinylated growth factors due to the very strong binding affinity of biotin for streptavidin

(dissociation constant Kd of ~10^{-15} M)[135] allows their efficient, non-covalent immobilization to streptavidin-modified PEG hydrogels and can be achieved both during and after gel formation. In contrast to naturally occurring and synthetic biomaterials functionalized with commercially available maleimide-streptavidin [125, 136], genetic engineering and recombinant expression provides the possibility to further modify streptavidin-linkers such as to integrate proteolytic cleavage sites for the tuning of growth factor release properties.

2.2.2 Production and characterization of streptavidin-modified TG-PEG hydrogels

The Gln-streptavidin linker was expressed in high yields (20 mg·L-1 culture) in E. coli strain BL21-Gold(DE3) pLysS (**Figure 2.2**A). It could be purified via biotin affinity chromatography, which additionally allowed for a selection of functional streptavidin (**Figure 2.2**B). The FXIIIa-mediated coupling of Gln-streptavidin to 8-PEG-MMPsensitive-Lys and the preservation of the biotin binding activity after the PEGylation reaction were confirmed by the detection of a high molecular weight PEGylated Gln-streptavidin on a Western blot using a biotinylated antibody (**Figure 2.2**C).

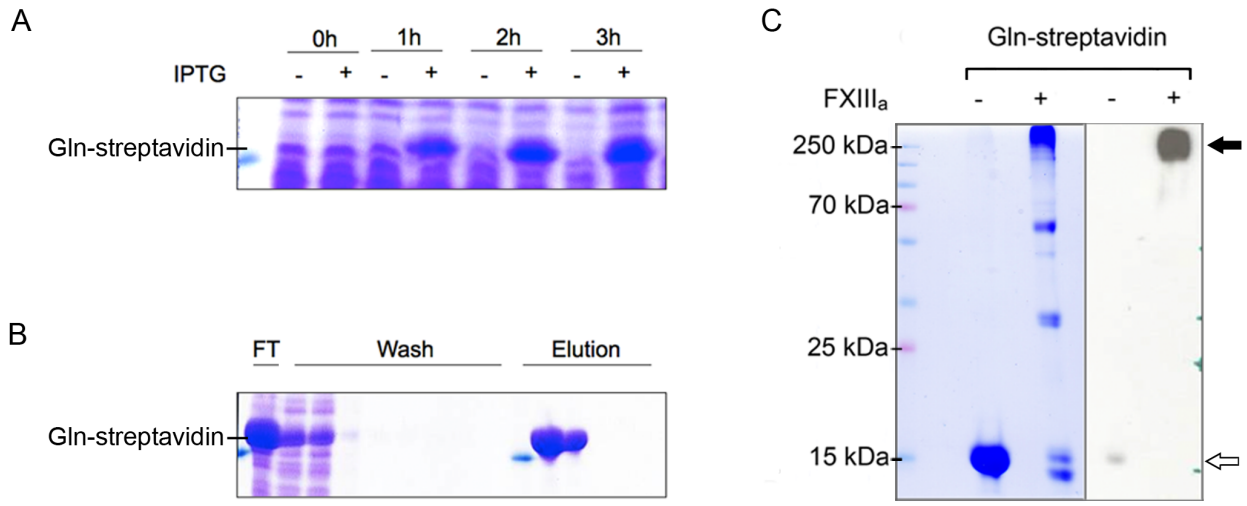

Figure 2.2. The Gln-streptavidin linker was produced, purified and assessed for functionality.

(A) The expression of Gln-streptavidin in *E. coli* BL21-Gold(DE3) pLysS was assessed at different time points after IPTG induction by SDS-PAGE of bacterial lysate samples. (B) Presence of the expressed Gln-streptavidin was determined at various steps of the purification process through an iminobiotin agarose column by SDS-PAGE (FT: flow-through). (C) The functionality of the Gln-streptavidin linker was evaluated for its TG-PEG hydrogel compatibility. Gln-streptavidin was reacted with 8-PEG-$MMP_{sensitive}$-Lys with or without $FXIII_a$ and cross-linking was evaluated by SDS-PAGE and Western blotting (with rat IgG-biotin, followed by anti-rat IgG-HRP). The white arrow indicates the non-cross-linked Gln-streptavidin and the black arrow shows the high molecular weight Gln-streptavidin that is cross-linked to 8-PEG-$MMP_{sensitive}$-Lys.

To show the ability of matrix-immobilized Gln-streptavidin to capture biotinylated proteins, hydrogels with increasing amounts of Gln-streptavidin linker were immersed in solutions containing biotinylated alkaline phosphatase (ALP-biotin). The amount of remaining ALP-biotin in the immersion solution was quantified by determination of the ALP activity over a period of 5 days. **Figure 2.3** shows that increasing the concentration of the Gln-streptavidin linker in the hydrogels leads to both an accelerated and more extensive uptake of ALP-biotin from its environment. Whereas with 5 µM Gln-streptavidin the enzymatic activity of the biotinylated ALP was reduced only to 42.9 ± 1.9%, with 125 µM the enzymatic activity had decreased to 7.6 ± 2.4% after 5 days. Of note, most of the protein is bound after the first 24 hours and equilibrium is almost reached after 48 hours with 125 µM Gln-streptavidin. Based on these results, a Gln-streptavidin concentration of 100 µM was chosen for the reliable binding of biotinylated proteins in all following experiments.

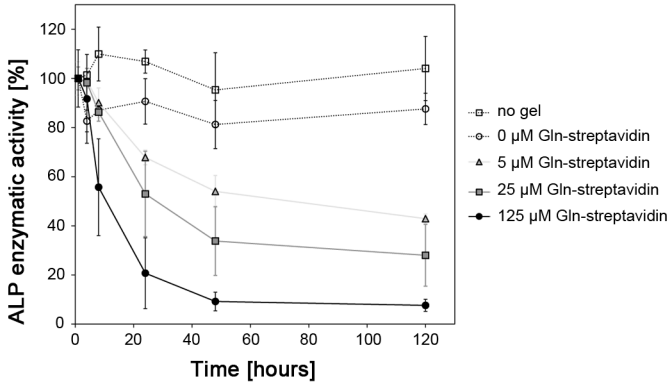

Figure 2.3. Streptavidin-modified hydrogels capture biotinylated proteins.

TG-PEG hydrogels containing 0, 5, 25 and 125 µM Gln-streptavidin were incubated in a solution containing ALP-biotin. The enzymatic activity of ALP-biotin in the solution was measured after 1, 4, 8, 24, 48 and 120 hours of incubation with the hydrogels via SEAP assay.

2.2.3 Biotinylation of BMP-2

Protein engineering not only is a labor-, time- and cost-intensive process, but is also associated with the risk of loss of functionality and stability by the proteins upon modification. It is thus tempting to speculate that this holds especially true for proteins like BMP-2, which in their native form can only be stably dissolved at higher concentrations than 200 nM at a low pH or in presence of chaotropic agents. For such proteins, biotinylation by commercially available bi-functional chemical linkers can be readily applied in a broad range of buffer conditions, which can be adjusted to the protein specific requirements, and is a straightforward alternative to modification by genetic engineering.

To generate fully functional rhBMP-2-biotin, commercially available amine-specific NHS-PEG4-Biotin was employed. Since the solubility of rhBMP-2 is relatively limited at physiological pH,[137] and the number of biotins per BMP molecule is inversely related to its biological function,[138] biotinylation was first tested at different molar ratios, reaction durations and pH conditions. As expected, the degree of biotinylation decreased with the reduction of molar ratio (NHS-PEG4-Biotin:protein), time, and pH (from 8.0 to 6.5) as determined by western blot analysis (**Figure 2.4**A, C). To determine the influence of biotinylation on the biological activity, preparations of the above-generated rhBMP-2 with variable incubation time and degree of biotinylation (**Figure 2.4**B, D) were employed to stimulate immortalized murine myoblastic C2C12 cells.

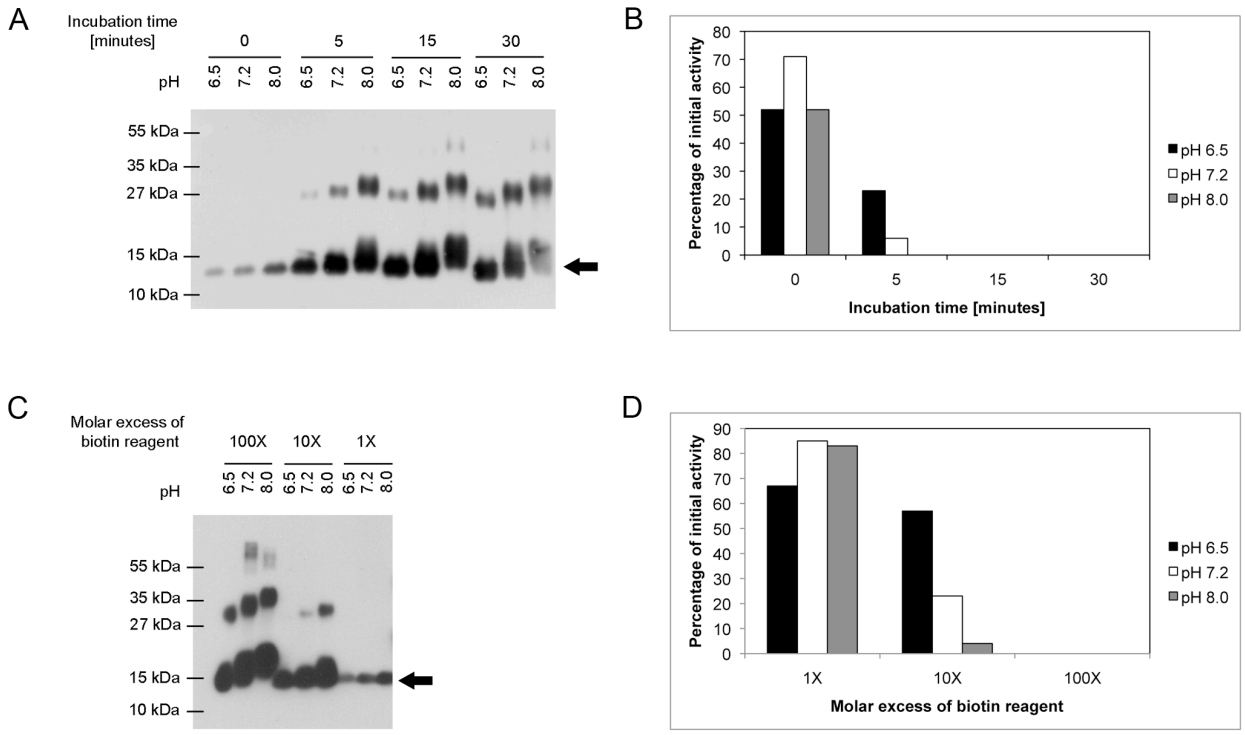

Figure 2.4. The rhBMP-2 biotinylation degree of depends on pH, time and molar ratio of biotin and influences its biological activity.

(A, C) rhBMP-2 was biotinylated at different incubation times or molar ratios of biotin reagent. Biotinylation was assessed by Western blotting. The black arrows indicate the bands representing rhBMP-2-biotin. A slight shift in molecular weight can be observed depending on the degree of biotinylation. (B, D) The biological activity of rhBMP-2 biotinylated at different incubation times and molar ratios of biotin was assessed on C2C12 cells with the ALP activity assay.

These cells upon stimulation with BMP-2 differentiate towards the osteogenic lineage, change their morphology from spindle-shaped to a cuboidal morphology, and in an almost linear dose-response curve increase the expression of alkaline phosphatase [139], making them a valuable tool to quantify the fraction of functional BMP. In agreement with previously published data by Hu et al.,[140] initial evaluations indicated that only a low degree of BMP-2 biotinylation was compatible with a high residual bioactivity, whereas higher degrees of biotinylation even resulted in

a complete loss of bioactivity (**Figure 2.4**D). Thus, final biotinylation of BMP-2 was performed for 30 minutes with a 1:2 molar excess of NHS-PEG4-Biotin at pH 6 and the obtained rhBMP-2-biotin retained almost 98% of its original biological activity, and was thus comparable to that of rhBMP-2 (**Figure 2.5**).

The level of biotinylation as quantified ranged between 3.7-3.9 moles of biotin per mole of dimeric rhBMP-2. Due to the lower pKa (7.6 to 8.0) of N-terminal α-amines than the one of α-amino group of lysine (10.0–10.2),[141] it can be assumed that under the chosen biotinylation conditions a substantial number of modifications are localized to the N-terminus. This is also consistent with the achieved high functionality of BMP-2-biotin and the observed number of modifications (approximately 4 moles of biotins per mole of dimeric BMP-2) under moderate pH (7.0) conditions, low molar excess of NHS (2-fold over BMP-2) and reaction time of 30 minutes.

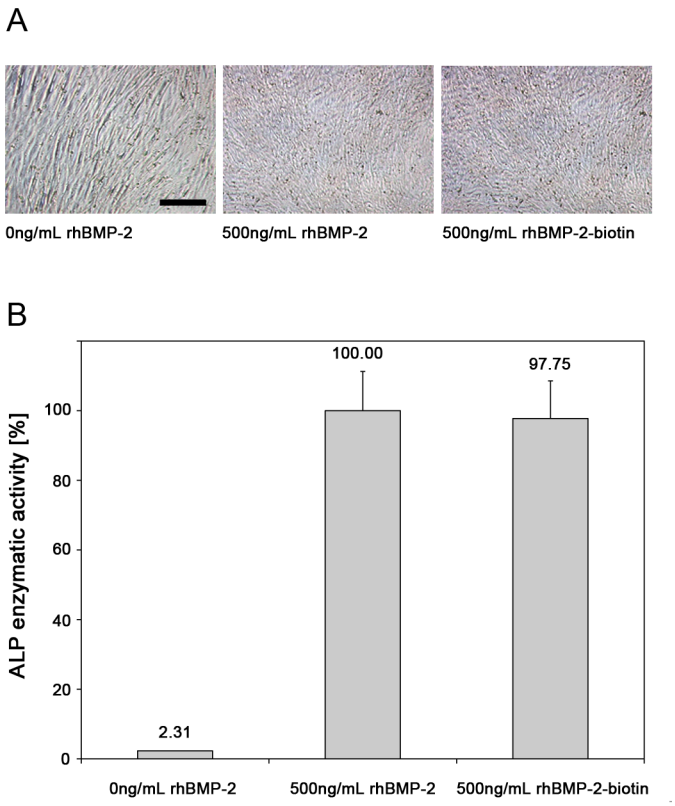

Figure 2.5. The biotinylation process was optimized for maximal functionality of rhBMP-2-biotin.

C2C12 cells were stimulated with 500 ng·mL^{-1} of either rhBMP-2 or rhBMP-2-biotin and the ALP activity was measured after 7 days in culture. (A) C2C12 cells exposed to rhBMP-2 or rhBMP-2-biotin assumed a cuboidal morphology compared to the spindle-shaped control C2C12 cells (scale bar = 250 μm). (B) Cells stimulated with rhBMP-2-biotin showed 98% of ALP enzymatic activity when compared to the enzymatic activity measured with rhBMP-2 stimulation.

2.2.4 Binding and release of rhBMP-2-biotin from Gln-streptavidin hydrogels

Next, we aimed at determining whether streptavidin-modified hydrogels could specifically capture rhBMP-2-biotin and whether the captured proteins remained bound to the gel over time. Therefore, 20 µL-sized TG-PEG hydrogel discs containing 0 or 100µM Gln-streptavidin were immersed in 200 µL cell culture medium, containing 250 ng·mL-1 rhBMP-2-biotin or rhBMP-2. BMP-2 ELISA measurements reveal that from the initial amount of rhBMP-2-biotin in the immersion solution 87.95% were captured by the streptavidin-modified hydrogel (13.05 % remained in solution) and even by thorough washing steps were not released. In contrast, after incubation with streptavidin linker-free hydrogels 84.19% of the rhBMP-2-biotin remained unbound and during washing steps most of the hydrogel-bound rhBMP-2-biotin was released (**Figure 2.6**). Together, these data show that streptavidin-modified TG-PEG hydrogels bind rhBMP-2-biotin with high specificity while streptavidin linker-free hydrogels indicate weak unspecific binding.

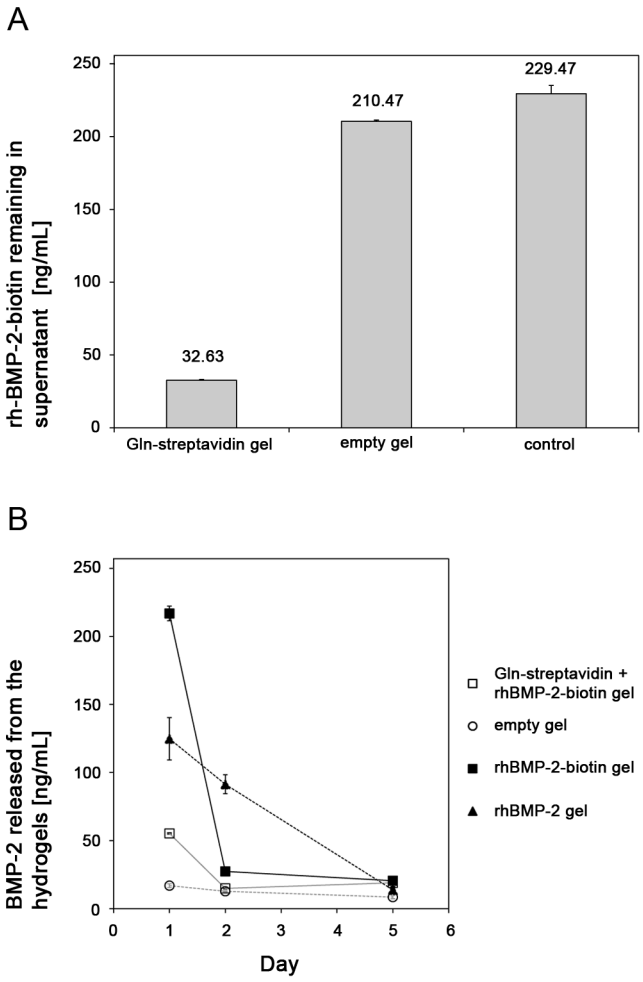

Figure 2.6. Uptake and release of rhBMP-2 from streptavidin-modified gels.

Hydrogels containing 0 or 100 µM Gln-streptavidin linker were incubated in a 250 ng·mL^{-1} solution of rhBMP-2-biotin at 4°C overnight. (A) RhBMP-2-biotin remaining in solution was determined by ELISA. A reaction tube containing the rhBMP-2-biotin solution but no hydrogel served as a control. (B) The release of rhBMP-2-biotin from the same hydrogels was measured over a

period of 5 days and compared to the BMP-2 release from streptavidin linker-free hydrogels containing soluble rhBMP-2 or rhBMP-2-biotin. The concentration of released BMP-2 was determined by ELISA. Data are presented as mean ± SD (n=3).

2.2.5 Osteogenic differentiation of C2C12 cells on hydrogels with immobilized BMP-2

The bioactivity of hydrogel-captured rhBMP-2-biotin was validated by differentiating C2C12 cells on BMP-2-presenting hydrogels towards the osteogenic lineage in an MSC-like process.[139] C2C12 cells were cultured for 5 days on top of TG-PEG hydrogels that contained 250 ng·mL-1 immobilized rhBMP-2-biotin on the surface, or throughout the bulk of the material by incorporating the growth factor together with Gln-streptavidin directly in the gel. Alongside, empty hydrogels (containing no Gln-streptavidin linker) with or without rhBMP-2-biotin added to the cell culture medium, and hydrogels with only the Gln-streptavidin linker were also formed as control conditions. Osteogenic differentiation in response to matrix-mediated BMP-2 presentation was assessed by colorimetric staining of ALP expressing cells of using 5-bromo-4-chloro-3-indolylphosphate (BCIP)/nitro blue tetrazolium (NBT).

The hydrogels presenting immobilized rhBMP-2-biotin contained differentiated cell clusters, which stained positive for ALP, whereas such staining was not observed in control conditions (**Figure 2.7**). Enzymatic ALP activity of cells stimulated with immobilized biotinylated rhBMP-2 was comparable to the one of cells stimulated with the soluble growth factor (84% of the enzymatic activity). Furthermore, binding of rhBMP-2-biotin to the PEG hydrogels was confirmed to be a specific interaction as seen in the binding and release study. Indeed, cells seeded on the empty hydrogel that had been incubated with rhBMP-2-biotin were not stimulated, indicating that the growth factor can be efficiently washed away. Also, the cells cultured on top of the gels containing only the Gln-streptavidin linker did not show any significant sign of ALP expression, excluding any effect due to the linker itself.

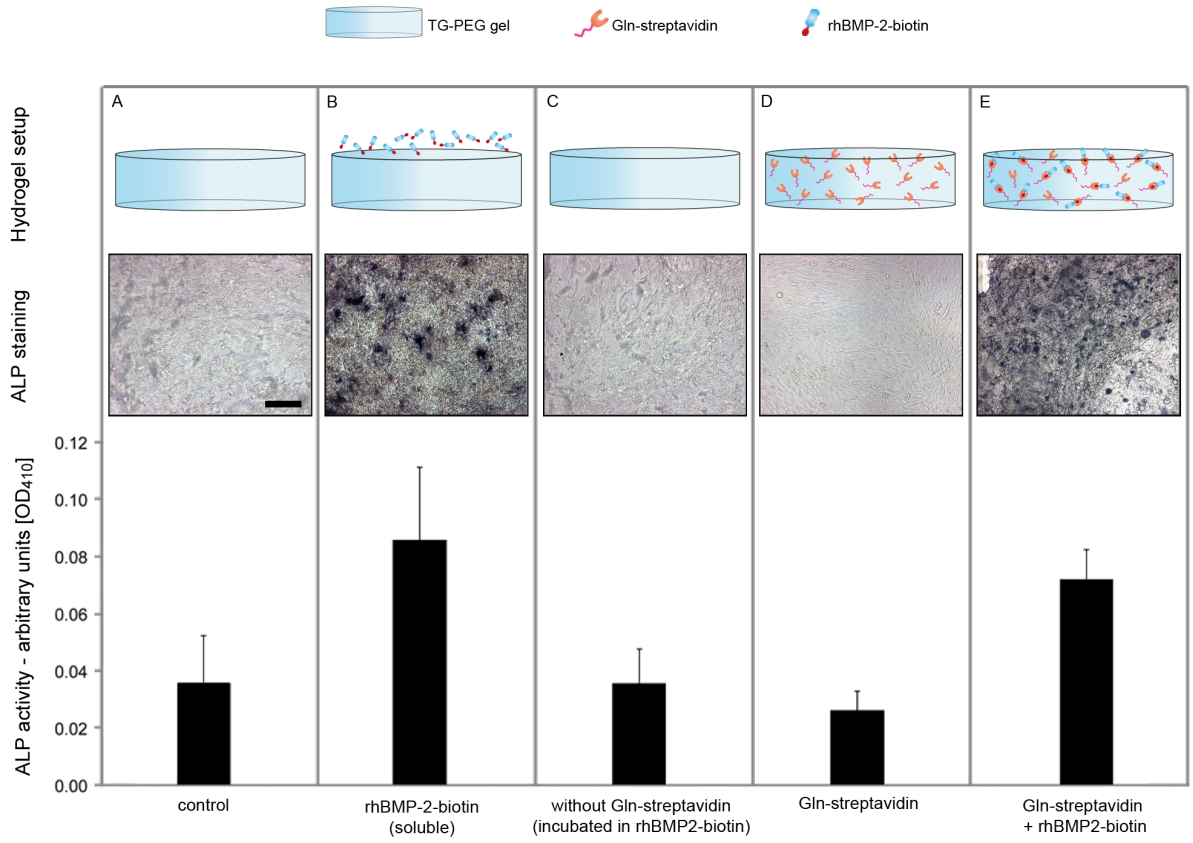

Figure 2.7. Differentiation of C2C12 cells on streptavidin-modified hydrogels.

C2C12 cells were cultured atop PEG hydrogels with or without immobilized rhBMP-2-biotin for 7 days and then assessed for ALP expression. The cells were either stimulated with soluble rhBMP-2 in the medium (B) or rhBMP-2-biotin bound to streptavidin-modified hydrogels (E). Additionally, cells were seeded on Gln-streptavidin linker-free hydrogels, which had been incubated with rhBMP-2-biotin and then washed (C), as well as on hydrogels containing only Gln-streptavidin (D). Cells seeded on an empty gel served as control. ALP expression was evaluated through colorimetric staining with the BCIP/NBT substrate solution and with ALP activity assay. Scale bar = 250; data are presented as mean ± SD (n=6).

2.2.6 Localized 3D osteogenic differentiation of mesenchymal stem cells

The ability of hydrogel-captured rhBMP-2 to specifically and locally induce the differentiation of either the C2C12 cell line or mesenchymal stem cells towards the osteogenic lineage was investigated by forming 3D-structured hydrogels which contained no, soluble or matrix immobilized rhBMP-2-biotin.

Localization of rhBMP-2 inside TG-PEG constructs was achieved by forming a small 5 µL PEG hydrogel containing 100 µM Gln-streptavidin and 5 µg·mL-1 rhBMP-2-biotin. This gel (inner gel) was then embedded in a bigger 20 µL PEG gel (outer gel) that contained no linker or growth factor (**Figure 2.1**B). Both gels contained equal concentrations of C2C12 cells, which were either incorporated as single cells or as cell spheroids. The importance of having bound growth factors was assessed with hydrogel constructs containing soluble rhBMP-2-biotin in the inner hydrogel without

Gln-streptavidin linker and looking at the cell differentiation. The constructs were then cultured for 9 days, so that the C2C12 cells in presence of rhBMP-2-biotin could differentiate towards the osteogenic lineage. As can be seen with BCIP/NBT staining (**Figure 2.8**A), cells exposed to the unbound rhBMP-2 showed only weak signs of ALP activity, whereas the cells presented with the bound rhBMP-2 environment expressed significant amounts of ALP. In addition, in the case of the unbound growth factor, cells both on the inner gel and the outer gel showed a very weak but similar staining for ALP, indicating that rhBMP-2 is diffusing out of the inner gel to the rest of the construct. In contrast, when rhBMP-2-biotin is bound via Gln-streptavidin, a strong localization of the differentiation pattern can be observed. These results could be observed in the case of single cells and cell spheroids.

Immunostaining of the cell spheroids furthermore revealed that there was a clear boundary between the differentiated and non-differentiated cells. C2C12 cells contained in the inner gel with the bound rhBMP-2-biotin expressed ALP throughout the bulk of the gel, whereas the cells located in the outer gel showed no staining for ALP with exception for a few cells located very close to the inner gel. Regarding the single cell experiment, the fluorescent signal after immunostaining was too low to detect any differences between the cells from the inner and outer gel, although these same cells showed localized differentiation with the colorimetric staining.

Finally, BM-MSCs, which crucially contribute to the biological healing of bone and other tissues, were locally differentiated by matrix-immobilized BMP-2-biotin. When single dispersed BM-MSCs were encapsulated in the hydrogels containing immobilized BMP-2 for up to 9 days, expression of ALP was insufficient to be detected with BCIP/NBT staining or immunostaining (data not shown). However, a localized cell differentiation could be achieved successfully with BM-MSCs spheroids. As shown in **Figure 2.8**B, a strong staining showing a clear limit between the ALP expressing cells in the BMP-2-presenting areas and the non-differentiated cells in the surrounding areas could be seen.

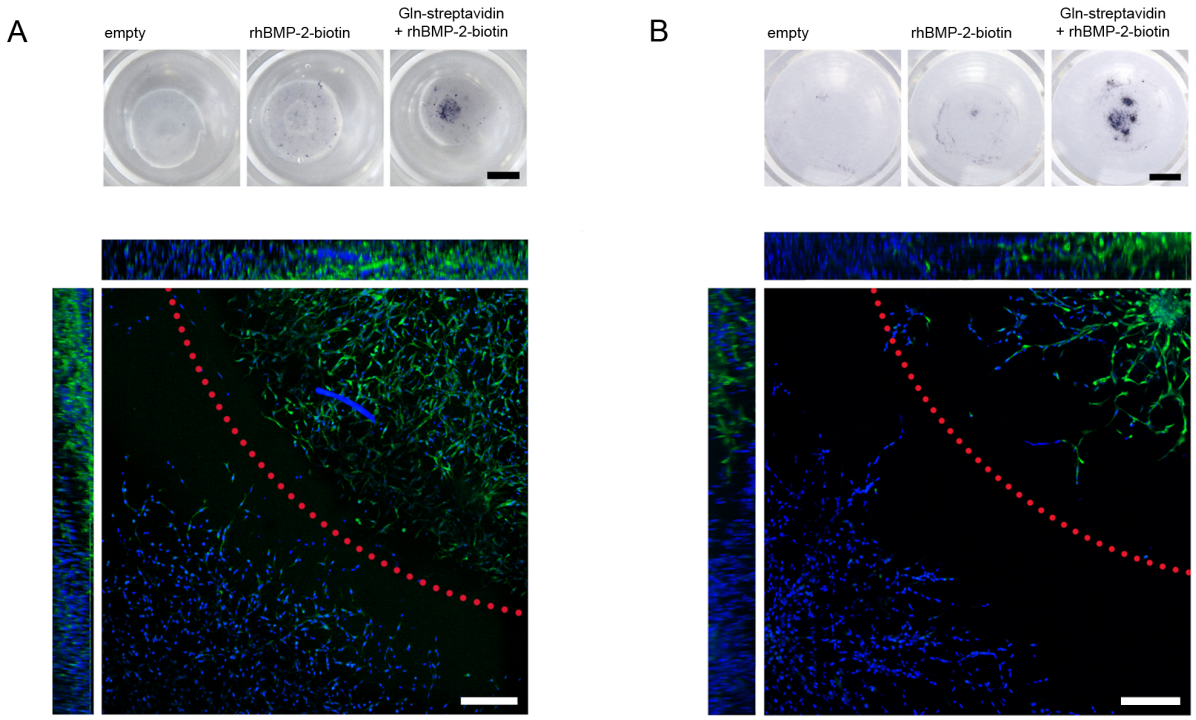

Figure 2.8. C2C12 cells and BM-MSCs could be locally differentiated with immobilized rhBMP-2-biotin.

PEG hydrogel constructs containing C2C12 cells (A) and BM-MSCs (B) were cultured for 9 days in TG-PEG hydrogel constructs containing a central area presenting either no, soluble or immobilized rhBMP-2-biotin. ALP expression was assessed via the colorimetric BCIP/NBT substrate staining (upper row, scale bar = 2 mm). The expression of ALP was confirmed by immunostaining (lower row, blue: nucleus, green: ALP, scale bar = 200 µm, xy axis in the main panel, xz and yz in the side panels).

To better understand the disparity between the ALP staining in BM-MSCs as single cells and as spheroids and to confirm the change in mRNA expression, an early osteogenic marker, Runt-related transcription factor 2 (Runx2) and the later osteogenic marker ALP[142] were assessed by quantitative real-time polymerase chain reaction (**Figure 2.9**). Expression levels of Runx2 in BM-MSCs after 9 days of culture and stimulation with various concentrations of rhBMP-2 were not significantly upregulated (**Figure 2.9**A). However, ALP expression levels correlated with concentrations of soluble rhBMP-2 (**Figure 2.9**B). Expression levels of ALP in response to 100 ng·mL-1 of soluble rhBMP-2 were stimulated in BM-MSCs, which were cultured as single dispersed cells (ca. 36-fold) and as micro-tissues (ca. 3-fold) (**Figure 2.9**C). In contrast, for equal amounts of bound rhBMP-2-biotin ALP expression was not increased in single cells, while it showed a significant expression when cells were seeded as spheroids (ca. 6-fold), confirming our previous findings.

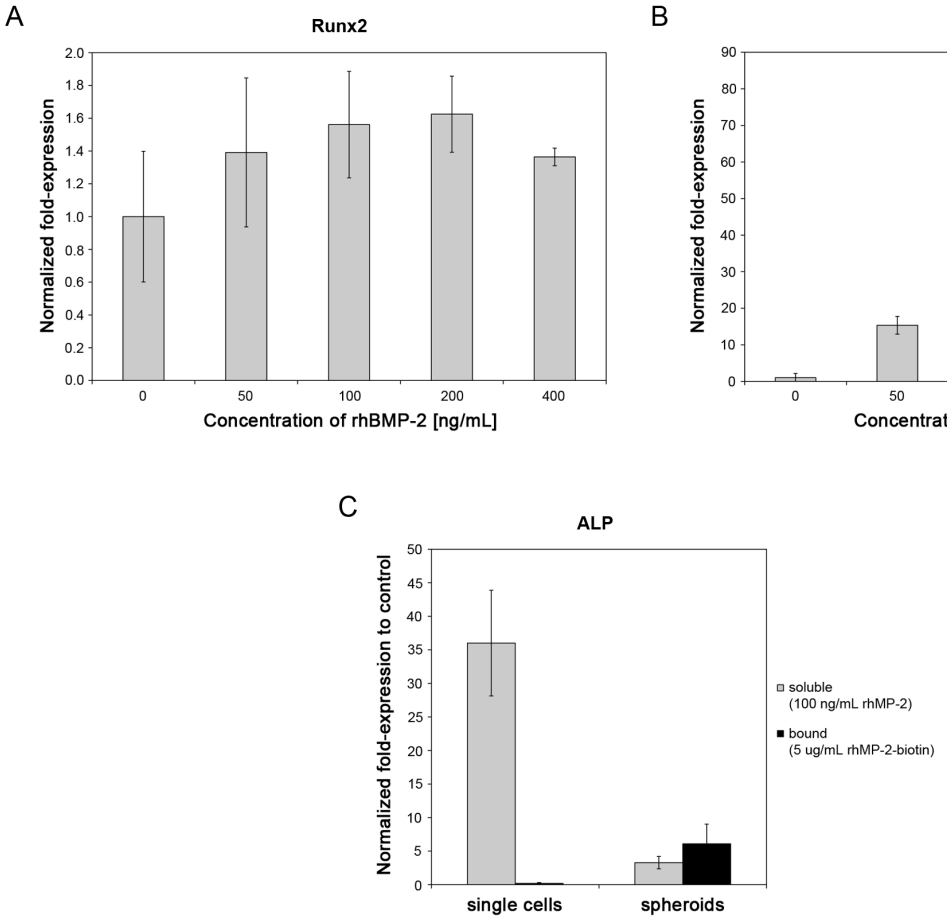

Figure 2.9. mRNA expression of two standard osteogenic markers.

BM-MSCs were seeded in TG-PEG hydrogels as single cells and stimulated with increasing concentrations of soluble rhBMP-2 supplemented to the culture medium. Expression levels of mRNA for Runx2 (A) and ALP (B) were measured via qPCR. (C) Expression levels of ALP mRNA were compared between BM-MSCs present in the hydrogels as single cells or spheroids and in presence of soluble rhBMP-2 or rhBMP-2-biotin bound to the hydrogel via Gln-streptavidin.

The tethering of growth factors to the hydrogel matrix with high affinity (Kd of ~10^{-15} M) results in a repository only with a very limited release of the payload through dissociation. Thus, the availability of the immobilized growth factor will largely depend on the proteolytic degradation of the matrix backbone or the immobilization linker. This, in turn, will be the result of the cell secreted proteases and the proteolytic susceptibility of the hydrogel components. As the release of proteolytic enzymes in the vicinity of cell clusters is expected to be manifold higher than in the vicinity of single dispersed cells, the absence of ALP-activity in encapsulated single cells indicates limited availability of BMP-2 under these conditions. Furthermore, the significant increase in ALP activity in micro-tissues embedded in hydrogels containing bound BMP-2 indicates that cells are mainly stimulated by released BMP-2. Thus, tuning the release properties of BMP-2 by proteolytically sensitive streptavidin linker peptides could be a mean to control the release efficiency and consequently tailor the differentiation of tissue progenitor cells.

Bi-functional peptide linkers such as Gln-streptavidin represent an elegant way for the development of biomimetic scaffolds. In combination with similar linker peptides that recognize and bind different tags (such previously described Gln-ZZ linker[81] that allows the immobilization of Fc-tagged proteins), the controlled immobilization of several growth factors in distinct patterns becomes conceivable. This important feature is critical for the spatial control of cell behavior, which is normally regulated by the ECM.

2.3 Conclusion

We investigated the use of modular designed, streptavidin-modified PEG hydrogels for the controlled presentation of rhBMP-2 and the consequent 3D-localized differentiation of MSCs. This system was shown to be an alternative and efficient way to deliver bioactive molecules, which cannot be easily produced as engineered fusion proteins. As it is compatible with other modes of growth factor delivery biotin/streptavidin based immobilization of rhBMP-2 will provide a basis for the creation of 3D multi-factorial growth factor presentation and delivery as will be needed for the generation of more sophisticated tissue mimetics *in vitro*. The advantage of growth factors, which strongly interact with the matrix, would be their tightly controlled effect on differentiation of cells in confined areas while preventing their influence on other cell types and tissue areas.

Overall, this PEG-based BMP-2 delivery strategy holds great promise to become a printable ink which would be needed for example for the formation (by printing, microfluidics or direct molding) of distinct osteogenic areas during the *in vitro* creation 3D-bone-mimicking tissues.

Furthermore, this tool can be adapted for the controlled immobilization and tunable release of other growth factors and can be of high value for the development of specific cell-instructive bio-inks, which will ideally be designed to mimic ECM properties occurring in natural microenvironments. In future, the highly localized assembly of various cell types in their matched cell-instructive matrices holds great promise for the fabrication of 3D tissue mimetics, which recapitulate histoarchitectures of native tissues.

2.4 Experimental Section

Cloning of the Gln-streptavidin linker:

To construct plasmid pPL8 (PT7-α2PI1–8-Strep), the streptavidin sequence from pWW801 [143] was cloned (NheI/BamHI) into pPL19 [81], resulting in an expression vector for the Gln-streptavidin linker protein under control of the phage T7 promoter.

Production of the Gln-streptavidin linker:

Expression and purification of the Gln-streptavidin linker protein was adapted from Humbert et al. describing the production of T7-Tag mature streptavidin in E. coli [144]. In brief, pPL8 was transformed into E. coli Bl21-Gold(DE3) pLysS (Agilent Technologies, La Jolla, CA, USA) and pre-cultures were grown overnight at 37°C in 200 ml LB medium (Scharlab, S.L., Barcelona, ES) containing 60 µg·mL-1 carbenicillin and 34 µg·mL-1 chloramphenicol under orbital shaking (230 RPM). Main cultures of 1 L LB medium containing 60 µg·mL-1 carbenicillin, 34 µg·mL-1 chloramphenicol and 0.4% glucose were inoculated to OD600 = 0.1 and grown at 37°C under orbital shaking (230 RPM). Expression was induced with 1 mM IPTG at OD600 = 1.0 and cells were harvested three hours after induction by centrifugation (4'000 RPM, 4°C, 10 min). The cell pellet was resuspended in denaturing buffer (15 mL per 1 L initial culture volume, 6 M guanidium hydrochloride pH 1.5). Cell disruption was achieved by French press lysis (Thermo Fisher Scientific, Waltham, MA, USA) at 15'000 psi and cell debris were eliminated by centrifugation (14'000 RPM, 4°C, 60 min). The cell lysate was dialyzed (10'000 kDa MWCO, Thermo Scientific, Rockford, IL, USA) against denaturing buffer for 24 hours at room temperature, renaturing buffer (20 mM Tris-HCl pH 7.4) for 24 hours at room temperature, and dialysis against iminobiotin-binding buffer (50 mM Na2Co3 0.5 M NaCl pH 9.8) for 24 hours at 4°C. Protein precipitates were removed by centrifugation (47'000 x g, 30 min, 3°C) followed by filtration using a 0.45 µm filter and a 0.22 µm filter. Protein solution was loaded onto a 2-iminobiotin agarose column (I4507, Sigma-Aldrich, Switzerland) and washed with iminobiotin-binding buffer until no protein could be detected by measuring optical density at 280 nm in the eluted fractions. Bound protein was eluted with 5 column volumes elution buffer (0.1 M acetic acid pH 2.9) into 1.25 column volumes neutralization solution (2 M Tris-HCl pH 7.4). Pure protein was dialyzed against storage buffer (50 mM Tris-HCl pH 7.6) for 24 hours at 4°C and concentrated by ultrafiltration (10 kDa MWCO, Millipore, Carrigtwohill, IE). Protein was passed through a 0.22 µm syringe filter and stored at -80°C. Protein content was determined by A280 nm measurements. The FXIIIa-mediated coupling of Gln-streptavidin to 8-PEG-MMPsensitive-Lys was verified by Western blotting of reaction mixtures of both components in presence or absence of FXIIIa. A rat anti-mouse IgG-biotin (eBioScience, Switzerland) followed by a goat anti-rat IgG-HRP (Life Technologies, Switzerland) were used for detection.

Formation of hydrogels:

TG-PEG hydrogels were formed by FXIIIa cross-linking of equimolar blends of two 8-arm PEG macromeres (8-PEG-MMPsensitive-Lys and 8-PEG-Gln) as previously described [74, 75]. Briefly, FXIII (200 U·mL-1, Fibrogammin P, CSL Behring, Switzerland) was activated with thrombin (2 U·mL-1, Sigma-Aldrich, Switzerland) for 30 minutes at 37°C and stored in small aliquots at -80°C. Stoichiometrically balanced solutions of 8-PEG-Gln and 8-PEG-MMPsensitive-Lys were prepared in 50 mM Tris, pH 7.6 buffer containing 50 mM calcium chloride. Precursor solutions for hydrogels with a final dry mass content of 1.7, 2 or 5% TG-PEG were prepared leaving a spare volume of 12.5% v/v for the addition of growth factors, RGD and linker peptides. The cross-linking reaction was initiated by addition of 10 U·mL-1 FXIIIa followed by vigorous mixing. Disc-shaped matrices were obtained by sandwiching the liquid reaction mixtures between sterile hydrophobic glass microscope slides (treated with SigmaCote, Sigma-Aldrich, Switzerland) separated by 1 mm thick spacers, clamped with binder clips and incubated for additional 30 minutes at 37°C.

Binding of biotinylated alkaline phosphatase to the Gln-streptavidin linker:

The Gln-streptavidin linker was incorporated into 20 µL PEG (2% w/v) hydrogels via FXIIIa cross-linking to final concentrations of 0, 5, 25 and 125 µM. The polymerized gels were then incubated in Eppendorf tubes containing 500 µL of Tris Buffered Saline (TBS; 50 mM Tris, 150 mM NaCl, pH 7.6) and left on a shaker at 4°C overnight to wash out any unbound linker. Gels were transferred to Eppendorf tubes containing 5.5 µg·mL-1 biotinylated alkaline phosphatase (ALP) (Thermo Scientific, Switzerland) in 500 µL TBS and incubated at 4°C for 5 days. Buffer samples of 20 µL were taken from the tubes after 1, 4, 8, 24, 48 and 120 hours and the remaining content of biotinylated ALP was quantified with the secreted alkaline phosphatase (SEAP) assay.

SEAP assay:

For each sample, 1 µL of buffer containing biotinylated ALP was diluted in 80 µL TBS. 100 µL of assay buffer (20 mM L-homoarginine, 1mM CaCl2, 21% diethanolamine, pH 9.8) were mixed with 20 µL of 120 mM p-nitrophenyl phosphate (diluted in assay buffer) and then added to 80 µL of diluted samples or TBS (blank) in a 96-well plate. Absorbance was measure at 405 nm every minute for 15 minutes in a microplate reader (Synergy HT, Bio-Tek Instruments, Switzerland). The absorbance was plotted against time and slope of each curve was determined. Enzymatic activity was calculated by subtracting the slope value of the blank from all other slope values and multiplying by the constant 256.8 (calculated from the Beer-Lambert law) and the dilution factor.

Biotinylation of BMP-2:

Dimeric rhBMP-2 was produced as previously described [145]. RhBMP-2 was biotinylated using EZ-Link NHS-PEG4-Biotin reagent (No Weigh™ Format, Thermo Scientific, Switzerland) according to the manufacturer's guidelines. The reaction was carried out in 20 mM HEPES, 6M urea at pH 7.2 with a 2-fold molar excess of biotin reagent for 30 minutes on ice. The reaction was stopped by the addition of the same volume of 50mM Tris, pH 7.6 buffer. Finally, rhBMP-2-biotin was dialyzed (Spectra/Por 3, MWCO 3500, Spectrum Laboratories, Germany) against 20 mM HEPES, 6M urea at pH 7.2 for 2 days at 4°C to remove any excess un-reacted biotin reagent. Biotinylation of rhBMP-2 was verified by Western blot. 500 ng of rhBMP-2 and rh-BMP-2-biotin were separated on a 15% SDS-PAGE gel and transferred to a nitrocellulose membrane (Protran® Nitrocellulose Transfer Membranes, Schleicher & Schuell, Germany). The membrane was incubated with 1% dry milk, 0.1% Triton X-100 in TBS overnight at 4°C. After washing (3 x 5 minutes) in TBS, the membrane was incubated with anti-biotin-POD (Fab Fragments, Roche, Switzerland) at a 1:200 dilution in TBS for 1 hour at room temperature. After washing, detection was performed with ECL™ Western Blotting Detection Reagents (GE Healthcare, United Kingdom).

Quantification of the biotinylation was performed with Pierce® Biotin Quantitation Kit (Thermo Scientific, Switzerland) using the manufacturer's protocol. Biotinylated ALP was used as a standard to determine the number of moles of biotin per mole of rhBMP-2.

Uptake and release of rhBMP-2 from Gln-streptavidin hydrogels:

For the uptake, 20 µL PEG hydrogels (5% w/v) were formed with 0 or 100 µM of Gln-streptavidin linker. The polymerized gels were then incubated in Eppendorf tubes with 500 µL TBS and left on a shaker at 4°C overnight to wash out any unbound linker. Gels were then transferred to Eppendorf tubes containing 200 µL TBS with or without rhBMP-2-biotin at 250 ng·mL-1 and incubated on a shaker at 4°C overnight. As a control, an Eppendorf tube with 200 µL TBS containing 250 ng·mL-1 rhBMP-2-biotin was incubated along without any gel.

For the release, the gels were retrieved and placed in an Eppendorf tube containing 200 µL Dulbecco's modified Eagle's medium (DMEM). Additionally, 20 µL PEG hydrogels (5% w/v, streptavidin linker-free) containing 50 ng of either rhBMP-2 or rhBMP-2-biotin were formed and also placed in Eppendorf tubes with 200 µL DMEM. The medium was then collected and replaced with fresh medium each day during 5 days. The concentration of rhBMP-2 and rh-BMP-2-biotin remaining in the buffer and medium was quantified via ELISA.

ELISA of BMP-2:

ELISAs were performed using the Human BMP-2 ELISA Development Kit (PeproTech, United Kingdom) according to the manufacturer's guidelines. Samples and standard solutions were diluted in DMEM. The standard curve was established with the rhBMP-2 that was used for all other experiments.

Binding of biotinylated BMP-2 to Gln-streptavidin hydrogels: 40 µL PEG hydrogels (5% w/v) containing 50 µM Lys-RGD were formed with 0 or 100 µM of Gln-streptavidin. The polymerized gels were then incubated in Eppendorf tubes with 500 µL TBS and left on a shaker at 4°C overnight to wash out any unbound linker. Gels were transferred to Eppendorf tubes containing 500 µL TBS with or without rhBMP-2-biotin at 250 ng·mL-1 and incubated on a shaker at 4°C overnight. All hydrogels were finally washed for 48 hours in DMEM at 4°C with gentle shaking.

Cell culture:

All cells were cultured at 37°C in a humidified atmosphere at 5% CO2.

Myoblastic mouse C2C12 cells (ATCC® CRL-1772™) were maintained in DMEM supplemented with 10% fetal calf serum (FCS), 1% penicillin-streptomycin and 2mM L-glutamine. The cells were trypsinized and passaged every 2-3 days at 70% confluence. For differentiation assays, cells were cultured in differentiation medium (Minimum Essential Medium Alpha (MEMα) supplemented with 10% FCS, 1% penicillin-streptomycin and 50 µg·mL-1 L-ascorbic acid).

Bone marrow-derived mesenchymal stem cells (BM-MSCs) [146] were maintained in MEMα supplemented with 10% FCS, 1% penicillin-streptomycin and 5 ng·mL-1 bFGF. For differentiation assays, the cells were cultured in the same medium supplemented with 50 µg·mL-1 L-ascorbic acid.

Stimulation of C2C12 cells with rhBMP-2-biotin:

For comparing the biological activity of rhBMP-2-biotin to rhBMP-2, C2C12 cells were seeded in a 24-well plate at a density of 4 · 104 cells·cm-2 with 1 mL per well of differentiation medium. The cells were stimulated with 250 ng·mL-1 of either rhBMP-2 or rhBMP-2-biotin for 5 days and then processed for the measurement of ALP activity.

For immobilization of the rhBMP-2, PEG hydrogels containing 0 or 100 µM Gln-streptavidin were formed. They were then incubated in a solution of 250 ng·mL-1 rhBMP-2-biotin, at 4°C overnight. Biotinylated rhBMP-2 was also added directly in the hydrogel at concentration of 250 ng·mL-1, by incubating it first with the linker for 1 hour and then adding it directly to the hydrogel precursor solution before the onset of gelation. For all conditions, the hydrogels were washed for 48 hours in DMEM to remove any unbound protein. The PEG gels were then glued on the bottom of a 24-well plate and C2C12 cells were seeded on top of the gels at a density of 4 · 104 cells·cm-2. As a positive control, C2C12 cells were seeded on top of empty PEG hydrogel (containing no linker), and their culture medium was supplemented with either 0 or 250 ng·mL-1 rhBMP-2. The cells were cultured on the hydrogels for 5 days and then either stained with an ALP staining kit or lysed and further processed for measurement of ALP activity.

Alkaline phosphatase colorimetric staining and activity assay:

ALP staining was performed using SIGMAFAST™ BCIP®/NBT tablets (Sigma-Aldrich, Switzerland). Medium was removed from the wells and the cells were washed with PBS. To each well 500 µL of ALP substrate solution at dilutions recommended by the manufacturer was added. When visually sufficient color has developed in positive controls (5-10 minutes) the solution was replaced with PBS in all conditions and cells were imaged with a light microscope.

To measure ALP activity, the medium was removed from the wells and the cells were washed with PBS. For each well, cells were collected in 500 µL lysis buffer (0.56 M 2-amino-2-methyl-1-propanol, 0.2% Triton X-100, pH 10 in H2O) and homogenized for 1 minute. The cell lysate was centrifuged at 10'000 RPM for 10 minutes and the supernatant was collected. ALP reagent (20 mM 4-nitrophenyl phosphate disodium salt hexahydrate, 4 mM MgCl2 in lysis buffer) was added to the cell lysates in a 96-well plate and incubated at 37°C for 10-20 minutes before absorbance was measure at 410 nm with a microplate reader.

Local differentiation of cells in 3D and immunostaining of ALP:

Small 5 µL PEG gels (1.7 % w/v) containing 50 µM Lys-RGD and 10 µM Gln-Alexa Fluor® 546 and combinations of either 0 or 100 µM Gln-streptavidin linker, 0 or 5 µg·mL-1 rhBMP-2 and 0 or 5 µg·mL-1 rhBMP-2-biotin were formed with either single cells at the concentration of 0.2 · 106 cells·mL-1 or cell spheroids at 500 cells/spheroid. These gels were then embedded into 20 µL PEG gels (1.7% w/v) containing 50 µM Lys-RGD and cells, but no linker or growth factor. The gels were then glued to the bottom of a well plate and covered with the corresponding cell culture medium. Medium was replaced every day for C2C12 cells and every second day for BM-MSCs and cells were cultured for up to 9 days. The constructs were then stained for alkaline phosphatase, followed by fixation in 4% paraformaldehyde for 20 minutes and immunostaining. Cell nuclei were stained with DAPI and presence of ALP was

assessed with mouse anti-bone alkaline phosphatase primary antibody (Abcam, United Kingdom) at a 1:500 dilution and goat anti-mouse IgG H&L (Alexa Fluor® 488) secondary antibody (Abcam, United Kingdom) at a 1:1000 dilution.

RNA isolation and quantitative polymerase chain reaction for Runx2 and ALP:

BM-MSCs were seeded in 10 µL PEG hydrogels (1.7% w/v) containing 50 µM Lys-RGD, 100 µM Gln-streptavidin, with or without 5 µg·mL-1 rhBMP-2-biotin, either as single cells (1 · 106 cells·mL-1) or as spheroids (500 cells/spheroid). The cells were cultured with either 0, 50, 100, 200, 400 ng·mL-1 soluble rhBMP-2 in the medium or hydrogel-bound rhBMP-2-biotin for 9 days and then the hydrogels were dissolved with a 2 mg·mL-1 collagenase A solution (Roche, Switzerland) for 20 minutes on ice. Total RNA was extracted using the RNeasy kit (Qiagen, Switzerland). Reverse transcriptions were performed in 50 µL reactions using Transcriptor First Strand cDNA Synthesis Kit (Roche, Switzerland). Reactions were incubated for 10 minutes at 25°C, followed by 60 minutes at 50°C and finally 5 minutes at 85°C. After cDNA synthesis, reactions were frozen at −80°C. The resultant cDNA was subjected to real-time PCR with the corresponding gene-specific primers (Qiagen, Switzerland) using FastStart SYBR Green Master (Roche, Switzerland) and MyIQ detection system (Bio-Rad) according to the manufacturer's instructions.

2.5 References

[74] M. Ehrbar, S. C. Rizzi, R. G. Schoenmakers, B. S. Miguel, J. A. Hubbell, F. E. Weber, and M. P. Lutolf, *Biomacromolecules,* 2007, *8*, 3000.

[75] M. Ehrbar, S. C. Rizzi, R. Hlushchuk, V. Djonov, A. H. Zisch, J. A. Hubbell, F. E. Weber, and M. P. Lutolf, *Biomaterials,* 2007, *28*, 3856.

[77] A. Sala, P. Hanseler, A. Ranga, M. P. Lutolf, J. Voros, M. Ehrbar, and F. E. Weber, *Integr. Biol. (Camb),* 2011, *3*, 1102.

[81] P. S. Lienemann, M. Karlsson, A. Sala, H. M. Wischhusen, F. E. Weber, R. Zimmermann, W. Weber, M. P. Lutolf, and M. Ehrbar, *Adv Healthc Mater,* 2013, *2*, 292.

[114] W. Tan, and T. A. Desai, *Biomedical Microdevices,* 2003, *5*, 235.

[115] B. Derby, *Science,* 2012, *338*, 921.

[116] K. R. Stevens, M. D. Ungrin, R. E. Schwartz, S. Ng, B. Carvalho, K. S. Christine, R. R. Chaturvedi, C. Y. Li, P. W. Zandstra, C. S. Chen, and S. N. Bhatia, *Nat Commun,* 2013, *4*, 1847.

[117] D. Huh, G. A. Hamilton, and D. E. Ingber, *Trends Cell Biol,* 2011, *21*, 745.

[118] C. C. Lin, and K. S. Anseth, *Pharm Res,* 2009, *26*, 631.

[119] C. A. DeForest, and K. S. Anseth, *Annu Rev Chem Biomol Eng,* 2012, *3*, 421.

[120] K. S. Masters, *Macromol Biosci,* 2011, *11*, 1149.

[121] O. Jeon, C. Powell, L. D. Solorio, M. D. Krebs, and E. Alsberg, *J Control Release,* 2011, *154*, 258.

[122] K. Lee, E. A. Silva, and D. J. Mooney, *J. R. Soc. Interface,* 2011, *8*, 153.

[123] A. K. Silva, C. Richard, M. Bessodes, D. Scherman, and O. W. Merten, *Biomacromolecules,* 2009, *10*, 9.

[124] S. Tada, T. Kitajima, and Y. Ito, *Int J Mol Sci,* 2012, *13*, 6053.

[125] R. G. Wylie, S. Ahsan, Y. Aizawa, K. L. Maxwell, C. M. Morshead, and M. S. Shoichet, *Nat Mater,* 2011, *10*, 799.

[126] M. Ehrbar, R. Schoenmakers, E. H. Christen, M. Fussenegger, and W. Weber, *Nat Mater,* 2008, *7*, 800.

[127] M. M. Kampf, E. H. Christen, M. Ehrbar, M. Daoud-El Baba, G. Charpin-El Hamri, M. Fussenegger, and W. Weber, *Adv Funct Mater,* 2010, *20*, 2534.

[128] R. G. Wylie, and M. S. Shoichet, *Biomacromolecules,* 2011, *12*, 3789.

[129] A. I. Caplan, *J Cell Physiol,* 2007, *213*, 341.

[130] D. Marolt, M. Knezevic, and G. V. Novakovic, *Stem Cell Res Ther,* 2010, *1*, 10.

[131] Y. C. Chen, R. Z. Lin, H. Qi, Y. Yang, H. Bae, J. M. Melero-Martin, and A. Khademhosseini, *Adv Funct Mater,* 2012, *22*, 2027.

[132] O. Tsigkou, I. Pomerantseva, J. A. Spencer, P. A. Redondo, A. R. Hart, E. O'Doherty, Y. Lin, C. C. Friedrich, L. Daheron, C. P. Lin, C. A. Sundback, J. P. Vacanti, and C. Neville, *Proc Natl Acad Sci U S A,* 2010, *107*, 3311.

[133] M. Ehrbar, A. Sala, P. Lienemann, A. Ranga, K. Mosiewicz, A. Bittermann, S. C. Rizzi, F. E. Weber, and M. P. Lutolf, *Biophys. J.,* 2011, *100*, 284.

[134] C. M. Madl, M. Mehta, G. N. Duda, S. C. Heilshorn, and D. J. Mooney, *Biomacromolecules,* 2014, *15*, 445.

[135] N. M. Green, *Adv. Protein Chem.,* 1975, *29*, 85.

[136] S. Cosson, and M. P. Lutolf, *Methods Cell Biol,* 2014, *121*, 91.

[137] R. Ruppert, E. Hoffmann, and W. Sebald, *Eur J Biochem,* 1996, *237*, 295.

[138] H. Uludag, J. Golden, R. Palmer, and J. M. Wozney, *Biotechnol Bioeng,* 1999, *65*, 668.

[139] T. Katagiri, A. Yamaguchi, M. Komaki, E. Abe, N. Takahashi, T. Ikeda, V. Rosen, J. M. Wozney, A. Fujisawa-Sehara, and T. Suda, *J. Cell Biol.,* 1994, *127*, 1755.

[140] J. Hu, and W. Sebald, *Int J Pharm,* 2011, *413*, 140.

[141] S. S. Wong, *Chemistry of Protein Conjugation and Cross-Linking*. CRC Press, Boca Raton, FL, USA, 1991.

[142] P. Ducy, R. Zhang, V. Geoffroy, A. L. Ridall, and G. Karsenty, *Cell,* 1997, *89*, 747.

[143] W. Weber, J. Stelling, M. Rimann, B. Keller, M. Daoud-El Baba, C. C. Weber, D. Aubel, and M. Fussenegger, *Proc Natl Acad Sci U S A,* 2007, *104*, 2643.

[144] N. Humbert, P. Schurmann, A. Zocchi, J. M. Neuhaus, and T. R. Ward, *Methods Mol Biol,* 2008, *418*, 101.

[145] F. E. Weber, G. Eyrich, K. W. Gratz, R. M. Thomas, F. E. Maly, and H. F. Sailer, *Biochem Biophys Res Commun,* 2001, *286*, 554.

[146] O. Frank, M. Heim, M. Jakob, A. Barbero, D. Schafer, I. Bendik, W. Dick, M. Heberer, and I. Martin, *J Cell Biochem,* 2002, *85*, 737.

Chapter 3 *Engineered poly(ethylene glycol) matrices for cell-dependent proteolytic release of growth factors*

Adapted from:

S Metzger, U Blache, PS Lienemann, M Karlsson, FE Weber, W Weber, M Ehrbar, **Cell-mediated proteolytic release of growth factors from poly(ethylene) glycol matrices**, submitted for publication.

3.1 Introduction

In order to engineer functional tissues as faithfully as possible, various cell types need to be assembled in their specific 3D microenvironment. In living tissue, this microenvironment is determined by cell-cell as well as cell-matrix interactions, physical cues and soluble or matrix-immobilized biochemical cues comprising hormones, cytokines or growth factors.[27, 147, 148] Growth factors and cytokines (henceforth referred to only as growth factors) are proteins that regulate cell behavior and trigger cellular processes such as proliferation, migration or differentiation. Therefore, they are widely applied in tissue engineering to instruct cellular behavior in 3D scaffolds.[149] Importantly, distribution, availability and function of growth factors in living tissue are significantly modulated by their binding to the extracellular matrix (ECM). This results in the spatiotemporal and the physiologically relevant presentation of growth factors, which then interact with cell-surface receptors to influence cell behavior.[52, 150] Additionally during physiological or healing-induced tissue remodeling, participating cells degrade ECM components by the tightly regulated secretion and local activation of proteases or polysaccharide lyases, resulting in the release of matrix fragments and growth factors from the ECM "reservoir".[48, 151] Proteases that most significantly contribute to the ECM degradation belong to the families of matrix metalloproteinases (MMPs).[152, 153] These facts together with appreciation that adequate, engineering-compatible growth factor presentation strategies are required have encouraged the development of smart biomaterials that can mimic the ECM and present and/or release growth factors.[73, 122] In this regard, synthetic materials such as poly(ethylene glycol) (PEG) hydrogels have been used for the substitution of the naturally occurring ECM as they can be tailored toward specific requirements.[34, 154, 155] PEG hydrogels are synthetic matrices that are formed under chemically controlled conditions and are biocompatible,

biologically inert, besides offering a highly tunable platform in order to support cell growth. We have previously developed an enzymatically cross-linked PEG system in which eight-arm star-shaped PEG precursors, containing either a glutamine acceptor substrate (8-PEG-Gln) or a MMP-degradable lysine donor substrate (8-PEGMMP$_{sensitive}$-Lys), are cross-linked by the transglutaminase (TG) Factor XIII (FXIII) to form hydrogels.[74, 75] When functionalized with the adhesion peptide RGD, the resulting hydrogels were shown to be excellent *in vitro* platforms for 3D cell culture reaching from short-term culture of preosteoblastic cells to long-term microvascularized osteogenic tissue mimics.[77, 80, 133] Moreover, we have used this platform to functionally immobilized growth factors into the PEG matrix by stable or affinity-based immobilization.[75, 79, 81, 156] For instance, we have covalently incorporated a streptavidin linker consisting of an FXIII-substrate peptide (Gln-streptavidin) in TG-PEG hydrogels by FXIII cross-linking. By this we were able to locally immobilize biotinylated recombinant human bone morphogenetic protein-2 (rhBMP-2-biotin) via the Gln-streptavidin linker to PEG and obtained the corresponding localized osteogenic differentiation of human bone marrow-derived mesenchymal stem cells (hBM-MSCs).[79]

Although working, this system relies on a PEG hydrogel that contains a type I collagen-derived degradation sequence (GPQGIWGQ) sensitive to multiple MMPs, as it was previously optimized towards cell migration and spreading.[72, 157] Due to the relatively slow degradation kinetic of this sequence and the dependence of growth factor release on hydrogel degradation,[158] it is assumed that a significant portion of the immobilized BMP-2 remains inaccessible for the encapsulated cells, causing a dampening of the expected growth factor effect *in vitro*.

Here, we aimed at the decoupling of the hydrogel backbone properties from the mode of growth factor release in order to generate advanced modular building blocks that allow both more specific tailoring and the release of growth factors on cellular demand by proteases (**Figure 3.1**). Toward this goal, we selected the previously described peptide VPMSMRGG, being sensitive to MMP-1 and 2.[158, 159] Subsequently, we designed a new streptavidin linker consisting of a hydrogel immobilization Gln-sequence followed by three repetitions of the MMP-degradable sequence and a streptavidin domain, named Gln-M$_3$-streptavidin (**Figure 3.1**B). To characterize the new degradable streptavidin linker, we assessed its FXIII$_a$ mediated cross-linking to hydrogel backbone precursors as well as its degradability by proteases. We show that hydrogels modified with this new engineered streptavidin linker have the capacity to capture biotinylated proteins from cell culture medium and stably retain them under cell culture conditions. Streptavidin-modified hydrogels containing immobilized rhBMP-2-biotin could present the growth factor to C2C12 cells and hBM-MSCs and induce their osteogenic differentiation. Finally, higher enzyme activity of the osteogenic differentiation marker alkaline phosphatase (ALP) was achieved when rhBMP-2-biotin was presented by the new degradable Gln-M$_3$-streptavidin linker to cells, which shows the potential of a cell-responsive linker as a tool for the engineering of tissue mimetics.

3.2 Results and Discussion

3.2.1 Design of a proteolytically degradable streptavidin peptide linker

The previously developed streptavidin linker [79] is composed of a glutamine acceptor peptide fused to the N-terminus of a streptavidin monomer. This linker peptide can be covalently incorporated in TG-PEG hydrogels via $FXIII_a$ cross-linking and the streptavidin domain is used to bind biotinylated molecules with a strong affinity ($K_d \approx 10^{-15}$ M).[135] To design the new proteolytically degradable linker, three repeats of the protease cleavage site VPMSMRGG (sensitive to MMP-1 and MMP-2) selected from a list of peptide sequences tested for their MMP sensitivity[158, 159] were inserted in between these two domains, as illustrated in **Figure 3.1**B. The amino acid sequences of the non-degradable linker (Gln-streptavidin) and the new MMP-sensitive linker (Gln-M_3-streptavidin) are indicated in **Table 3.1**.

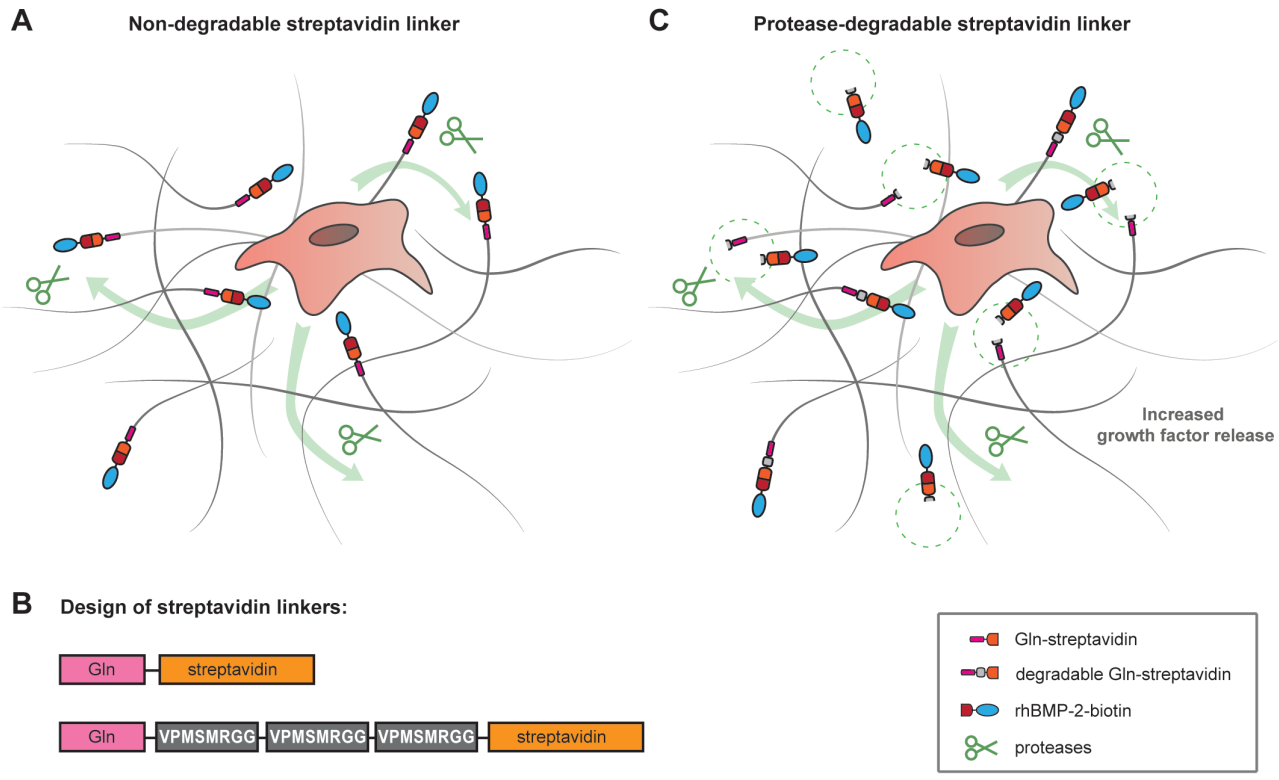

Figure 3.1. Rationale behind the design of the protease-degradable linkers.

A) 3D encapsulated cells by secretion and activation of proteases degrade the surrounding synthetic network and by matrix degradation release matrix immobilized growth factors. B) The protease-sensitive linker contains three repeats of a proteolytically degradable site between the $FXIII_a$ substrate sequence Gln and the streptavidin domain of Gln-streptavidin and was designed to be highly susceptible to MMP degradation. C) In slowly proteolytically degradable hydrogels such fast degradable linkers allow decoupling of growth factors and matrix degradation.

Linker Name	Size [kDa]	Proteolytic site	Sequence[1]
Gln-streptavidin	17.8	-	MNQEQVSPLAS*MTGGQQMGRDQEAGITGTWYNQLGSTFIVTAGA DGALTGTYESAVGNAESRYVLTGRYDSAPATDGSGTALGWTVAW KNNYRNAHSATTWSGQYVGGAEARINTQWLLTSGTTEANAWKST LVGHDTFTKVKPSAASIDAAKKAGVNNGNPLDAVQQGSL*
Gln-M_3-streptavidin	21.4	MMP-1, MMP-2	MNQEQVSPLASVD**VPMSMRGG**SVD**VPMSMRGG**SVD**VPMSMRG G**SVD*MTGGQQMGRDQEAGITGTWYNQLGSTFIVTAGADGALTGT YESAVGNAESRYVLTGRYDSAPATDGSGTALGWTVAWKNNYRN AHSATTWSGQYVGGAEARINTQWLLTSGTTEANAWKSTLVGHDT FTKVKPSAASIDAAKKAGVNNGNPLDAVQQGSL*

Table 3.1. Amino acid sequences of the streptavidin linkers.

(1) The glutamine acceptor substrate Gln indicated by a single underline, the proteolytically degradable sites are in bold and the streptavidin sequence is in italics and indicated by a dashed underline. Peptide orientation is from N-terminus to C-terminus.

3.2.2 Production and characterization of the degradable streptavidin linker

The linker was produced in Escherichia coli with yields varying between 5 and 20 mg per 1L of bacterial culture. Purification was carried out via biotin affinity chromatography, also ensuring the bioactivity of the streptavidin domain. The covalent cross-linking of the linker to the 8-PEG-$MMP_{sensitive}$-Lys component of the TG-PEG system was assessed via polyacrylamide gel electrophoresis (SDS-PAGE) and Western blot analysis of streptavidin. As shown in **Figure 3.2**A, a shift of the streptavidin linkers to higher molecular weight was detected when cross-linked to 8-PEG-$MMP_{sensitive}$-Lys by $FXIII_a$ indicating the successful incorporation of the linkers into the PEG component (the strong bands at 65 kDa in the Coomassie blue staining are caused by BSA used as carrier protein for $FXIII_a$). Next, we examined if the engineered streptavidin linker was indeed cleavable by MMP-1 and MMP-2. To answer this question we incubated the new linker as well as the non-degradable linker with the corresponding proteases and analyzed the degradation products via SDS-PAGE followed by Coomassie blue staining. After 1 hour of incubation with either 10 or 50 nM of MMP-1 or MMP-2, the Gln-streptavidin remained stable as no band shift is visible on the SDS-PAGE (**Figure 3.2**B).

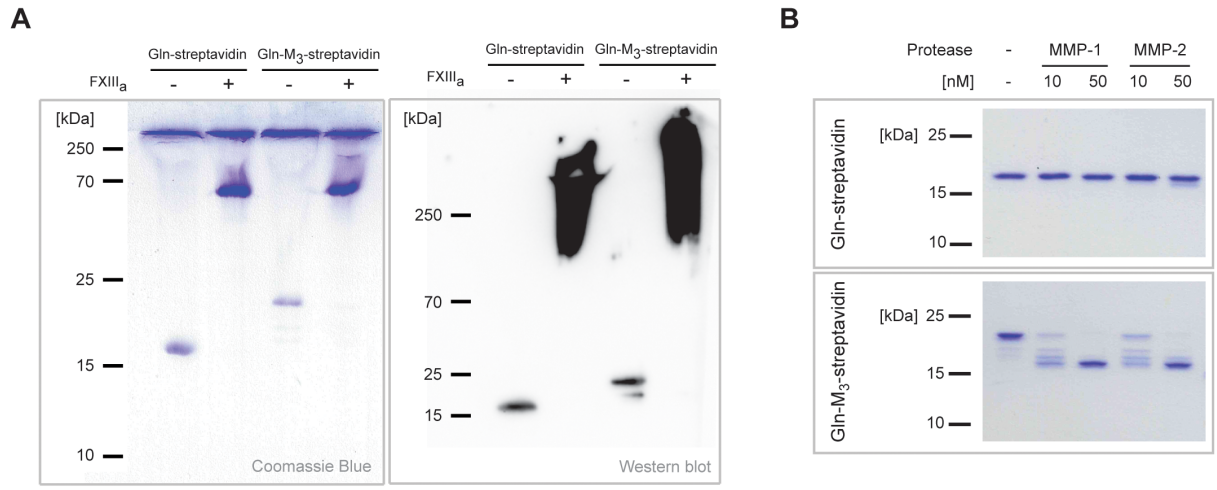

Figure 3.2. Characterization of the streptavidin linkers.

(A) The incorporation of the two different linkers into the PEG system by $FXIII_a$ was assessed via SDS-PAGE and Western blotting against streptavidin. Samples without or with $FXIII_a$ are indicated by - or + respectively. (B) The degradation of the linkers by the proteases MMP-1, MMP-2 (both at 10 or 50 nM) was assessed after 1 hour incubation via SDS-PAGE and Coomassie blue staining to detect the different degradation products.

Similarly, increasing the incubation time to 20 h did not lead to degradation of Gln-streptavidin by MMPs (**Figure 3.3**). In contrast, all MMP conditions resulted in the degradation of the MMP-sensitive Gln-M_3-streptavidin linker. More in detail, 50 nM of either MMP-1 or MMP-2 lead to the full cleavage of all three MMP-sensitive sites already after 1 h of incubation, resulting into a single band at 17.5 kDa. Interestingly, 1 h of incubation at lower MMP concentration (10 nM) revealed four different bands representing the original size of Gln-M_3-streptavidin at 21.5 kDa, the two intermediates containing two (19.5 kDa) or one (18.5 kDa) MMP-sensitive sites, and the final fragment lacking all three MMP-sensitive sites at 17.5 kDa (**Figure 3.2**B). However, all three MMP-sensitive sites were fully cleaved after 20 h of incubation with lower MMP concentration (**Figure 3.3**).

Taken together the degradation results reveal that Gln-M_3-streptavidin is as planned and designed sensitive to MMP-1 and MMP-2 whereas Gln-streptavidin is robust against MMPs.

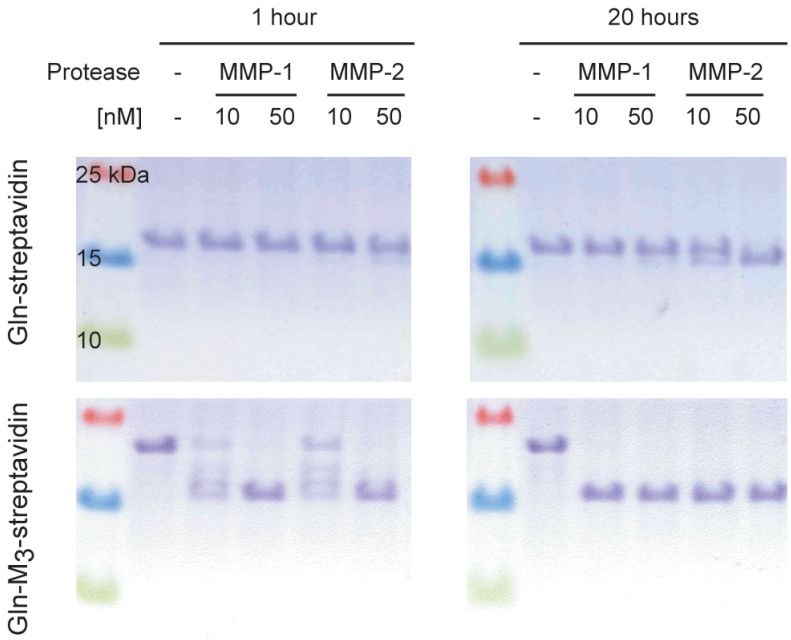

Figure 3.3. Proteolytic degradation of the streptavidin linkers over 1 and 20 hours.

The degradation of the linkers by the proteases MMP-1, MMP-2 (both at 10 or 50 nM) and plasmin (150 nM = 0.025 U mL^{-1}) was assessed after 1 hour and 20 hours incubation via SDS-PAGE and Coomassie blue staining to detect the different degradation products.

3.2.3 Binding of biotinylated proteins to streptavidin hydrogels

In order to demonstrate the biotin-binding ability of matrix-immobilized streptavidin linkers, TG-PEG hydrogels were prepared with both variants of streptavidin linkers (i.e. Gln-streptavidin and Gln-M_3-streptavidin) at 5 and 100 µM and incubated in a solution containing biotinylated alkaline phosphatase (ALP-biotin). To determine the fraction of hydrogel captured ALP-biotin, the ALP enzymatic activity remaining in the solution was quantified after 0, 1, 4, 8, 24, 48 and 120 hours. **Figure 3.4**A shows that ALP-biotin is captured faster and more extensively with 100 µM than with 5 µM for both types of linkers. Gln-streptavidin showed a faster and more efficient uptake of ALP-biotin than Gln-M_3-streptavidin. Although both variants possess the same streptavidin domain, the slight differences in uptake dynamics were found throughout all uptake experiments, indicating that flanking regions could have an effect on the streptavidin binding affinity. However, the concentration of streptavidin linker (5 or 100 µM) had far less influence on the binding of ALP-biotin if the biotinylated molecule was coupled to the linkers (in a 1:2 or 1:40 molar ratio respectively) in advance by a pre-incubation step before being incorporated into the hydrogel. Here, total release of ALP-biotin from hydrogels was assessed over a period of 7 days, with or without the streptavidin linkers (**Figure 3.4**B). Almost the entirety of the immobilized ALP-biotin remained bound to the hydrogels when it was coupled to either one of the streptavidin linkers, independently of the linker concentration, whereas ALP-biotin was almost completely released into the surrounding buffer in absence of linker. This shows that the linkers have very comparable binding

efficacy when there is a pre-incubation step with biotinylated molecule and that they are capable of immobilizing it very efficiently in non-proteolytic conditions.

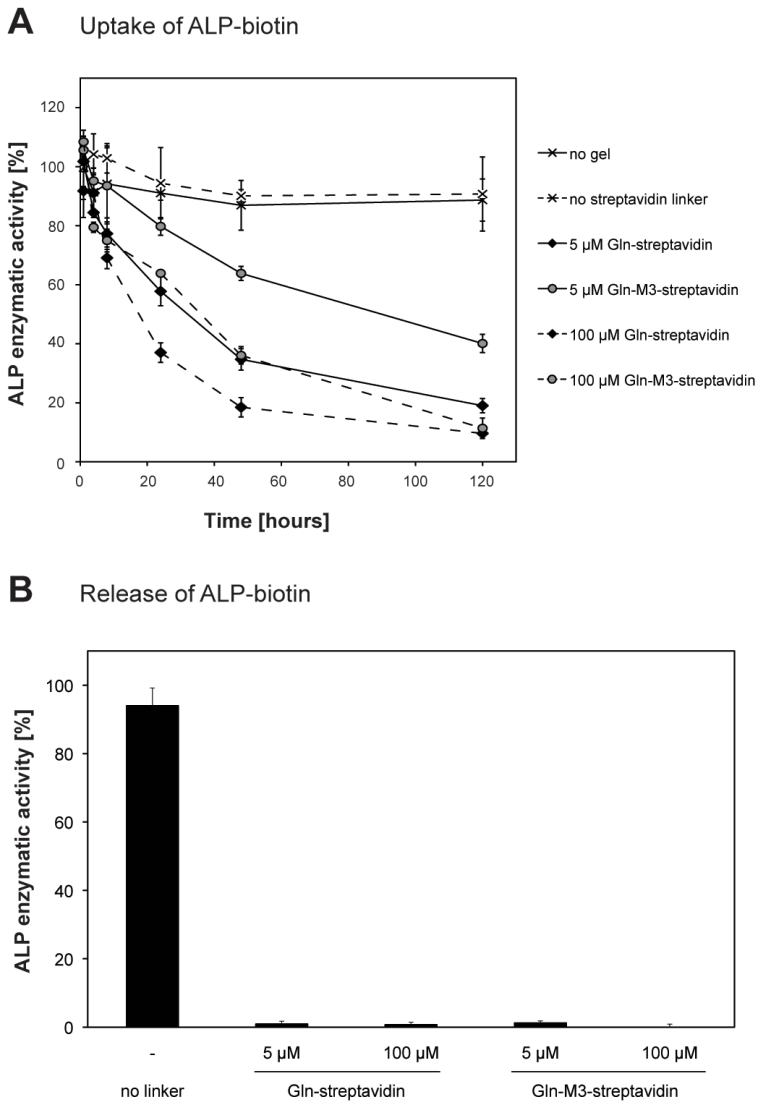

Figure 3.4. Uptake and release from streptavidin hydrogels.

(A) Uptake of biotinylated ALP by streptavidin-modified hydrogels. TG-PEG hydrogels containing 5 or 100 µM of linker were incubated in a solution containing ALP-biotin. The enzymatic activity of the remaining ALP-biotin in the solution was measured with the SEAP assay over a period of 5 days and compared to the initial enzymatic activity at the start of the experiment. Error bars represent standard deviation, n = 4. (B) Release of immobilized ALP-biotin from streptavidin-modified hydrogels. The release of ALP-biotin incorporated in TG-PEG hydrogels containing the different streptavidin linkers was assessed in Tris buffer after a period of 7 days. Error bars represent standard deviation, n = 3.

3.2.4 Release of rhBMP-2-biotin from streptavidin hydrogels

To test the functionality and efficiency of this immobilization strategy for tissue engineering applications, we chose to use a model of osteogenic differentiation of myoblastic and mesenchymal stem cells by BMP-2 in 3D TG-PEG hydrogels. To this end, we first evaluated the immobilization efficiency of rhBMP-2, which was biotinylated as previously described[79] and immobilized into PEG hydrogels via the different streptavidin linkers. In the following experiments, rhBMP-2-biotin was directly coupled to the streptavidin linker by incubating both components for 30 minutes at room temperature before their incorporation in the TG-PEG hydrogel mix. In detail, 5 µM of streptavidin linker and 50 ng of rhBMP-2-biotin (approximately 25-fold molar excess of streptavidin ensures sufficient binding efficacy) were incubated before incorporating the rhBMP-2/streptavidin complex into TG-PEG hydrogels. Hydrogels were then incubated in a microcentrifuge tube containing 500 µL of Tris buffer with 0.5% BSA for up to 7 days. Subsequently, we confirmed the successful immobilization of rhBMP-2-biotin by measuring non-bound and therefore diffused/released rhBMP-2 via ELISA. In the case of a 100% release into the buffer or medium, the expected rhBMP-2-biotin concentration is approximately 100 ng mL^{-1}. As can be seen in **Figure 3.5**, rhBMP-2-biotin incorporated in hydrogels that did not contain any linker was almost completely released after 2 days, with a burst release of 75% of the total rhBMP-2-biotin in the first 24 hours. In contrast, the hydrogels containing rhBMP-2-biotin immobilized with either Gln-streptavidin or Gln-M_3-streptavidin only released around 20% of the total rhBMP-2-biotin in the course of a 7 days incubation period, meaning that the majority of rhBMP-2-biotin remains immobilized in the hydrogels.

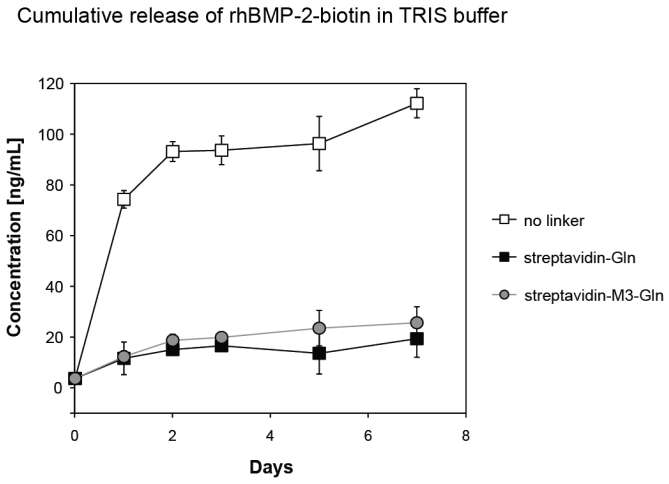

Figure 3.5. Cumulative release of immobilized rhBMP-2-biotin from streptavidin-modified hydrogels.

The release of rhBMP-2-biotin incorporated in TG-PEG hydrogels containing the different streptavidin linkers was assessed in Tris buffer over a period of 7 days. Error bars represent standard deviation, n = 3.

3.2.5 Osteogenic differentiation of cells in streptavidin hydrogels

To determine if the incorporation of proteolytically cleavable sites in the streptavidin linker improved the biological efficiency of immobilized growth factors, we cultivated C2C12 cells in streptavidin-modified TG-PEG hydrogels for each type of linker with the same total amount of bound rhBMP-2-biotin. C2C12 cells are a myoblastic cell line that differentiates toward the osteogenic lineage when exposed to BMP-2 in a dose-dependent manner.[139] Therefore, C2C12 cells were cultivated in the rhBMP-2-biotin/streptavidin-modified hydrogels and analyzed for osteogenic differentiation. As a positive control, C2C12 cells embedded in hydrogels were stimulated with the same amount of rhBMP-2-biotin, but soluble in the cell culture medium. After 9 days of culture, the enzymatic activity of the early osteogenic marker alkaline phosphatase (ALP) was analyzed. **Figure 3.6**A and B illustrates the enzymatic activity of ALP as shown by ALP substrate staining and by measurement of the ALP activity of retrieved cells. As expected, soluble rhBMP-2-biotin can strongly induce the ALP activity. Presenting rhBMP-2-biotin with the Gln-streptavidin linker resulted in an induction as well, however, ALP activity was lower than in the soluble rhBMP-2-biotin condition. Importantly, the measured ALP activity was the highest and significantly higher than the other conditions (including the soluble condition) when rhBMP-2-biotin was immobilized by Gln-M_3-streptavidin. Furthermore, we also showed that binding of rhBMP-2-biotin to the different streptavidin linkers did not influence the bioactivity of the growth factor, since the ALP activity of cells stimulated with the linker/growth factor complex in soluble form in the cell culture medium was comparable to stimulation with only rhBMP-2-biotin soluble in the medium (**Figure 3.6**C).

Of note, although the total amount of rhBMP-2-biotin was matched throughout the different conditions, comparisons between soluble and streptavidin-bound BMP-2 conditions should only be made very carefully as the manner in which the BMP-2 is presented influences the local concentration perceived by cells. Indeed although 50 ng of total rhBMP-2-biotin was used for both bound and soluble conditions, the local concentration of bound protein was 5 µg mL^{-1} in relation to the hydrogel volume, whereas the soluble protein concentration was 100 ng mL^{-1} in the cell culture medium.

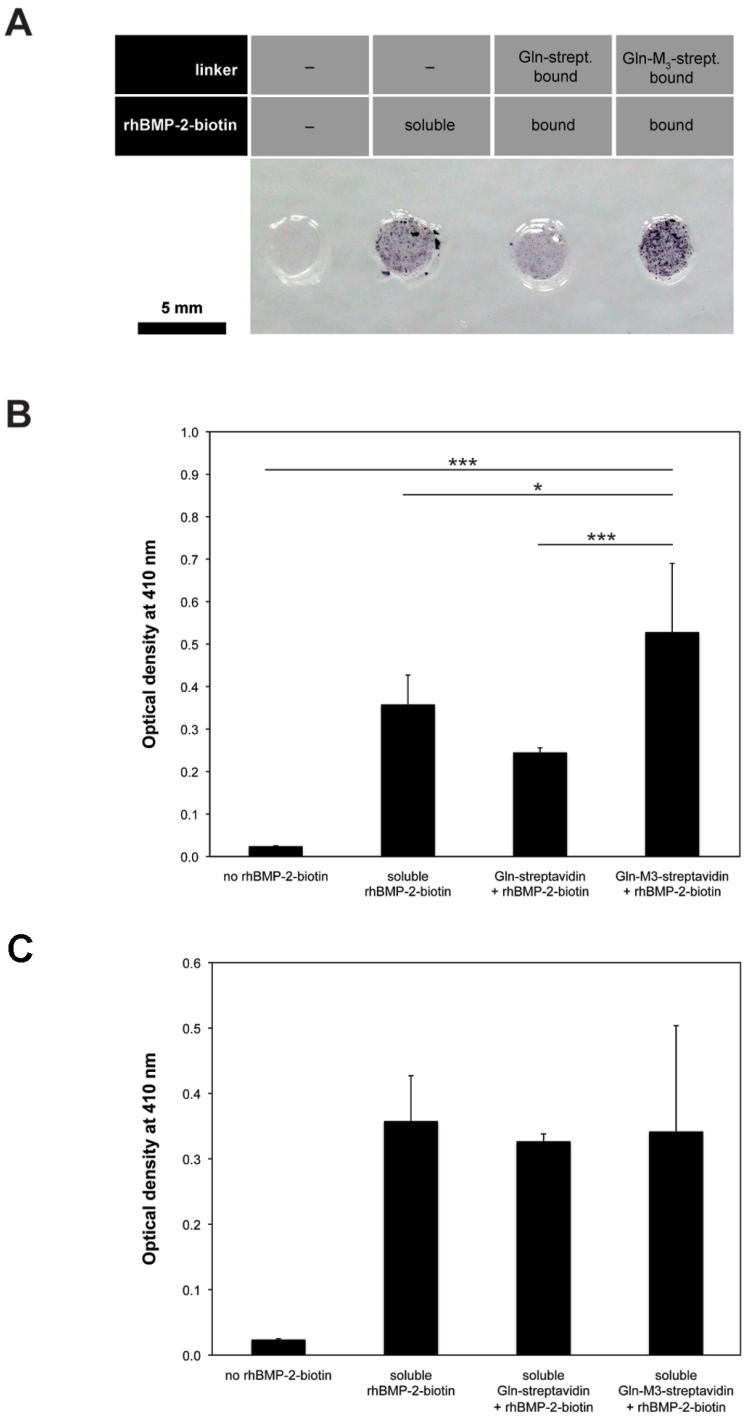

Figure 3.6. ALP activity of C2C12 cells cultivated in streptavidin-modified hydrogels for 9 days.

(A) Enzymatic activity of the osteogenic marker ALP was assessed using a substrate stain of TG-PEG hydrogels with various formulations of streptavidin linkers and rhBMP-2-biotin. (B) ALP enzymatic activity was correlated with the hydrolysis of a substrate (with absorption maximum at 410 nm) for each type of linkers with immobilized rhBMP-2-biotin. (C) ALP enzymatic activity was also determined for the soluble streptavidin-linker/rhBMP-2-biotin complexes. Error bars represent standard deviation, n = 4, * $p < 0.05$; ** $p < 0.01$; *** $p < 0.001$ and 'no rhBMP-2-biotin' was significantly different from all other conditions with $p < 0.001$. Samples were analyzed by one-way ANOVA followed by a Bonferroni post hoc test.

Furthermore, as can be seen in **Figure 3.7**, Gln-M_3-streptavidin can also be employed for the 3D localized differentiation of cells, in an analogous manner as previously shown with Gln-streptavidin.[79] TG-PEG hydrogel constructs containing MSCs were formed with a central area presenting rhBMP-2-biotin immobilized via Gln-M_3-streptavidin and an outer region without rhBMP-2. After 9 days of culture, ALP substrate stains and immunostaining against ALP showed a high ALP activity in the central area of Gln-M_3-streptavidin containing hydrogels, while the ALP activity in the outer area as well as in the other hydrogels was much weaker.

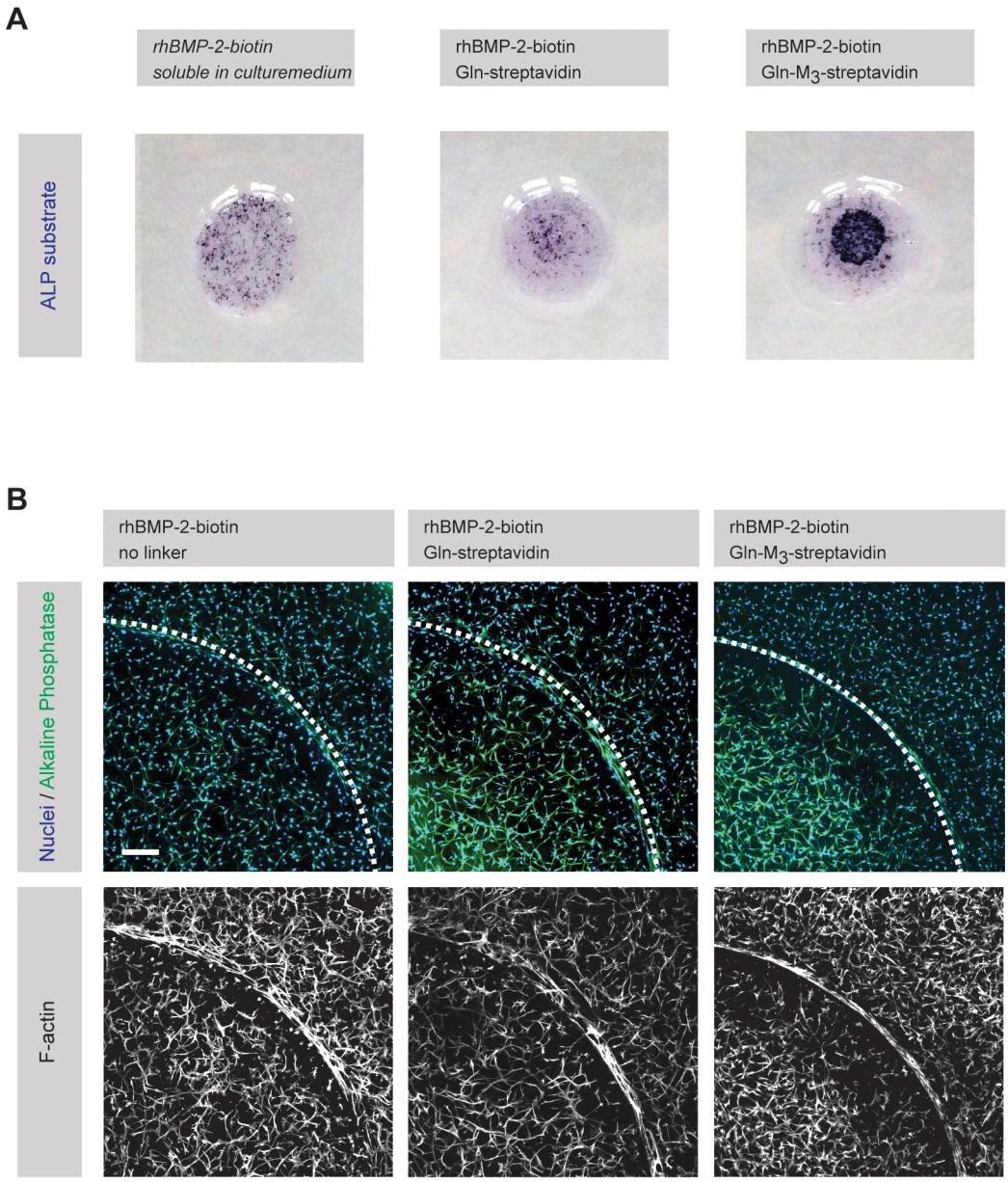

Figure 3.7. 3D-localized osteogenic differentiation of mesenchymal stem cells.

MSCs were encapsulated in hydrogel constructs made from an inner part with and an outer part without streptavidin-linker immobilized rhBMP-2. Osteogenic differentiation was assessed via presence of ALP, which was detected with both a substrate staining (A) and by immunostaining (B).

Finally, we selected the Gln-M_3-streptavidin linker, which gave the strongest ALP response in the previous experiment in order to take a closer look at the effect of BMP-2 dose. We compared the ALP activity of both C2C12 cells and MSCs inside TG-PEG hydrogels when different doses of rhBMP-2-biotin (ranging from 0 to 50 ng) were presented to them in soluble form or in bound but MMP releasable form. As can be seen in **Figure 3.8**A and Figure 3.9, we obtained a significantly higher ALP activity when rhBMP-2-biotin was bound to the hydrogel via the degradable Gln-M_3-streptavidin linker than when it was soluble in the cell culture medium. Availability and efficiency of the immobilized rhBMP-2 was thus improved by the addition of MMP-sensitive sites in the streptavidin linker, providing a cell-triggered release of growth factors.

To confirm the osteogenic differentiation by streptavidin-based BMP-2 delivery, C2C12 cells were encapsulated and cultured in TG-PEG hydrogels, which presented 50 ng rhBMP-2-biotin by MMP-degradable streptavidin linker. Samples cultured in absence or presence of soluble BMP-2-biotin (50 ng in total at 200 ng mL-1) served as controls. Quantitative PCR analysis after 7 days of culture revealed that consistent with ALP activity both early (ALP) and late (Sp7/osterix) and collagen type I alpha 1 (Col1) osteogenic markers were significantly upregulated by rhBMP-2-biotin (Figure 6B). The expression of these genes was highest in hydrogels where rhBMP-2-biotin was presented by Gln-M3-streptavidin. Runt-related transcription factor 2 (Runx2), a gene which is induced very early in osteogenic differentiation is only upregulated in samples where rhBMP-2-biotin is presented by Gln-M3-streptavidin. This data demonstrate that hydrogel immobilized rhBMP-2-biotin can induce osteogenic differentiation. However, whether the enhanced osteogenic differentiation of C2C12 cells with rhBMP-2-biotin bound to the MMP-degradable streptavidin linker is due to increased BMP availability or more efficient internalization and intracellular trafficking needs further evaluation.

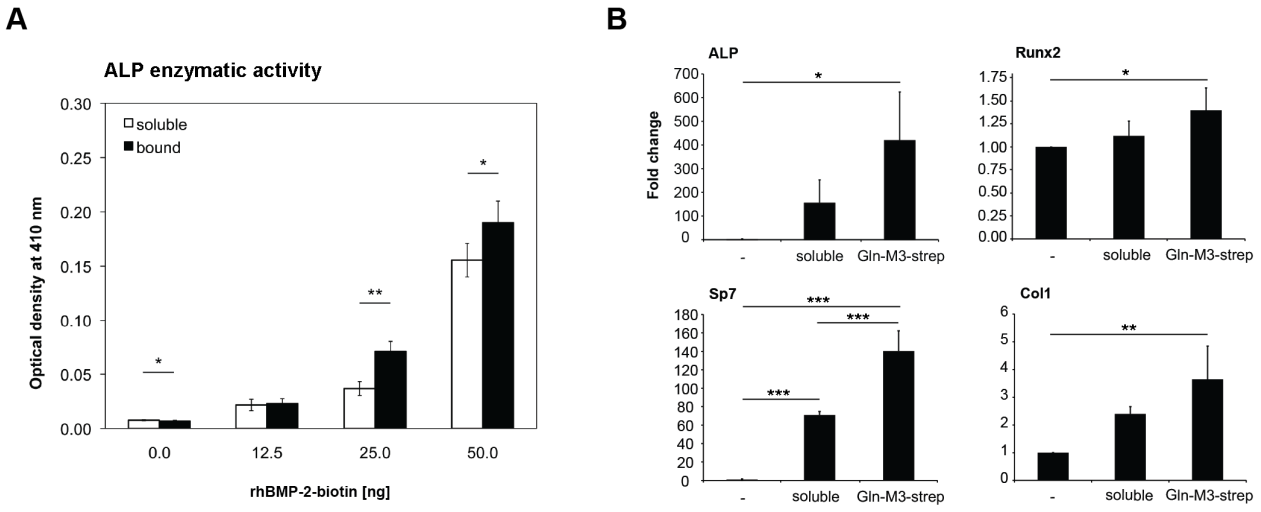

Figure 3.8. Immobilization of BMP-2 via Gln-M_3-streptavidin with C2C12 cells.

A) The enzymatic activity of the osteogenic marker ALP of C2C12 cells was measured for different doses of BMP-2 immobilized with Gln-M_3-streptavidin. Error bars represent standard deviation, n = 3, * $p < 0.05$; ** $p < 0.01$. Samples were analyzed by one-way ANOVA followed by a Bonferroni post hoc test. B) Gene expression of osteogenic markers in PEG hydrogels were measured by means of qRT-PCR and normalized on GAPDH expression. Error bars represent standard deviation, n = 3, * $p < 0.05$; ** $p < 0.01$, *** $p < 0.001$. Samples were analyzed by one-way ANOVA followed by a Bonferroni post hoc test.

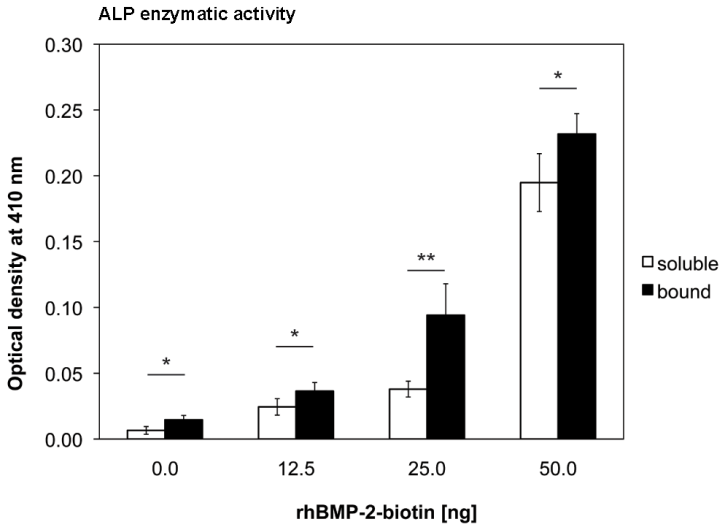

Figure 3.9 Immobilization of BMP-2 via Gln-M3-streptavidin with hBM-MSCs.

The enzymatic activity of the osteogenic marker ALP was measured for different doses of BMP-2 immobilized with Gln-M3-streptavidin. Error bars represent standard deviation, n = 3, * $p < 0.05$; ** $p < 0.01$. Samples were analyzed by one-way ANOVA followed by a Bonferroni post hoc test.

3.2.6 Degradable linkers for the immobilization and release of growth factors

The presentation of growth factors by biomaterials is desirable due to various reasons. On the one hand, the successful immobilization of growth factors can decrease the amounts of growth factors needed for biological effects, which is an important goal for the medical application of biomaterials in combination with growth factors.[149] On the other hand, the immobilization of growth factors is essential for relevant *in vitro* studies, as *in vivo* many growth factors are presented by the ECM.[122] By presenting the osteoinductive growth factor BMP-2 via two different types of streptavidin linkers to C2C12 cells and MSCs we compared the functionality and performance of a novel linker for tissue engineering and 3D cell biology approaches. Importantly, the highest osteogenic induction of C2C12 cells (measured by ALP activity) was achieved with the MMP-sensitive Gln-M_3-streptavidin linker, which was able to double the response in comparison to the previous non-degradable Gln-streptavidin linker. Moreover, when rhBMP-2-biotin was presented by Gln-M_3-streptavidin, C2C12 cells as well as MSC differentiated more efficiently than when the same overall amount of BMP-2 was applied soluble. These results suggest that the effect of growth factors depend on the

way in which they are presented and how they become available for cells. In this context, the proteolytic release of BMP-2 from TG-PEG hydrogels, independently of hydrogel stability, resulted in the local availability of BMP-2 on cellular demand and enhanced the biological net effect of BMP-2 in the system.

Taking advantage of the strong affinity between streptavidin linkers and biotin, and the availability of commercial biotinylation methods, our system offers a relatively simple strategy for the binding of growth factors. The advantage of this indirect immobilization strategy, as opposed to the direct incorporation of growth factors into the PEG matrix, is its versatility. Various growth factors can be easily and rapidly biotinylated and immobilized while using the same linker strategy, which represents a powerful alternative to genetic engineering of proteins. In this study we extended our toolbox by introducing a proteolytically degradable streptavidin/biotin system to immobilize growth factors into synthetic cell-friendly hydrogels. Such streptavidin linkers can be readily cloned with multiple alternative features, efficiently purified from bacterial expression systems, as herein demonstrated by MMP- or plasmin-sensitive sites. Additionally, refined individual functional properties of novel linkers can be tested by *in vitro* assays allowing for their efficient selection. Therefore, we are convinced that herein described approach will be applicable to develop novel, cell and application specific biomimetic materials for the recapitulation of more sophisticated tissues microenvironments.

3.3 Conclusion

We have established proteolytically degradable streptavidin-based growth factor binding linker modules, which allow the cell-mediated release of biotinylated growth factors from hydrogels. Our degradable streptavidin linker provides a growth factors release strategy, which mimics the ECM binding and release as it has been described for multiple factors in native tissues.[52, 150, 151]

This work demonstrates that indeed by the appropriate engineering of a release system, a growth factor can be delivered very locally and in such a way that it outperforms the cell culture medium supplemented soluble form. Therefore these results suggest that the effect of growth factors depends on the way in which they are presented and how they become available for cells.

3.4 Experimental Section

Cloning of the Degradable Streptavidin Linker:

To construct the plasmid pPL22 (Gln-M_3-streptavidin), three repeats of an MMP-1-sensitive sequence (VPMSMRGG)[159] were cloned into the pPL8 (Gln-streptavidin),[79] so as to be inserted between the transglutaminase sequence (Gln) and the streptavidin sequence. The expression of the streptavidin linker is under control of a T7 promoter.

Production of the Streptavidin Linker:

The plasmid pPL22 was transformed into E. coli BL21-Gold (DE3)pLysS (Agilent Technologies, La Jolla CA, USA). Expression and purification of the streptavidin linker was done as described previously for Gln-streptavidin.[79]

Cross-Linking of the Streptavidin Linkers to PEG:

Mixtures of Gln-streptavidin or Gln-M_3-streptavidin (5 µg) with 8-PEG-$MMP_{sensitive}$-Lys (molecular weight: 40'000 Da) were incubated for 30 minutes at 37°C in absence or presence of $FXIII_a$. Cross-linking of the linker proteins was assessed via 15% SDS-PAGE followed by Coomassie Blue staining. For Western blot detection, mixtures were loaded on a 4–20% gradient SDS-PAGE (Bio-Rad, Switzerland) and blotted on a PVDF membrane (Millipore, Switzerland). Streptavidin was detected by 1:1000 mouse monoclonal primary antibody (sc-52234, Santa Cruz, USA) followed by 1:2500 polyclonal goat anti-mouse IgG-HRP (P 0447, DAKO, Switzerland), both in 5% dry milk. IgG-HRP was visualized by the Lumi-Light Western Blotting Substrate (Roche, Switzerland) using the Fusion Fx Imaging System (Vilber).

Degradation of the Streptavidin Linkers with Proteases:

Each streptavidin linker (10 µM; 10 µg/50 µl) was incubated in degradation buffer (50 mM Tris, 50 mM NaCl, 10 mM $CaCl_2$, 0.05% (w/v) Brij 35, pH 7.5) for 1 and 20 hours at 37°C with either 10 or 50 nM MMP-1 (PeproTech, United Kingdom), 10 or 50 nM MMP-2 (PeproTech, United Kingdom) or 0.025 U mL^{-1} of plasmin (Sigma-Aldrich, Switzerland). Degradation products were loaded on a 15% SDS-PAGE for analysis.

Formation of Hydrogels:

TG-PEG hydrogels were formed by the cross-linking of two PEG components (8-PEG-Gln and 8-PEG-$MMP_{sensitive}$-Lys, molecular weight: 40'000 Da) via $FXIII_a$ as previously described.[74, 75] Briefly, a 200 U mL^{-1} solution of FXIII (Fibrogammin P, CSL Behring, Switzerland) was activated with 2 U mL^{-1} thrombin (Sigma-Aldrich, Switzerland) for 30 min at 37°C. Equimolar solutions of 8-PEG-Gln and 8-PEG-$MMP_{sensitive}$-Lys were prepared in 50 mM Tris, 50 mM calcium chloride, pH 7.6 buffer. Precursor solutions for hydrogels with a final dry mass content of 1.7 or 2% TG-PEG were prepared and growth factors, RGD, linker peptides and cells were added according to experiment. The cross-linking

reaction was initiated by addition of 10 U mL^{-1} $FXIII_a$. Disc-shaped hydrogels were obtained by placing the reaction mixtures between sterile hydrophobic microscope glass slides (treated with SigmaCote, Sigma-Aldrich, Switzerland) separated by 1 mm thick spacers, clamped with binder clips and incubated for 20 minutes at 37°C to allow polymerization.

Uptake of Biotinylated Alkaline Phosphatase by Streptavidin Hydrogels:

20 µL PEG hydrogels (2% w/v) containing 0, 5 and 100 µM of Gln-streptavidin or Gln-M_3-streptavidin were formed via $FXIII_a$ cross-linking. The hydrogels were then washed in microcentrifuge tubes containing 500 µL of Tris buffer (50 mm Tris, pH 7.6) at 4°C overnight on a shaker. Hydrogels were then transferred to microcentrifuge tubes containing 500 µL of a solution of 5.5 µg mL^{-1} biotinylated ALP (Thermo Scientific, Switzerland) in Tris buffer. The hydrogels were incubated at 4°C for 5 days. 20 µL buffer samples were collected after 1, 4, 8, 24, 48 and 120 hours and the remaining content of biotinylated ALP was quantified by means of enzymatic activity with the secreted alkaline phosphatase (SEAP) assay as described previously.[79]

Release of Biotinylated Alkaline Phosphatase by Streptavidin Hydrogels:

20 µL TG-PEG hydrogels (1.7% w/v) containing approximately 2.3 µM of ALP-biotin with 0, 5 or 100 µM streptavidin linker were formed for both types of linker. The hydrogels were incubated in 500 µL of 50 mM Tris, 0.5% BSA, pH 7.6 buffer and incubated at 4°C on a shaker. The buffer or medium was collected after 7 days. The ALP activity in the solution was determined with the secreted alkaline phosphatase (SEAP) assay as described previously.[79]

Binding of Biotinylated rhBMP-2 by Streptavidin Hydrogels:

10 µL TG-PEG hydrogels (1.7% w/v) containing 50 ng of rhBMP-2-biotin[79] with 0 or 5 µM streptavidin linker were formed for both types of linker. The hydrogels were incubated in 500 µL of 50 mM Tris, 0.5% BSA, pH 7.6 buffer and incubated at 4°C on a shaker. The buffer or medium was collected and freshly replaced on day 1, 2, 3, 5 and 7. The concentration of released rhBMP-2-biotin was determined via ELISA.

ELISA of BMP-2:

All BMP-2 ELISAs were performed using the human BMP-2 ELISA Development Kit (PeproTech, United Kingdom) according to the manufacturer's guidelines. The solution in which the samples were diluted was used as diluent for both samples and standards. The standard curves were established with the same rhBMP-2-biotin used for the experiments.

Cell culture:

Cells were cultured at 37°C in a humidified atmosphere at 5% CO_2. C2C12 cells (ATCC, USA) were expanded in DMEM supplemented with FBS (10%), penicillin-streptomycin (1%) and L-Glutamine (2mM). The cells were passaged every 2-3 days at 70% confluence. Human bone marrow-derived mesenchymal stem cells were isolated as described previously[160] from bone marrow aspirated of healthy donors obtained during orthopedic surgical procedures after

informed consent and in accordance with the local ethical committee (University Hospital Basel; Prof. Dr. Kummer; approval date 26/03/2007 Ref Number 78/07). The cells were maintained in Minimum Essential Medium Alpha (MEMα) supplemented with FBS (10%), penicillin-streptomycin (1%) and bFGF (5 ng mL^{-1}) and passaged every 2-3 days at 70-80% confluence.

For differentiation assays, both cell types were cultured in MEMα supplemented with FBS (10%), penicillin-streptomycin (1%) and L-ascorbic acid (50 µg mL^{-1}).

3D differentiation of cells in hydrogels with immobilized rhBMP-2-biotin:

10 µL TG-PEG hydrogels (1.7 % w/v) containing Lys-RGD (50 µM) and different combinations of either 0 or 5 µM of streptavidin linker and 0 or 50 ng rhBMP-2-biotin were formed with a final single cell concentration of 1.5×10^6 cells mL^{-1}. After polymerization, the hydrogels were glued to the bottom of a 48-well plate with a TG-PEG (2% w/v) solution and cultured with the appropriate medium for 7-9 days.

Alkaline Phosphatase Colorimetric Staining and Enzymatic Activity Assay:

For the colorimetric staining, medium was removed from the wells and the hydrogels were washed with PBS. 250 µL of substrate solution made from SIGMA*FAST* BCIP/NBT tablets (Sigma-Aldrich, Switzerland) and prepared according to the manufacturer's guidelines were added to each well followed by incubation at 37°C. Once enough color had visually developed (5-10 minutes), the substrate solution was removed and the hydrogels were fixed with a 4% paraformaldehyde solution for 10 minutes. Finally the hydrogels were washed with PBS and imaged with a light microscope. For the enzymatic activity assay, the medium was removed from the wells and the hydrogels were washed with PBS. Each hydrogel was collected and transferred to a microcentrifuge tube and digested in an equivalent volume of collagenase A solution (2 mg/mL in PBS, Roche, Switzerland) at 37°C for 10 minutes or until completely dissolved. Lysis buffer (0.56 M 2-amino-2-methyl-1-propanol, 0.2% Triton X-100, pH 10 in ddH_2O) was then added to each tube for a final volume of 500 µL and the cell lysates were incubated at room temperature for 30 minutes, followed by 1 minute of homogenization (Omni TH220 tissue homogenizer, Omni International, USA). After centrifugation of the cell lysate at 10'000 rpm for 10 minutes, the supernatant was collected. 50 µL of cell lysate was mixed with 50 µL of ALP reagent (20mM 4-nitrophenyl phosphate disodium salt hexahydrate, 4 mM MgCl2 in lysis buffer) in a 96-well plate and incubated at 37°C for 10 minutes before reading absorbance at 410 nm with a microplate reader. For each sample, the absorbance values were normalized to the total protein content in the cell lysate, which was measure via Bradford assay.

Gene expression analysis using qRT-PCR:

C2C12 cells were encapsulated in 10 µL PEG hydrogels (1.7% PEG, 50 µm RGD) at a final concentration of 1.5×10^6 mL^{-1}. Hydrogels were cultured for 7 days in MEMα, FCS (10%), penicillin-streptomycin (1%) and 50 ng BMP-2 presented soluble in the cell culture medium or bound to the PEG hydrogel by 5 µm Gln-M3-streptavidin linker. After 7 days, hydrogels were digested in 30 µL of collagenase A solution (2 mg mL-1 in PBS, Roche, Switzerland) for 30 min at 37°C. Next, cells were collected by centrifugation and total RNA was isolated from the cells by the RNeasy Micro Kit

(Qiagen) according to the manufacturer's instructions. For quantitative real-time PCR (qRT-PCR), 200 ng RNA were converted into 40 µL cDNA by means of the High-Capacity cDNA Reverse Transcription Kit (Applied Biosystems). qRT-PCR was carried out using 2 µL cDNA template, the TaqMan Universal PCR Master Mix (Applied Biosystems) and the StepOnePlus Real-Time PCR System (Applied Biosystems). The following TaqMan primer/probe sets were used for gene expression tests: Mm00475834_m1 (Alpl), Mm00501584_m1 (Runx2), Mm04209856_m1 (Sp7), Mn00801666_g1 (Col1a1). Data were normalized on Mm99999915_g1 (Gapdh) and relative gene expression was calculated by the comparative Ct method.

Localized 3D differentiation of cells in hydrogels:

Small 10 µL TG-PEG hydrogels (1.7% w/v) containing Lys-RGD (50 µM) and combinations of the different streptavidin linkers (5 µM) with or without rhBMP-2-biotin (50 ng) were formed with single cells at a final concentration of 2 $\times 10^6$ cells mL^{-1}. These hydrogels were then embedded in a second 20 µL hydrogel with the same formulation except that no rhBMP-2-biotin was included. The hydrogel constructs were then glued at the bottom of a 48-well plate and cultured in the appropriate cell culture medium. Medium was replaced every second day and cells were cultured up to 9 days. The hydrogel constructs were then either stained with ALP substrate or fixed in 4% paraformaldehyde for 10 minutes before proceeding to immunostaining.

Immunostaining of alkaline phosphatase:

The hydrogel constructs were fixed in 4% paraformaldehyde for 20 minutes. Cell nuclei were stained with Hoechst and presence of ALP was assessed with mouse anti-bone alkaline phosphatase primary antibody (Abcam, United Kingdom) at a 1:500 dilution and goat anti-mouse IgG H&L (Alexa Fluor® 488) secondary antibody (Abcam, United Kingdom) at a 1:1000 dilution. Images were acquired with a confocal laser scanning microscope Leica SP5, 150 µm stack with 2.5 µm z-step.

3.5 References

[27] C. Frantz, K. M. Stewart, and V. M. Weaver, *J Cell Sci,* 2010, *123*, 4195.

[34] J. Zhu, *Biomaterials,* 2010, *31*, 4639.

[48] M. F. Brizzi, G. Tarone, and P. Defilippi, *Curr Opin Cell Biol,* 2012, *24*, 645.

[52] R. O. Hynes, *Science,* 2009, *326*, 1216.

[72] M. P. Lutolf, J. L. Lauer-Fields, H. G. Schmoekel, A. T. Metters, F. E. Weber, G. B. Fields, and J. A. Hubbell, *Proceedings of the National Academy of Sciences of the United States of America,* 2003, *100*, 5413.

[73] M. P. Lutolf, and J. A. Hubbell, *Nat. Biotechnol.,* 2005, *23*, 47.

[74] M. Ehrbar, S. C. Rizzi, R. G. Schoenmakers, B. S. Miguel, J. A. Hubbell, F. E. Weber, and M. P. Lutolf, *Biomacromolecules,* 2007, *8*, 3000.

[75] M. Ehrbar, S. C. Rizzi, R. Hlushchuk, V. Djonov, A. H. Zisch, J. A. Hubbell, F. E. Weber, and M. P. Lutolf, *Biomaterials,* 2007, *28*, 3856.

[77] A. Sala, P. Hanseler, A. Ranga, M. P. Lutolf, J. Voros, M. Ehrbar, and F. E. Weber, *Integr. Biol. (Camb),* 2011, *3*, 1102.

[79] S. Metzger, P. S. Lienemann, C. Ghayor, W. Weber, I. Martin, F. E. Weber, and M. Ehrbar, *Adv Healthc Mater,* 2015, *4*, 550.

[80] U. Blache, S. Metzger, Q. Vallmajo-Martin, I. Martin, V. Djonov, and M. Ehrbar, *Adv Healthc Mater,* 2015.

[81] P. S. Lienemann, M. Karlsson, A. Sala, H. M. Wischhusen, F. E. Weber, R. Zimmermann, W. Weber, M. P. Lutolf, and M. Ehrbar, *Adv Healthc Mater,* 2013, *2*, 292.

[122] K. Lee, E. A. Silva, and D. J. Mooney, *J. R. Soc. Interface,* 2011, *8*, 153.

[133] M. Ehrbar, A. Sala, P. Lienemann, A. Ranga, K. Mosiewicz, A. Bittermann, S. C. Rizzi, F. E. Weber, and M. P. Lutolf, *Biophys. J.,* 2011, *100*, 284.

[135] N. M. Green, *Adv. Protein Chem.,* 1975, *29*, 85.

[139] T. Katagiri, A. Yamaguchi, M. Komaki, E. Abe, N. Takahashi, T. Ikeda, V. Rosen, J. M. Wozney, A. Fujisawa-Sehara, and T. Suda, *J. Cell Biol.,* 1994, *127*, 1755.

[147] T. Dvir, B. P. Timko, D. S. Kohane, and R. Langer, *Nat Nanotechnol,* 2011, *6*, 13.

[148] J. K. Mouw, G. Ou, and V. M. Weaver, *Nat Rev Mol Cell Biol,* 2014, *15*, 771.

[149] A. C. Mitchell, P. S. Briquez, J. A. Hubbell, and J. R. Cochran, *Acta Biomater.,* 2015.

[150] G. S. Schultz, and A. Wysocki, *Wound. Rep. Reg.,* 2009, *17*, 153.

[151] C. Streuli, *Curr. Opin. Cell Biol.,* 1999, *11*, 634.

[152] P. Lu, K. Takai, V. M. Weaver, and Z. Werb, *Cold Spring Harb Perspect Biol,* 2011, *3*.

[153] T. E. Cawston, and D. A. Young, *Cell Tissue Res,* 2010, *339*, 221.

[154] C. M. Kirschner, and K. S. Anseth, *Acta Mater.,* 2013, *61*, 931.

[155] C. C. Lin, *RSC Adv.,* 2015, *5*, 39844.

[156] P. S. Lienemann, M. P. Lutolf, and M. Ehrbar, *Adv. Drug Deliv. Rev.,* 2012, *64*, 1078.

[157] H. Nagase, and G. B. Fields, *Biopolymers,* 1996, *40*, 399.

[158] J. Patterson, and J. A. Hubbell, *Biomaterials,* 2011, *32*, 1301.

[159] J. Patterson, and J. A. Hubbell, *Biomaterials,* 2010, *31*, 7836.

[160] A. Papadimitropoulos, E. Piccinini, S. Brachat, A. Braccini, D. Wendt, A. Barbero, C. Jacobi, and I. Martin, *PLoS One,* 2014, *9*, e102359.

Chapter 4 *Evaluation of growth factors modulating angiogenesis*

4.1 Introduction

Blood vessels growth is an important factor in regenerative medicine and in the design of engineered tissues. On the one hand, gaining knowledge on angiogenesis allows developing strategies for the treatment of ischemic diseases. On the other hand, vascularization is a factor that can strongly limit the size of engineered constructs and that is critical to ensure their viability upon transplantation, by providing oxygen and nutrients to the cells and their microenvironment. Angiogenesis *in vivo* is a complex process that is tightly regulated. In order to allow the growth of new vascular structures, angiogenic signals require proper spatial and temporal localization in the ECM, an aspect that is crucial to include in the engineering of tissue constructs.[161, 162]

Amongst the most commonly employed angiogenic factors for such scaffold engineering approaches are VEGF, FGF-2 and PDGF, which all play a role in endothelial cell recruitment, capillary formation and vessel maturation.[163] The ephrins and their Eph receptors (described in **Section 1.5.3**) represent another category of growth factors, which have also been studied for their role in angiogenesis. Eph receptors are an important family of receptor tyrosine kinase, which bind to their ephrin counterparts and play an important role in cell-cell interactions. They are involved in many biological processes as mediators of cell adhesion, repulsion, migration and ECM attachment and are of particular interest due to their ability to induce bi-directional signaling during cell-cell interactions.[105] In recent years, many studies have shown their involvement in vascular development. They are commonly used as markers to differentiate between venous and arterial endothelial cells during the early stages of vessel formation, and can be expressed by mesenchymal supporting cells as well.[104, 107] Ephrins and Eph receptors represent thus an interesting target for the study and recapitulation of vascular networks and could potentially serve as important co-factor alongside angiogenic factors to obtain controlled blood vessel formation in engineered tissues. For this work, four different ephrin proteins were selected to assess their effect on endothelial cell migration and the development of vascular structures: ephrin-A1, ephrin-A5, ephrin-B1 and ephrin-B2. Expression of ephrin-A1 has been shown to be present in vasculature during mouse embryonic development,[164] and is also involved in vascular signaling pathways in conjunction to VEGF and TNF-α, as well as in EC migration and assembly, along with its receptor EphA2.[104, 165, 166] Ephrin-A5 has mainly been studied in the context of neurogenesis and cancer for its repulsive effect on cell migration,[167, 168] and although little is known on its function in angiogenesis, its high affinity for the EphB2 receptor that normally binds ephrinB1 and ephrinB2 (both involved in angiogenesis) makes it an interesting candidate.[107, 167]

Ephrin-B1 has been shown to have a pro-angiogenic role and is assumed to be involved in EC attachment to the ECM by activation of integrins.[107, 169, 170] Finally, ephrin-B2 plays an important role in vascular development by regulating remodeling, vessel maturation, VEGF-induced angiogenesis, and is involved in spatial guidance and discrimination between arterial and venous structure.[89, 169-171] Furthermore the role of netrin-4, which has been described in **Section 1.5.3**, was assessed in the context of blood vessel development by evaluating its anti-angiogenic effects on the chicken chorioallantoic membrane assay.

The chicken chorioallantoic membrane (CAM) is an easily accessible, technically simple, rapid and cost-effective model for the screening of tissue-engineered constructs.[171, 172] The CAM is an extra-embryonic membrane present during the development of the chick embryo and is mainly responsible for gas exchange and distribution of nutrients. It is highly vascularized and is thus commonly used to study angiogenesis in short-term and large-scale screenings.[173] Typically, the CAM starts forming on day 3-4 after incubation and is mainly composed of undifferentiated blood vessels distributed across the mesoderm. These vascular structures develop and grow rapidly until day 8, when some vessels start differentiating into capillaries that will form a network at the base of the ectoderm. The capillary network continues to develop and is generally completed by day 10. By day 13-14 the capillary network is fully differentiated and has reached the surface of the ectoderm, just beneath the shell membrane. From a histological view, the CAM is composed of two epithelial layers that border a thin layer of stroma. The capillary plexus is located in the upper portion of the stroma, lining the upper epithelium. The rest of the vasculature as well as lymphatic vessels are distributed across the stroma.[171, 174]

Due to its ease of access, cost-effectiveness and its extensive vascularization, the chicken CAM is often used to evaluate angiogenic processes and to determine the effects of certain molecules and growth factors on vascular development and morphogenesis or for studying tumor growth.[174]. This can be done by a variety of methods, including stimulation with pro- and anti-angiogenic factors, and vascularization of tissue grafts.[171] Furthermore, the CAM vasculature develops in a short time, which offers a window for the study of processes at different stages of vascular growth and of developmental pathways, with relatively low immunogenic responses from the CAM. But it is important to mention that limitations can arise due to species-related incompatibilities. Nevertheless, the chicken CAM assay represents an attractive model for the rapid screening of factors and their angiogenic effects.

Taken together, these different aspects of vascular development in tissue engineering show that the selected factors could be interesting targets for the development of pre-vascularized tissue constructs, especially in regards to spatial and temporal control of vessel growth combined to a modular PEG hydrogel platform for support. And to understand the roles of these growth factors on vasculature, the CAM assay represents a relatively easy method for obtaining the first insights on the effect of ephrin signaling on vascular morphology and development.

4.1.1 Objective

With the tools in hand to design and assemble tunable microenvironment for cells, it becomes important to assess if these strategies can be combined with vascularization. The TG-PEG platform used here has recently been shown to be able to host microvascular-like networks formed co-cultures of BM-MSC and ECs.[80] Therefore, it would be an advantage to have a relatively simple and fast method for the first screening of angiogenic factors, which could facilitate the formation, guidance and maintenance of pre-vascular structures in TG-PEG hydrogels. To this purpose, we studied the effects of such angiogenic factors on the vasculature of the chicken CAM. Netrin-4 was selected due to its potential anti-angiogenic effect, which was assessed on the chicken CAM. Ephrin-A1, A5, B1 and B2 were selected for their known role as cell guidance cues and role in the regulation of angiogenesis and their effect was evaluated on the chicken CAM as well as in cell migration assays. VEGF-A was chosen as a benchmark pro-angiogenic factor, since its implication in angiogenesis[99, 175] and its effect on the chicken CAM have already been characterized.[75, 176, 177]

4.2 Results and discussion

4.2.1 Anti-angiogenic effect of netrin-4 on the chicken CAM[2]

The chicken CAM vasculature was stimulated with full-length netrin-4 over a period of 48 hours. To do so, soluble netrin-4 was incorporated in TG-PEG hydrogels, which were placed on the surface of the CAM vasculature on day 9 after incubation of the eggs. BSA incorporated in the hydrogels was used as protein control and to ensure that the application of the TG-PEG hydrogel itself had no influence on the vasculature. Results were furthermore compared to areas of the vasculature that had received no treatment. The effects of netrin-4 were then assessed 12, 24 and 48 hours post-treatment. For each time point and treatment, images of the chicken CAM blood vessels were acquired via fluorescent microscopy after injection of a FITC-Dextran solution in the vascular network. The vascularized area for the treatment and control was quantified with a semi-automated image analysis script that measures the hole area of the capillary plexus. As can be seen in **Figure 4.1**A, the percentage of the vascularized area in CAMs treated with netrin-4 (~75%) already showed a slight decrease in comparison to the control (~80%) after 12 hours. Following 24 and 48 hours, the decrease in vascularized area became even more significant reaching approximately 70% then 55% respectively, whereas the control area remained constant (~80%). Additionally, we performed histological stainings (eosin and hematoxylin) of the CAMs after 48 hours of treatment to highlight the changes in capillary density (**Figure 4.1**B). Control area of the CAMs showed a dense distribution of the capillary lining the epithelium, but netrin-4 treated regions only possessed a few capillaries dispersed along the epithelial layer.

[2] *Adapted from*: R Reuten, S Metzger, Z Zhou, J Kaltenberg, KK McKee, M McDougall, T Bald, K Pool, T Tüting, B Brachvogel, P Zigrino, J Stetefeld, V Djonov, W Bloch, PD Yurchenco, E Pöschl, M Ehrbar, M Koch, **Netrin-4 regulates functional vascular basement membrane assembly and neo-angiogenic events**, submitted for publication, 2016.

As netrin is known to be able to strongly interact with laminin[178, 179] we hypothesized that netrin-4 could potentially influence the vascular basement membrane by interacting with laminin. This could in turn have an effect on pericytes and on the stability of the vascular epithelium. Therefore we performed ultrastructural analysis of the CAM after 48 hours of treatment to assess the state of the basement membrane (**Figure 4.1**C). In CAMs treated with netrin-4, pericytes appeared detached from ECs, compared to the control where pericytes are normally in close contact with ECs. Additionally, where the basement membrane can be seen surrounding and embedding pericytes and ECs in the control, it was almost completely absent in the CAMs treated with netrin-4. These results show that netrin-4 has a detrimental effect on the capillary network, in the context of the chicken CAM. Furthermore, this effect seems to be linked with the stability of the basement membrane and the stabilizing interactions between pericytes and ECs, which are compromised in presence of netrin-4. This shows the strong potential of netrin-4 as an anti-angiogenic factor, which could be used in order to regulate angiogenesis.

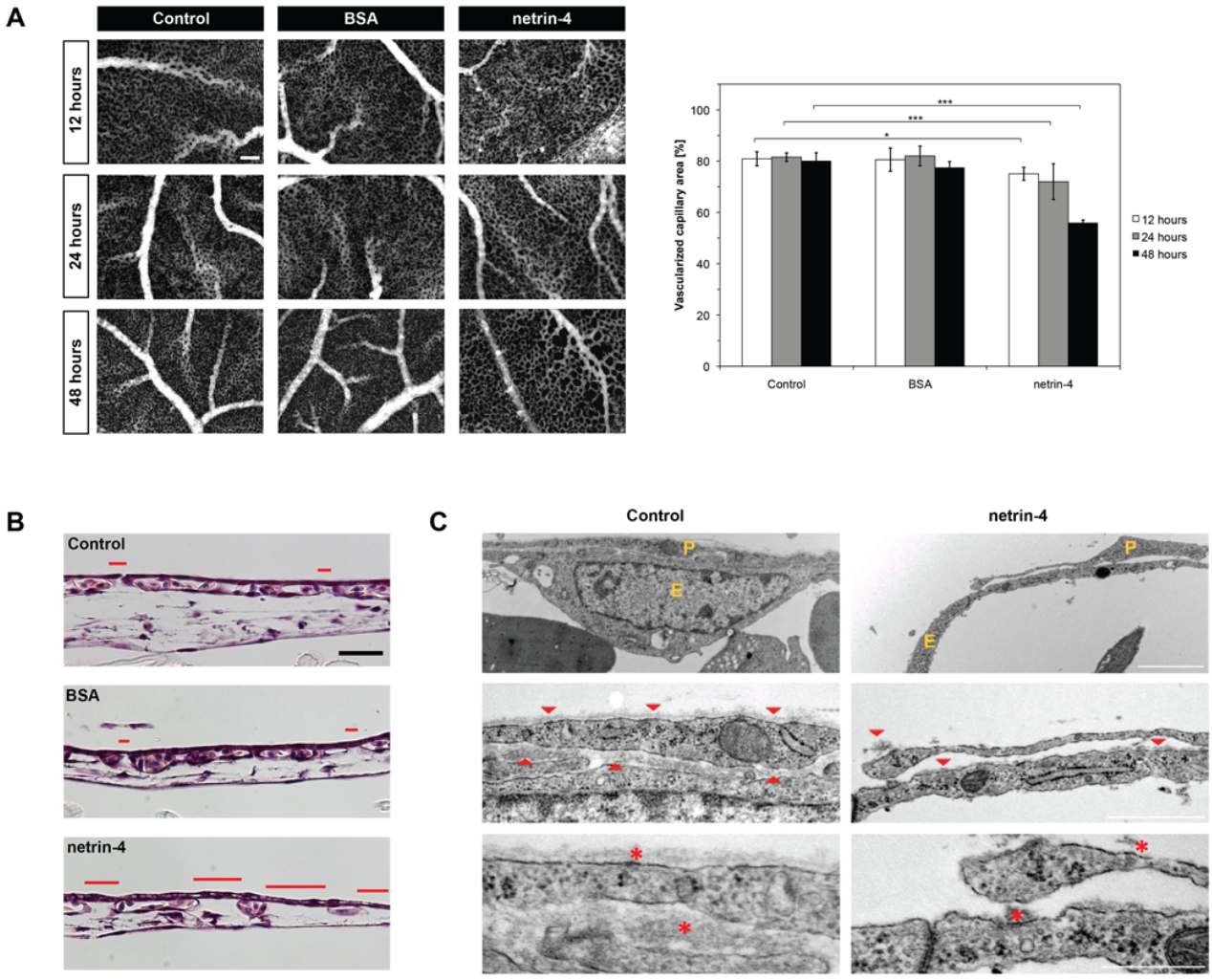

Figure 4.1. Netrin-4 inhibits angiogenesis in the *ex ovo* chicken CAM assay.

A) Visualization of capillaries via FITC-dextran injection of untreated (ctrl), BSA- and netrin-4-treated CAMs after 12, 24 and 48 h, scale bars = 100 µm. The vascularized area from different protein treatments was determined at 12, 24 and 48 h (mean ± s.d.; *n* = 5;

****P < 0.0001, Student's t-test). B) H&E staining of untreated (ctrl), BSA- and netrin-4-treated CAMs after 48 h. Red lines indicate holes in the capillary plexus. Scale bar = 20 µm. C) Ultrastructural analyses of control and netrin-4 treated CAMs using transmission electron microscopy. Images show the capillary endothelium surrounded by perivascular cells. The endothelium E is shown and perivascular cells (PVCs) are indicated as P. Electron microscopy images highlight the vascular basement membrane [vBM, red arrow heads (middle) and red asterisks (bottom)] between the endothelium and PVCs, which are surrounded by a vBM layer. Scale bars = top: 2 µm; middle: 1 µm; bottom: 0.5 µm.

4.2.2 Effects of ephrins and VEGF on the chicken CAM

To determine if ephrins could be candidates in the establishment of a hydrogel platform allowing controlled vascularization, we assessed their effects on the capillary network of the chicken CAM. To do so, we stimulated the chicken CAM with ephrin-A1, A5, B1 and B2, which were delivered in soluble form via TG-PEG hydrogel placed on the surface of the CAM capillary network on day 9 after incubation of the eggs. Treatment with $VEGF_{165}$ was used as pro-angiogenic control, whereas non-treated areas served as negative control (control). Hydrogels containing no protein were used as an additional control to ensure that the hydrogel itself had no effect on the CAM (not shown). The vasculature was imaged using fluorescence microscopy after injection of a FITC-Dextran solution in the vascular network. Looking at the morphology of the blood vessels and capillaries in **Figure 4.2**, $VEGF_{165}$ treatment resulted in thicker blood vessels and more chaotic architecture compared to the control. Furthermore, the blood vessels presented the typical spiral-like or "corkscrew-like" structures, as described in other studies about the effects of VEGF on the CAM vasculature.[180, 181] The capillary density seemed increased as well, as can be seen from the higher fluorescent background. Ephrin-A1, B1, and B2 all seemed to have rather pro-angiogenic effects on the vasculature to some extent, as could be seen from the chaotic vessel growth, the spiral-like structures and the increase in vessel diameter. Ephrin-A1 treatment induced particularly more spiral-like structures, especially on blood vessels of lower hierarchy that connect to the capillary plexus. For both ephrin-A1 and B1, the capillary density was also increased and appeared almost leaky in some areas. Ephrin-B2 induced a blood vessel morphology that was very similar to the effect of $VEGF_{165}$ with thick wavy vascular structures. Ephrin-A5 had a very different effect and reduced the overall vascularization. The blood vessels appeared very thin and with less hierarchical structure. The strongest effect could be seen on the capillary plexus, where large non-vascularized areas in the form of hole in the capillary network are present. Although the role of ephrin-A5 in angiogenesis if any is not yet well understood, it has been shown to interact with the EphB2 receptor, which is involved in vascular development.[107, 167] We thus hypothesize that ephrin-A5 could be used as an anti-angiogenic guiding cue to set boundaries to the development of blood vessels.

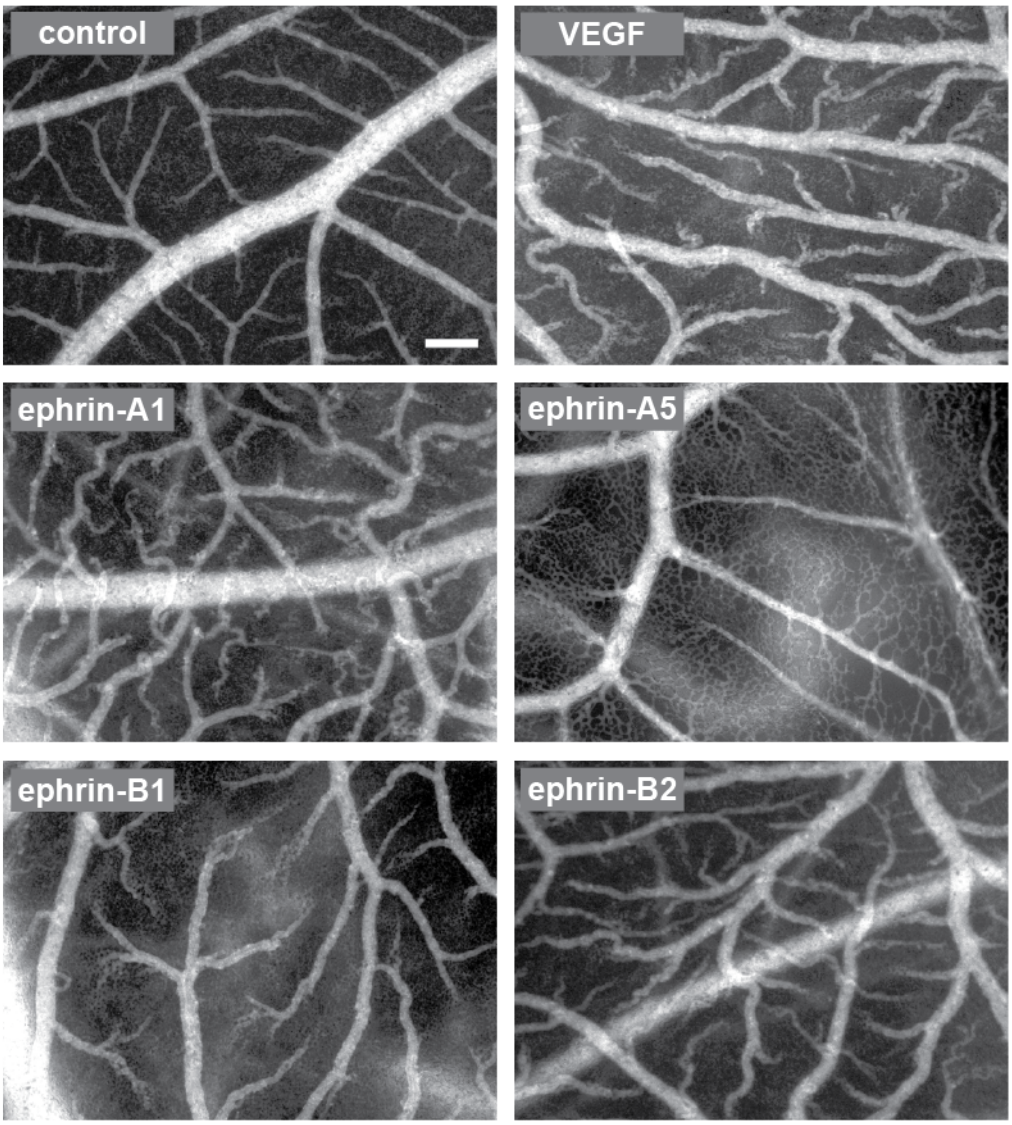

Figure 4.2. Effects of ephrins and VEGF on the morphology of the CAM vasculature.

Visualization of the capillaries via FITC-dextran injection in untreated CAMs (control), or CAMs stimulated with either VEGF, ephrin-A1, ephrin-A5, ephrin-B1 or ephrin-B2 at 48 h post-treatment (scale bar = 250 µm).

Due to the chaotic morphology and increased capillary density (leading to a high background noise), the image analysis used to quantify the effect of netrin-4 under **Section 4.2.1** could not be used to quantify the effects of VEGF and the selected ephrins. However it would be of great interest to have access to an automated and reliable method that could analyze different morphological parameters such as branching, vessel length, number and diameter. The next section addresses the possibility of developing such method.

4.2.3 Casting of the CAM with polyurethane for µCT quantification

Because morphological analysis of the vasculature could not be automated for the images obtained from $VEGF_{165}$, and ephrin treatment with live fluorescence microscopy, we developed a technique that allowed us to inject a polyurethane solution in the CAM vasculature for corrosion casting (**Figure 4.3**). Using a syringe pump, untreated CAMs were first perfused with a 1% PFA solution in order to flush the blood and fix the vasculature. Next the CAM vasculature was perfused with polyurethane resin, again with the help of the syringe pump to obtain a constant and controlled flow rate. The polyurethane solution polymerized to a hard plastic within 1 hour and the remaining soft tissues were dissolved during 24 hours using a 7.5% KOH solution, followed by a neutralization step of 12 hours in a 5% formic acid solution. After the polyurethane cast was allowed to dry, 6mm-biopsy punches were retrieved from the CAMs and processed by µCT imaging. The obtained images were then reconstructed to obtain 3D model of the vascular network. This shows that casting of CAMs and µCT imaging could be an efficient method for the computed analysis of the CAM vasculature, as has been successfully done with the same polyurethane resin in mice.[182, 183]

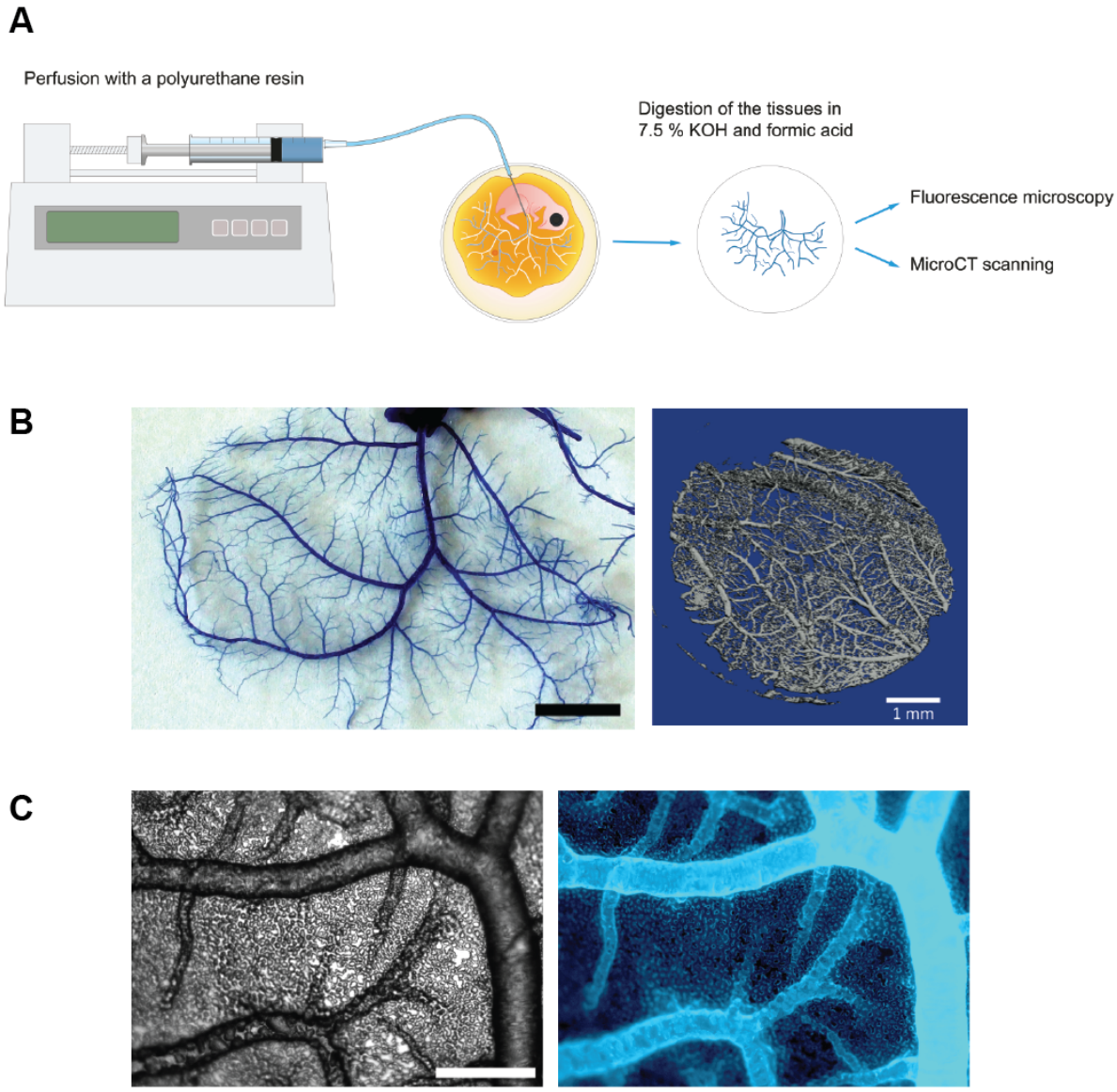

Figure 4.3. Polyurethane casting of the chicken CAM and analysis.

A) The cast is obtained by injecting polyurethane resin in the vascular system of the CAM. The resin polymerizes within 1 h and the soft tissues can then be dissolved. B) Left - remaining polyurethane cast after complete digestion of the soft tissues, right - 3D representation of µCT scan obtained from a 6mm biopsy punch of a cast. Scale bars = 1 cm and 1 mm respectively. C) Brightfield and fluorescence microscopy images of the cast. Scale bar = 250 µm.

4.2.4 Effects of ephrins cell migration

After showing that ephrins could influence blood vessel morphology and capillary density of the CAM vasculature, we wanted to assess their effect on the migration of cells as ephrins are often described acting as guidance cues.

4.2.4.1 Ephrins and 2D cancer cell migration

In order to study cell migration upon ephrin stimulation, we wanted to develop a system using our synthetic TG-PEG hydrogels. To establish the system, we chose to study the cell migration of the cancer cell line PC-3, as a previous study[168] showed and quantified how ephrins could influence the migration direction of these cells in 2D. We seeded PC-3 cells on the surface of TG-PEG hydrogels patterned with four different types of Fc-tagged ephrins (Fc-ephrin-A1, Fc-ephrin-A5, Fc-ephrin-B1 and Fc-ephrin-B2). The ephrins were immobilized via the Gln-ZZ[81] linker that was incorporated in the hydrogels. Because clustering of ephrins is known to affect ephrin signaling, the experiment was also carried out with ephrin cluster patterns, obtained from multimerizing the Fc-tagged ephrins with human anti-IgG antibody before patterning. Cell migration was then recorded via time-lapse microscopy over a period of 24 hours (**Figure 4.4**). Using an image analysis script, cells randomly selected within the patterned regions were tracked and total migration distance was quantified and compared to cells seeded outside of the ephrin patterns.

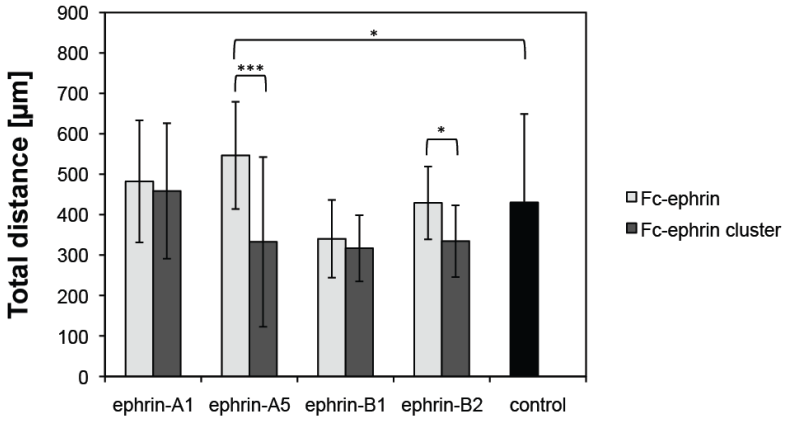

Figure 4.4. Effects of ephrin presentation on the 2D migration of PC-3 cells.

Total distance travelled was measured by cell tracking for each condition. (*, $p < 0.05$; **, $p < 0.01$; ***, $p < 0.001$, Student's t-test).

The acquired data showed that the total migration distance was only significantly affected by stimulation with Fc-ephrin-A5, which showed an increase in distance. Also, cells migrated on shorter distances when stimulated with Fc-ephrin-A5 clusters. Fc-ephrin-B2 did not show significant changes in migratory behavior, but the clustering of the factor reduced the migration of cells. Although Fc-ephrin-A1 stimulation hinted towards an increase in migration and Fc-ephrin-B1 stimulation created a slightly decreased migration, results were not significantly different from the control. Furthermore both Fc-ephrin-A1 and Fc-ephrin-B1 clustering did not have a significant effect.

These preliminary results suggested that Fc-ephrin-A5 and Fc-ephrin-B2 could be potential candidates for studying the effects of ephrins on cell migration, but further experiments are necessary. However, during the development of this migration assay, technical and biological limitations made it evident that a 3D experiment setup was needed. Indeed

studying the cell migration in 3D conditions would be more pertinent to our goal of designing cell-instructive microenvironments. Moreover distribution and immobilization of ephrins in 3D matrices would be more relevant, as 2D patterning of ephrins make it difficult to determine the appropriate concentrations needed for stimulation and is far from physiological conditions.

4.2.4.2 Ephrins and 3D endothelial cell migration

To have a better adapted method for the assessment of ephrin effects on endothelial cell migration, we chose to study the 3D cell sprouting from spheroids. Cell spheroids were formed with HUVECs incorporated in TG-PEG hydrogels. Cell migration from the spheroids was assessed for 24 hours after stimulation with the four different ephrins, which were added solubly at a concentration of 1µg/mL to the culture medium. The cell spheroids were stimulated with the clustered ephrins as well for comparison. The positive control for migration was soluble $VEGF_{165}$ at a concentration of 100ng/mL and the negative control was the medium without addition of any protein. Cell migration was recorded by time-lapse microscopy over a period of 24 hours (**Figure 4.5**).

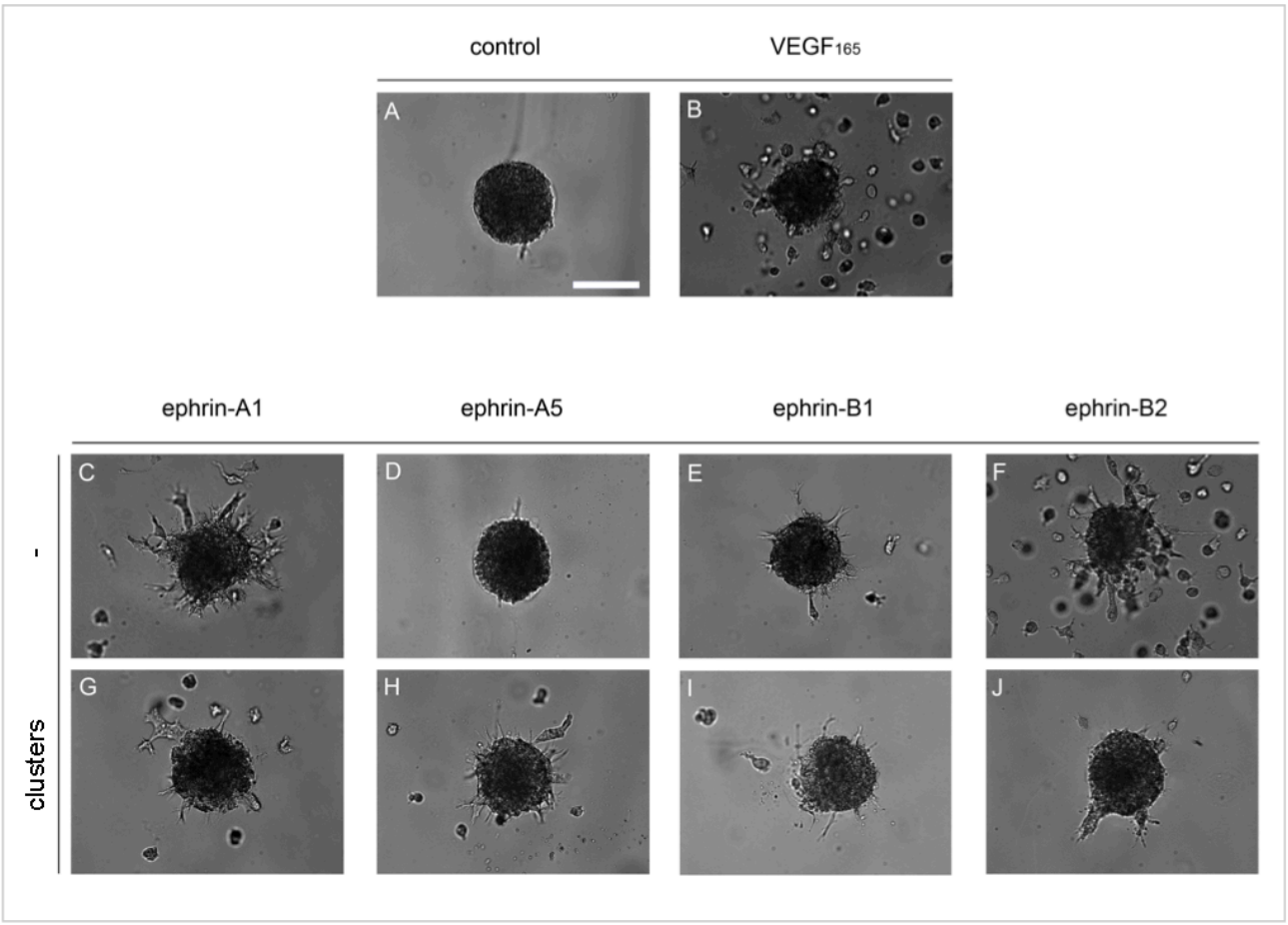

Figure 4.5. HUVEC sprouting from spheroids after 18 hours of stimulation with ephrins and VEGF (scale bar = 100 µm).

Our preliminary results indicated that ephrin-A1 induced some migration from the spheroids, which was however not comparable to the positive control ($VEGF_{165}$). Clustering the protein with antibody did not seem to influence the effect on cell migration. Stimulation with ephrin-A5 appeared to completely prevent cells from migrating out of the spheroids, although the cells remained active as could be seen from the extension of filopodia. Interestingly, clustering of ephrin-A5 canceled this effect and cells could sprout from the spheroid. For ephrin-B1, only a few cells migrated out of the spheroids and clustering did not have any significant effect. Ephrin-B2 induced the strongest migration amongst the tested ephrins (comparable to $VEGF_{165}$) and its effect seemed to be decreased when pre-clustered with an antibody. Moreover, these results follow the same trends observed in the 2D migration assay under **Section 4.2.4.1**, i.e. that clustering of ephrin-A5 and ephrin-B2 seem to alter their effect on cells, but not for ephrin-A1 and B1.

These data show again that ephrins, in particular ephrin-A5 and ephrin-B2, can influence cell migration and could be integrated in our TG-PEG hydrogel platform to regulate cell migration. Additional experiments are of course necessary to fully understand if and how these proteins can be used for that purpose.

4.3 Conclusion

We have shown the effect of the angiogenic factors netrin-4, VEGF, ephrin-A1, A5, B1 and B2 on the vascularization of the chicken CAM and demonstrated that ephrins are able to influence EC migration.

Netrin-4 had a very strong anti-angiogenic effect on the capillaries and blood vessels of the CAM and induced a decrease in capillary density as well as a reduction in blood vessel diameter. We hypothesized that netrin-4 could destabilize the basement membrane by interacting with laminin and were able to show a disrupted basement membrane in the CAM vasculature with netrin-4 treatment.

Amongst the ephrins used to treat the CAM, ephrin-A5 and ephrin-B2 showed the strongest and perhaps more interesting effects. Ephrin-A5 had a strong anti-angiogenic effect that lead to the degradation of the capillary network, whereas ephrin-B2 induced chaotic vascular structures and increased blood vessel diameter and a blood vessel morphology similar to the effect of $VEGF_{165}$. Interestingly, these results could be paralleled in the context of our cell migration experiment, where ephrin-A5 prevented the sprouting of ECs from cell spheroids, whereas ephrin-B2 stimulated cell migration in a comparable manner as $VEGF_{165}$.

These preliminary data indicate that these factors play an important role in the formation of blood vessel and thus it would be of great interest to incorporate them to our modular TG-PEG hydrogel platform in order to facilitate or even induce the formation of microvascular structures.

4.4 Experimental Section

Chick Chorioallantoic Membrane (CAM) angiogenesis assay and live imaging:

The ex ovo culture of the chicken embryos was adapted from Auerbach et al.[184]. Briefly, fertilized Ross chicken eggs (Wüthrich Brüterei AG, Switzerland) were incubated at 37°C for 3 days in humidified atmosphere. On day 3, the eggs were carefully opened and their content was transferred into 100 x 20 mm Petri dishes (Corning, Switzerland). The chicken embryos were incubated in the same conditions for 6 more days. On day 9, the PEG hydrogels with and without growth factors were placed on the surface of the CAM. 15 µL PEG hydrogels were formed by Factor $XIII_a$-catalyzed cross-linking of two 8-arm PEG components (8-PEG-Gln and 8-PEG-$MMP_{sensitive}$-Lys) in 50 mM Tris pH 7.6, 50 mM $CaCl_2$ buffer to a final PEG concentration of 2% (w/v).[75]

In **Section 4.2.1**, hydrogels contained 4.25 µg of recombinant netrin-4 per gel. In **Section 4.2.2**, hydrogels either contained 1 µg/mL recombinant Fc-ephrin protein or 100 ng/mL VEGF.

After 48 h of treatment, 100 µl of 2.5% FITC-dextran (MW 20,000, Sigma-Aldrich, Switzerland) in 0.9% NaCl solution were injected intravenously in the CAM. The vasculature was visualized by fluorescence microscopy and images around the treatment site were collected.

The images collected by fluorescence microscopy were analyzed using the ImageJ software (ImageJ 1.48, http://imagej.nih.gov/) using a script based on the quantification method developed by Blacher et al.[185] Background of each image was evened out and the contrast was enhanced. Then the threshold was adjusted manually do discriminate the vascularized area from the non-vascularized area, and the image was transformed into a binary image. A series of filters were applied then to refine the capillary structures. ROIs were set manually to exclude second-order and higher-ranking blood vessels and regions with underlying blood vessels. The non-vascularized areas within the ROIs, as well as the total ROI area, were measured. The obtained values were used to determine the distribution non-vascularized areas in the capillary network.

Immunohistochemistry of the CAM:

After live imaging, the CAMs were fixed with 4% paraformaldehyde solution by applying the solution both on top and beneath the CAM membranes and incubated at room temperature for 1 h. The area around the treatment site was carefully cut out and placed between cellulose sheets before being processed for paraffin embedding. Tissue sections of 4 µm were cut with a microtome and mounted on glass slides for hematoxylin and eosin staining.

Transmission electron microscopy analyses of the capillary structure within the CAM:

After live imaging, CAMs were fixed with 2.5% glutaraldehyde (buffered with 0.1M sodium-cacodylate, pH 7.4, 540 mOsm.) by applying the solution both on top and beneath the CAM membranes. They were post-fixed in 1% OsO_4 (0.1M sodium-cacodylate, pH 7.4, 340mOsm), dehydrated in ethanol, and embedded in Epon 812 (Fluka, Buchs,

Switzerland). Semi-thin sections were prepared, stained with toluidine blue, and analyzed with a light microscope[186]. Representative areas were selected and further imaged by transmission electron microscopy.

Corrosion casting of the CAM:

After live imaging, the CAMs were perfused via the umbilical artery with 4% PFA in PBS using a syringe pump (Pico Pump, KD Scientific, USA) at a flow rate of 5 µL/min. Immediately following perfusion, a solution of polyurethane PU4ii supplemented with fluorescent UV dye (vasQtec, Switzerland) prepared according to manufacturer's notice was infused with the syringe pump at a flow rate of 3 µL/min. After resin curing for 1-2 hours at room temperature, the soft tissues were macerated in 7.5% KOH for 24 hours at room temperature, followed by decalcification in 5% formic acid solution for 12 hours at room temperature. Casts were washed with distillated water and dried.

For microCT, 6mm CAM biopsy punches of the treated areas were sent to b-cube AG (Switzerland) for imaging with a µCT 40 desktop scanner (Scanco Medical AG, Switzerland) and 3D reconstruction.

2D cell migration assay:

20 µL PEG hydrogels (5% w/v) with a final concentration of 5 µM Gln-ZZ linker were formed as described previously. The Fc-ephrins were deposited as droplets on the surface of the PEG gels (2µL droplets containing 200ng Fc-ephrin) and given 2 hours to bind to the gel surface before washing in 50 mM Tris pH 7.6 buffer. FITC labeled antibody was added with each droplet to help localize the ephrin patterns. PC-3 cells were seeded on the surface of the gel ($0.5 \cdot 10^5$ cells/mL) and cell migration was recorded over a period of 24 hours by time-lapse microscopy. For analysis, 5 cells per patterned and control region (4 regions per condition) were randomly selected, insofar as the cells were not part of cell cluster, dividing during the duration of the time-lapse movie or migrating out of the frame. The cells were then tracked with the Manual Tracking plug-in (ImageJ). Mean velocity and total distance for each cell were analyzed.

3D endothelial cell spheroid sprouting assay:

Spheroids containing 500 HUVECs were formed overnight with the hanging drop technique and then incorporated at approximately 5 spheroids per PEG hydrogel (1.5% w/v). Each hydrogel was then glued to the bottom a well of a 48-well plate, and cultured in 500 µL DMEM:EBM-2 (4:1) medium (with 10% FCS), supplemented with either 1µg/mL of Fc-ephrin, 1 µg/mL of Fc-ephrin pre-clustered with 200ng/mL of anti-human IgG (Fc-specific) antibody (Sigma-Aldrich, Switzerland), or 100ng/mL of $VEGF_{165}$. Cell culture medium without addition of any protein served as control. Migration was recorded with by time-lapse microscopy (Leica, Switzerland) over a period of 24 hours.

4.5 References

[75] M. Ehrbar, S. C. Rizzi, R. Hlushchuk, V. Djonov, A. H. Zisch, J. A. Hubbell, F. E. Weber, and M. P. Lutolf, *Biomaterials,* 2007, *28*, 3856.

[80] U. Blache, S. Metzger, Q. Vallmajo-Martin, I. Martin, V. Djonov, and M. Ehrbar, *Adv Healthc Mater,* 2015.

[81] P. S. Lienemann, M. Karlsson, A. Sala, H. M. Wischhusen, F. E. Weber, R. Zimmermann, W. Weber, M. P. Lutolf, and M. Ehrbar, *Adv Healthc Mater,* 2013, *2*, 292.

[99] N. Ferrara, H. P. Gerber, and J. LeCouter, *Nat Med,* 2003, *9*, 669.

[104] N. Cheng, D. M. Brantley, and J. Chen, *Cytokine Growth Factor Rev,* 2002, *13*, 75.

[105] E. B. Pasquale, *Nat Rev Mol Cell Biol,* 2005, *6*, 462.

[107] B. Mosch, B. Reissenweber, C. Neuber, and J. Pietzsch, *J Oncol,* 2010, *2010*, 135285.

[161] H. M. Blau, and A. Banfi, *Nat Med,* 2001, *7*, 532.

[162] M. M. Martino, S. Brkic, E. Bovo, M. Burger, D. J. Schaefer, T. Wolff, L. Gurke, P. S. Briquez, H. M. Larsson, R. Gianni-Barrera, J. A. Hubbell, and A. Banfi, *Front Bioeng Biotechnol,* 2015, *3*, 45.

[163] E. C. Novosel, C. Kleinhans, and P. J. Kluger, *Adv Drug Deliv Rev,* 2011, *63*, 300.

[164] J. L. McBride, and J. C. Ruiz, *Mech Dev,* 1998, *77*, 201.

[165] N. Cheng, D. M. Brantley, H. Liu, Q. Lin, M. Enriquez, N. Gale, G. Yancopoulos, D. P. Cerretti, T. O. Daniel, and J. Chen, *Mol Cancer Res,* 2002, *1*, 2.

[166] D. M. Brantley-Sieders, J. Caughron, D. Hicks, A. Pozzi, J. C. Ruiz, and J. Chen, *J Cell Sci,* 2004, *117*, 2037.

[167] J. P. Himanen, M. J. Chumley, M. Lackmann, C. Li, W. A. Barton, P. D. Jeffrey, C. Vearing, D. Geleick, D. A. Feldheim, A. W. Boyd, M. Henkemeyer, and D. B. Nikolov, *Nat Neurosci,* 2004, *7*, 501.

[168] J. W. Astin, J. Batson, S. Kadir, J. Charlet, R. A. Persad, D. Gillatt, J. D. Oxley, and C. D. Nobes, *Nat Cell Biol,* 2010, *12*, 1194.

[169] T. Kojima, J. H. Chang, and D. T. Azar, *Am J Pathol,* 2007, *170*, 764.

[170] U. Huynh-Do, C. Vindis, H. Liu, D. P. Cerretti, J. T. McGrew, M. Enriquez, J. Chen, and T. O. Daniel, *J Cell Sci,* 2002, *115*, 3073.

[171] J. Borges, F. T. Tegtmeier, N. T. Padron, M. C. Mueller, E. M. Lang, and G. B. Stark, *Tissue Eng,* 2003, *9*, 441.

[172] S. Baiguera, P. Macchiarini, and D. Ribatti, *J Biomed Mater Res B Appl Biomater,* 2012, *100*, 1425.

[173] C. A. Staton, M. W. Reed, and N. J. Brown, *Int J Exp Pathol,* 2009, *90*, 195.

[174] P. Nowak-Sliwinska, T. Segura, and M. L. Iruela-Arispe, *Angiogenesis,* 2014, *17*, 779.

[175] N. Ferrara, *Am J Physiol Cell Physiol,* 2001, *280*, C1358.

[176] O. Baum, F. Suter, B. Gerber, S. A. Tschanz, R. Buergy, F. Blank, R. Hlushchuk, and V. Djonov, *Microcirculation,* 2010, *17*, 447.

[177] R. Hlushchuk, M. Ehrbar, P. Reichmuth, N. Heinimann, B. Styp-Rekowska, R. Escher, O. Baum, P. Lienemann, A. Makanya, E. Keshet, and V. Djonov, *Arterioscler Thromb Vasc Biol,* 2011, *31*, 2836.

[178] F. I. Schneiders, B. Maertens, K. Bose, Y. Li, W. J. Brunken, M. Paulsson, N. Smyth, and M. Koch, *J Biol Chem,* 2007, *282*, 23750.

[179] F. I. Staquicini, E. Dias-Neto, J. Li, E. Y. Snyder, R. L. Sidman, R. Pasqualini, and W. Arap, *Proc Natl Acad Sci U S A,* 2009, *106*, 2903.

[180] M. Ehrbar, V. G. Djonov, C. Schnell, S. A. Tschanz, G. Martiny-Baron, U. Schenk, J. Wood, P. H. Burri, J. A. Hubbell, and A. H. Zisch, *Circ Res,* 2004, *94*, 1124.

[181] L. W. Chow, R. Bitton, M. J. Webber, D. Carvajal, K. R. Shull, A. K. Sharma, and S. I. Stupp, *Biomaterials,* 2011, *32*, 1574.

[182] S. Heinzer, G. Kuhn, T. Krucker, E. Meyer, A. Ulmann-Schuler, M. Stampanoni, M. Gassmann, H. H. Marti, R. Muller, and J. Vogel, *Neuroimage,* 2008, *39*, 1549.

[183] P. Schneider, T. Krucker, E. Meyer, A. Ulmann-Schuler, B. Weber, M. Stampanoni, and R. Muller, *Microsc Res Tech,* 2009, *72*, 690.

[184] R. Auerbach, L. Kubai, D. Knighton, and J. Folkman, *Dev Biol,* 1974, *41*, 391.

[185] S. Blacher, L. Devy, R. Hlushchuk, E. Larger, N. Lamande, P. Burri, P. Corvol, V. Djonov, J. M. Foidart, and A. Noël, *Image Anal Stereol,* 2005, *24*, 169.

[186] V. G. Djonov, A. B. Galli, and P. H. Burri, *Anat Embryol (Berl),* 2000, *202*, 347.

Chapter 5 *Conclusion*

5.1 Achieved results

In the natural ECM, growth factors often interact with the proteoglycans that constitute the cellular microenvironment, which crucially contributes to the preservation of growth factor bioactivity and which can improve and is sometimes required to induce the desired signaling response. Different strategies exist that mimic these properties. Some are based on the chemical and genetic engineering of growth-factor binding sites into synthetic scaffolds or the modification of scaffolds and growth factors with corresponding affinity binding domains.[81, 120-128] Although many of these strategies are very promising, they can require time-consuming processes for the customization of each growth factor and can sometimes negatively impact growth factor functionality. Furthermore, vascularization is essential to the survival of tissues, enabling the exchange of gases and nutrients, and the perivascular ECM play a critical role in the development of blood vessels. It is therefore very desirable to reproduce vascular structures in engineered tissues.[83, 85, 163]

The overall objective of this work was thus to develop a cell-responsive artificial microenvironment for the modular presentation of growth factors, in order to regulate cell behavior in a controlled and 3D localized manner. Furthermore, we investigated potential growth factors for the establishment of pre-vascular networks in our scaffolds.

5.1.1 Streptavidin linker for the controlled and localized immobilization of growth factors

With these aspects in mind, the purpose of the work in **Chapter 2** was to develop a strategy for the immobilization of growth factors, with relative ease of implementation and flexibility in the selection of growth factors. We took advantage of the strong affinity of the streptavidin-biotin interaction to design and synthesize a peptide linker that could be covalently incorporated in our TG-PEG hydrogels. Several commercial biotinylation kits exist with different specificities for functional groups (such as primary amines, sulfhydryl groups or carbohydrate residues) and can be selected to biotinylate most of the desired growth factors without harming the target molecule, while the biotinylation conditions can also be further adapted to have a minimal impact on the growth factor biofunctionality.

To demonstrate the effectiveness of the synthesized streptavidin peptide linker, we chose to induce the differentiation of C2C12 cells and MSCs with immobilized biotinylated rhBMP-2. Not only could we successfully show the osteogenic differentiation in these cells, we were also able to obtained hydrogel constructs with 3D-localized cell differentiation corresponding to the immobilized rhBMP-2-biotin pattern. Although the constructs shown in this work had a very simple circular architecture, we hypothesize that this tool could be easily transferred to automated patterning technologies such as bio-printing. Thus, this platform represents a step towards the generation of more complex 3D cellular architectures to better mimic native tissues.

5.1.2 MMP-sensitive streptavidin linker for cell-dependent release of immobilized growth factors

In the above mentioned streptavidin-biotin immobilization strategy, the release of growth factor depended mainly on the degradation of the TG-PEG scaffold, which contains a collagen-derived protease-sensitive sequence. But despite successful cell differentiation, our results suggested that a portion of the immobilized growth factors remained inaccessible to the cells, decreasing the dose efficiency of the growth factor. The focus of **Chapter 3** was thus to design a peptide linker which allowed the release of growth factors independently from scaffold degradation. To achieve this, we developed and synthesized a streptavidin linker that contained three repeats of a proteolytically degradable domain specific to MMP-1 and MMP-2, in order to increase the rate of growth factor release in the immediate vicinity of the cells, depending on their proteolytic activity. As with the previously developed linker, we demonstrated its covalent incorporation in the TG-PEG hydrogel backbone and its ability to efficiently immobilize biotinylated proteins. We characterized and showed the specific proteolytic degradation by MMP-1 and MMP-2. Using the model of BMP-2 induced osteogenic differentiation of C2C12 cells and MSCs, we were able to demonstrate an improved response in comparison to the non-degradable linker. Additionally, our results showed that for the same total amount of rhBMP-2-biotin delivered, immobilization via the proteolytically degradable linker outperformed the presentation of soluble growth factor supplemented to the medium in relation to osteogenic differentiation. We believe that the availability of an MMP-sensitive peptide linker allows for an improved response to immobilized growth factors due to the better overall release.

5.1.3 Growth factors modulating angiogenesis

Furthermore, we addressed the vascularization of engineered tissues, which poses great limitations in the development of clinically relevant tissue constructs, by evaluating the potential of selected growth factors as guiding cues and regulators of angiogenesis. In **Chapter 4**, their effects on vascular morphology were assessed using the chicken CAM model and their influence on cell migration was studied in the prospect of establishing microvascular networks in tissue-engineered constructs.

5.1.3.1 Netrin-4 as an anti-angiogenic factor

In our investigation of factors regulating angiogenesis, we were able to demonstrate the role of netrin-4 as an anti-angiogenic factor using the chicken CAM model. By treating the vasculature of the CAM with netrin-4 delivered via TG-PEG hydrogels, we could observe the significant reduction of the vascularized area over a period of 48 hours, through live imaging of the vasculature and through histological staining of the membrane. Additionally, we investigated the integrity of the vascular basement membrane with ultrastructural analysis, since it has been reported that netrin-4 can interact with laminin. Indeed, we showed that in the capillary networks treated with netrin-4, the basement membrane surrounding the pericytes and ECs was almost completely disrupted and that the pericytes were detached from the endothelium. Our data thus suggest that netrin-4 could be used as an inhibitor of angiogenesis or as a tool to study the effects of basement membrane disruption.

5.1.3.2 Ephrins as guidance cues for vascular endothelial cell migration

In our search for potential cues for the establishment of pre-vascular structures in TG-PEG constructs, we reported the different effects of ephrin-A1, A5, B1 and B2 on the vascular development of the chicken CAM. We delivered the ephrins on the CAM vasculature and observed the changes in morphology. Ephrin-A1 and ephrin-B1 induced chaotic vessel growth and morphology as well as a slight increase in vessel diameter. Ephrin-A5 had a strong anti-angiogenic effect, disrupting the capillary network and resulting in thinner blood vessels. Ephrin-B2 had an effect very similar to treatment with the well-know pro-angiogenic factor $VEGF_{165}$, with the appearance of blood vessels with increased diameter, increased capillary density and chaotic vessel morphology.

Furthermore we collected preliminary data on the effects of ephrin in cell migration, as well as regarding the effects of ephrin clustering. Using the endothelial cell spheroid sprouting assay, we demonstrated the inhibitory effect of ephrin-A5 on cell migration. On the other hand, ephrin-B2 strongly stimulated the migration of cells out of the spheroid in a similar fashion to $VEGF_{165}$. Both ephrin-A1 and ephrin-B1 only slightly induced the migration of ECs. Regarding clustering of ephrins, both the endothelial cell spheroid sprouting assay with HUVECs and the 2D cancer cell migration assay with PC-3 cells showed that clustering of ephrin-A5 and B2 influenced their biological effect, whereas this could not be observed for ephrin-A1 and B1. In the 2D cell migration assay, clustering of both ephrin-A5 and B2 lead to a significant decrease of the measured migration distance. In 3D cell sprouting assay, clustering of ephrin-A5 and ephrin-B2 appeared to either invert or reduced their effects. Indeed stimulation with ephrin-A5 clusters cancelled the inhibitory effect on cell migration, whereas stimulation with ephrin-B2 clusters reduced the previously observed positive effect on cell sprouting.

These data support the hypothesis that ephrins can be used as regulators of endothelial cell migration, which could be a promising tool in the establishment of pre-vascular networks in tissue engineered constructs or for the stimulation of graft vascularization from the host upon transplantation.

5.2 Future developments

Altogether, this thesis presents useful advances for the development of tissue-engineered constructs. Two efficient strategies for the immobilization and delivery of growth factors in synthetic poly(ethylene glycol) scaffolds have been developed and used successfully for the controlled differentiation of cells. Additional growth factors, such has PDGF, FGF-2 and TGF-β, have been successfully biotinylated and are currently being tested in combination with the streptavidin linkers for different cell differentiation/recruitment approaches. We thus believe that the developed linkers are versatile and can allow the immobilization of large variety of growth factors, which can be biotinylated with relatively easy-to-use commercial biotinylation kits. The presented results also gave us valuable insights on the important role of growth factor immobilization and how the way in which they are presented and made available for cells can influence their biological effects.

The availability of a protease-sensitive linker also opens the possibility of using varying combinations of non-degradable and degradable linkers to fine-tune the release of immobilized growth factors and to mimic ECM properties even more closely. In order to do so, detailed release studies are needed to determine the influence of degradable vs. non-degradable mixture ratios on the release kinetics. An interesting aspect would be to determine if such mixtures of peptide linkers could help enhance the effect of the immobilized growth factors by providing a rapid cell-triggered release of factors for an immediate effect, while also guaranteeing the availability of bioactive factor on the long-term through the non-degradable peptide linker, in a similar manner to what happens in the natural ECM. For instance, the data on cell differentiation presented in this thesis never evaluated the effects of immobilized rhBMP-2-biotin for periods longer than 9 days. It would thus be important to assess the bioactivity of immobilized growth factors over longer time periods and to compare them with the bioactivity of growth factors presented in their soluble form in the cell culture medium. Furthermore, due to the simple and efficient production and purification of these small peptide linkers in bacteria in large amounts, the development of additional degradable linker with other known protease-specific domains[158, 159] seems straightforward. This would allow the creation of linkers customized for specific types of proteases and could be an interesting perspective in the design of cell-responsive microenvironments or for the adjustment of release kinetics.

Moreover, our TG-PEG hydrogel platform and the streptavidin linkers can be combined with other types of affinity linkers, such as the previously developed and compatible Gln-ZZ linker[81], to facilitate the controlled immobilization of several growth factors in the same constructs. Additionally, we believe that this platform could potentially be adapted to become a printable ink and used with available bio-printing technologies[82] in order to generate hydrogel constructs with precise 3D growth factors patterns. The next step for this project is the printing of controlled rhBMP-2-biotin regions in TG-PEG hydrogel mixtures and confirming that encapsulated cells still show localized osteogenic differentiation. If successful, such an approach could represent the first step to the formation of distinct osteogenic areas during the *in vitro* creation 3D-bone-mimicking tissues.

Overall, the development of both types of streptavidin linkers has lead up to several scientific collaborations. Currently, both types of streptavidin linkers are being used for the presentation of other growth factors and the development of different types of cellular microenvironment, notably for the establishment of microvascular networks using immobilized FGF-2 in TG-PEG scaffolds[187] and for the creation of a 3D cell culture system for the chondrogenic differentiation of MSCs using immobilized TGF-β3. In the domain of bone repair, the first *in vivo* study in mice involving Gln-streptavidin and rhBMP-2-biotin has been carried out, leading to promising results (**Figure 5.1**), where immobilized BMP-2 was shown to perform as well as soluble BMP and to contribute to bone healing.

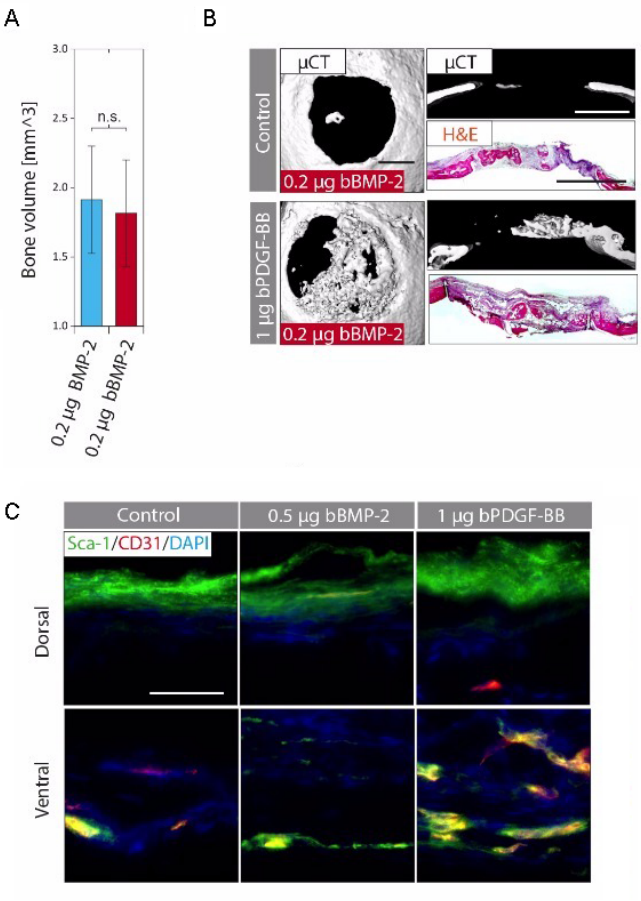

Figure 5.1. Effects of Gln-streptavidin-immobilized rhBMP-2-biotin in calvarial bone defects.[3]

A 4mm circular bone defect was created in the left and right parietal bones of C57Bl/6 mice. Preformed hydrogel implants with the indicated amount of soluble or matrix-immobilized BMP-2 were placed in the defect. A) Quantitative assessment of bone volume 4 weeks post-op (n≥5), depicted as mean ± SD, n.s. = not significant (1-way ANOVA with Tukey-Kramer post-hoc test), B) 4 weeks post-op bone regeneration was assessed ex vivo. Representative top (left panels) and side views (upper right panels) of 3D surface rendered micro-CT measurements and H&E stained sections (lower right panel) of coronal cross sections are displayed for the indicated conditions. Scale bars = 1 mm, C) 8 days post-op presence of Sca-1$^+$ cells and blood vessels on the dorsal and ventral sides of the hydrogel implants were assessed ex vivo using immunohistological stains against Sca-1 and CD31. Scale bar = 10 µm.

[3] *Adapted from*: PS Lienemann, P Papageorgiou, U Blache, S Metzger, A Kiveliö, V Milleret, Q Vallmajo-Martin, A Sala, S Hohnel, A Roch, R Reuten, M Koch, O Naveiras, FE Weber, W Weber, MP Lutolf, and M Ehrbar, **Top-down design of a biomimetic cell trap to amplify low-dose BMP-2 treatment for bone regeneration by augmenting homing of endogenous MSCs**, in preparation, 2016.

In future, we expect that the TG-PEG platform in combination with the streptavidin linkers will continue to be used *in vivo* for the improvement of bone healing strategies, but also serve for the *in vitro* localized assembly of various cell types in their customized cell-instructive matrices with complex structural features, especially if we can successfully combine this system with bio-printing.

Regarding the regulation of vascular processes, the work done in thesis has shown that various growth factors could play an important role as regulators of vascularization in synthetic scaffolds. Both netrins and ephrins are often studied as potential targets of cancer therapy, especially in the context of restraining tumor angiogenesis.[107, 188-190] We thus believe that these growth factors, in combination with other angiogenic factors such as VEGF, could be used to either form pre-vascular structures in tissue constructs before implantation, or help the anastomosis of the graft to the host vasculature. Because the angiogenic mechanisms of netrins and ephrins are not yet fully understood, it would be crucial to characterize their effect on developing vascular networks, such as the chicken CAM, but also to investigate their effects *in vitro* on cell migration by looking at receptors phosphorylation and at the activated signaling cascades. Ephrins are of particular interest, since they have been reported to regulate cell migration by modifying the actin cytoskeleton and by interactions between integrins and adhesion molecules.[105] Thus, they would be an ideal target for the improvement of engineered microenvironment, not only in terms of vascularization but also for cell guidance in general and establishment of tissue boundaries. We thus are convinced that these factors could become useful tools in combination with our modular TG-PEG hydrogel platform for the design of engineered tissues.

5.3 References

[81] P. S. Lienemann, M. Karlsson, A. Sala, H. M. Wischhusen, F. E. Weber, R. Zimmermann, W. Weber, M. P. Lutolf, and M. Ehrbar, Adv Healthc Mater, 2013, 2, 292.

[82] K. Pataky, T. Braschler, A. Negro, P. Renaud, M. P. Lutolf, and J. Brugger, Adv Mater, 2012, 24, 391.

[83] M. Lovett, K. Lee, A. Edwards, and D. L. Kaplan, Tissue Eng Part B Rev, 2009, 15, 353.

[85] F. A. Auger, L. Gibot, and D. Lacroix, Annu Rev Biomed Eng, 2013, 15, 177.

[105] E. B. Pasquale, Nat Rev Mol Cell Biol, 2005, 6, 462.

[107] B. Mosch, B. Reissenweber, C. Neuber, and J. Pietzsch, J Oncol, 2010, 2010, 135285.

[120] K. S. Masters, Macromol Biosci, 2011, 11, 1149.

[121] O. Jeon, C. Powell, L. D. Solorio, M. D. Krebs, and E. Alsberg, J Control Release, 2011, 154, 258.

[122] K. Lee, E. A. Silva, and D. J. Mooney, J. R. Soc. Interface, 2011, 8, 153.

[123] A. K. Silva, C. Richard, M. Bessodes, D. Scherman, and O. W. Merten, Biomacromolecules, 2009, 10, 9.

[124] S. Tada, T. Kitajima, and Y. Ito, Int J Mol Sci, 2012, 13, 6053.

[125] R. G. Wylie, S. Ahsan, Y. Aizawa, K. L. Maxwell, C. M. Morshead, and M. S. Shoichet, Nat Mater, 2011, 10, 799.

[126] M. Ehrbar, R. Schoenmakers, E. H. Christen, M. Fussenegger, and W. Weber, Nat Mater, 2008, 7, 800.

[127] M. M. Kampf, E. H. Christen, M. Ehrbar, M. Daoud-El Baba, G. Charpin-El Hamri, M. Fussenegger, and W. Weber, Adv Funct Mater, 2010, 20, 2534.

[128] R. G. Wylie, and M. S. Shoichet, Biomacromolecules, 2011, 12, 3789.

[158] J. Patterson, and J. A. Hubbell, Biomaterials, 2011, 32, 1301.

[159] J. Patterson, and J. A. Hubbell, Biomaterials, 2010, 31, 7836.

[163] E. C. Novosel, C. Kleinhans, and P. J. Kluger, Adv Drug Deliv Rev, 2011, 63, 300.

[187] U. Blache, S. Metzger, Q. Vallmajo-Martin, I. Martin, V. Djonov, and M. Ehrbar, Adv Healthc Mater, 2016, 5, 489.

[188] H. Q. Xi, X. S. Wu, B. Wei, and L. Chen, J Cell Mol Med, 2012, 16, 2894.

[189] C. Eveno, J. O. Contreres, P. Hainaud, J. Nemeth, E. Dupuy, and M. Pocard, Oncol Rep, 2013, 29, 73.

[190] C. Eveno, D. Broqueres-You, J. G. Feron, A. Rampanou, A. Tijeras-Raballand, S. Ropert, L. Leconte, B. I. Levy, and M. Pocard, Am J Pathol, 2011, 178, 1861.

Bibliography

[1] A. Atala, *Rejuvenation Res,* 2004, *7*, 15.

[2] Y. Ikada, *J R Soc Interface,* 2006, *3*, 589.

[3] C. M. Magin, D. L. Alge, and K. S. Anseth, *Biomed Mater,* 2016, *11*, 022001.

[4] S. Baiguera, L. Urbani, and C. Del Gaudio, *Biomed Res Int,* 2014, *2014*, 398069.

[5] A. Atala, S. B. Bauer, S. Soker, J. J. Yoo, and A. B. Retik, *Lancet,* 2006, *367*, 1241.

[6] P. Jungebluth, E. Alici, S. Baiguera, K. Le Blanc, P. Blomberg, B. Bozoky, C. Crowley, O. Einarsson, T. Gudbjartsson, S. Le Guyader, G. Henriksson, O. Hermanson, J. E. Juto, B. Leidner, T. Lilja, J. Liska, T. Luedde, V. Lundin, G. Moll, B. Nilsson, C. Roderburg, S. Stromblad, T. Sutlu, A. I. Teixeira, E. Watz, A. Seifalian, and P. Macchiarini, *Lancet,* 2011, *378*, 1997.

[7] A. Raya-Rivera, D. R. Esquiliano, J. J. Yoo, E. Lopez-Bayghen, S. Soker, and A. Atala, *Lancet,* 2011, *377*, 1175.

[8] T. Shin'oka, Y. Imai, and Y. Ikada, *N Engl J Med,* 2001, *344*, 532.

[9] A. Atala, F. K. Kasper, and A. G. Mikos, *Sci Transl Med,* 2012, *4*, 160rv12.

[10] A. Peloso, A. Dhal, J. P. Zambon, P. Li, G. Orlando, A. Atala, and S. Soker, *Stem Cell Res Ther,* 2015, *6*, 107.

[11] V. van Duinen, S. J. Trietsch, J. Joore, P. Vulto, and T. Hankemeier, *Curr Opin Biotechnol,* 2015, *35*, 118.

[12] N. T. Elliott, and F. Yuan, *J Pharm Sci,* 2011, *100*, 59.

[13] T. Kofidis, P. Akhyari, J. Boublik, P. Theodorou, U. Martin, A. Ruhparwar, S. Fischer, T. Eschenhagen, H. P. Kubis, T. Kraft, R. Leyh, and A. Haverich, *J Thorac Cardiovasc Surg,* 2002, *124*, 63.

[14] R. J. Thomas, R. Bhandari, D. A. Barrett, A. J. Bennett, J. R. Fry, D. Powe, B. J. Thomson, and K. M. Shakesheff, *Cells Tissues Organs,* 2005, *181*, 67.

[15] J. P. Miranda, S. B. Leite, U. Muller-Vieira, A. Rodrigues, M. J. Carrondo, and P. M. Alves, *Tissue Eng Part C Methods,* 2009, *15*, 157.

[16] T. M. DesRochers, L. Suter, A. Roth, and D. L. Kaplan, *PLoS One,* 2013, *8*, e59219.

[17] Y. S. Torisawa, C. S. Spina, T. Mammoto, A. Mammoto, J. C. Weaver, T. Tat, J. J. Collins, and D. E. Ingber, *Nat Methods,* 2014, *11*, 663.

[18] Q. Sun, Y. Gu, W. Zhang, L. Dziopa, J. Zilberberg, and W. Lee, *Bone Res,* 2015, *3*, 15026.

[19] J. S. Jeon, I. K. Zervantonakis, S. Chung, R. D. Kamm, and J. L. Charest, *PLoS One,* 2013, *8*, e56910.

[20] S. Bersini, J. S. Jeon, G. Dubini, C. Arrigoni, S. Chung, J. L. Charest, M. Moretti, and R. D. Kamm, *Biomaterials,* 2014, *35*, 2454.

[21] C. L. M. Bao, E. Y. Teo, M. S. K. Chong, Y. Liu, M. Choolani, and J. K. Y. Chan, 'Advances in Bone Tissue Engineering', in *Regenerative Medicine and Tissue Engineering*, ed. by P. J. A. Andrades InTech, 2013.

[22] S. Bose, S. Vahabzadeh, and A. Bandyopadhyay, *Materials Today,* 2013, *16*, 496.

[23] M. Mravic, B. Peault, and A. W. James, *Biomed Res Int,* 2014.

[24] C. Bonnans, J. Chou, and Z. Werb, *Nat Rev Mol Cell Biol,* 2014, *15*, 786.

[25] T. R. Cox, and J. T. Erler, *Dis Model Mech,* 2011, *4*, 165.

[26] W. P. Daley, S. B. Peters, and M. Larsen, *J Cell Sci,* 2008, *121*, 255.

[27] C. Frantz, K. M. Stewart, and V. M. Weaver, *J Cell Sci,* 2010, *123*, 4195.

[28] J. D. Humphrey, E. R. Dufresne, and M. A. Schwartz, *Nat Rev Mol Cell Biol,* 2014, *15*, 802.

[29] T. Rozario, and D. W. DeSimone, *Dev Biol,* 2010, *341*, 126.

[30] W. S. To, and K. S. Midwood, *Fibrogenesis Tissue Repair,* 2011, *4*, 21.

[31] S. K. Mitra, D. A. Hanson, and D. D. Schlaepfer, *Nat Rev Mol Cell Biol,* 2005, *6*, 56.

[32] S. H. Kim, J. Turnbull, and S. Guimond, *J Endocrinol,* 2011, *209*, 139.

[33] E. S. Place, N. D. Evans, and M. M. Stevens, *Nat Mater,* 2009, *8*, 457.

[34] J. Zhu, *Biomaterials,* 2010, *31*, 4639.

[35] S. Amano, N. Akutsu, Y. Matsunaga, T. Nishiyama, M. F. Champliaud, R. E. Burgeson, and E. Adachi, *Exp Cell Res,* 2001, *271*, 249.

[36] K. Brew, D. Dinakarpandian, and H. Nagase, *Biochim Biophys Acta,* 2000, *1477*, 267.

[37] I. M. Clark, T. E. Swingler, C. L. Sampieri, and D. R. Edwards, *Int J Biochem Cell Biol,* 2008, *40*, 1362.

[38] P. Olczyk, L. Mencner, and K. Komosinska-Vassev, *Biomed Res Int,* 2014, *2014*, 747584.

[39] G. S. Schultz, and A. Wysocki, *Wound. Rep. Reg.,* 2009, *17*, 153.

[40] G. S. Schultz, J. M. Davidson, R. S. Kirsner, P. Bornstein, and I. M. Herman, *Wound. Rep. Reg.,* 2011, *19*, 134.

[41] R. F. Diegelmann, and M. C. Evans, *Front Biosci,* 2004, *9*, 283.

[42] Y. S. Wu, and S. N. Chen, *Front Pharmacol,* 2014, *5*, 1.

[43] J. M. Reinke, and H. Sorg, *Eur Surg Res,* 2012, *49*, 35.

[44] S. Guo, and L. A. Dipietro, *J Dent Res,* 2010, *89*, 219.

[45] J. M. Shah, E. Omar, D. R. Pai, and S. Sood, *Indian J Plast Surg,* 2012, *45*, 220.

[46] K. S. Midwood, L. V. Williams, and J. E. Schwarzbauer, *Int J Biochem Cell Biol,* 2004, *36*, 1031.

[47] G. C. Gurtner, S. Werner, Y. Barrandon, and M. T. Longaker, *Nature,* 2008, *453*, 314.

[48] M. F. Brizzi, G. Tarone, and P. Defilippi, *Curr Opin Cell Biol,* 2012, *24*, 645.

[49] K. Forsten-Williams, C. L. Chu, M. Fannon, J. A. Buczek-Thomas, and M. A. Nugent, *Ann Biomed Eng,* 2008, *36*, 2134.

[50] M. M. Martino, and J. A. Hubbell, *FASEB J,* 2010, *24*, 4711.

[51] M. M. Martino, P. S. Briquez, A. Ranga, M. P. Lutolf, and J. A. Hubbell, *Proc Natl Acad Sci U S A,* 2013, *110*, 4563.

[52] R. O. Hynes, *Science,* 2009, *326*, 1216.

[53] F. Gattazzo, A. Urciuolo, and P. Bonaldo, *Biochim Biophys Acta,* 2014, *1840*, 2506.

[54] J. Schlessinger, A. N. Plotnikov, O. A. Ibrahimi, A. V. Eliseenkova, B. K. Yeh, A. Yayon, R. J. Linhardt, and M. Mohammadi, *Mol Cell,* 2000, *6*, 743.

[55] M. Mohammadi, S. K. Olsen, and R. Goetz, *Curr Opin Struct Biol,* 2005, *15*, 506.

[56] N. Ortega, F. E. L'Faqihi, and J. Plouet, *Biol Cell,* 1998, *90*, 381.

[57] C. J. Robinson, and S. E. Stringer, *J Cell Sci,* 2001, *114*, 853.

[58] G. H. Mahabeleshwar, W. Feng, K. Reddy, E. F. Plow, and T. V. Byzova, *Circ Res,* 2007, *101*, 570.

[59] P. R. Somanath, N. L. Malinin, and T. V. Byzova, *Angiogenesis,* 2009, *12*, 177.

[60] P. Lijnen, and V. Petrov, *Methods Find Exp Clin Pharmacol,* 2002, *24*, 333.

[61] X. Pan, Z. Chen, R. Huang, Y. Yao, and G. Ma, *PLoS One,* 2013, *8*, e60335.

[62] T. A. Wilgus, *Adv Wound Care (New Rochelle),* 2012, *1*, 249.

[63] A. L. Sieron, N. Louneva, and A. Fertala, *Cytokine,* 2002, *18*, 214.

[64] M. Kisiel, A. S. Klar, M. Ventura, J. Buijs, M. K. Mafina, S. M. Cool, and J. Hilborn, *PLoS One,* 2013, *8*, e78551.

[65] E. N. Blaney Davidson, E. L. Vitters, P. L. van Lent, F. A. van de Loo, W. B. van den Berg, and P. M. van der Kraan, *Arthritis Res Ther,* 2007, *9*, R102.

[66] R. J. Wade, and J. A. Burdick, *Materials Today,* 2012, *15*, 454.

[67] W. E. Hennink, and C. F. van Nostrum, *Adv Drug Deliv Rev,* 2002, *54*, 13.

[68] J. L. Drury, and D. J. Mooney, *Biomaterials,* 2003, *24*, 4337.

[69] D. Seliktar, *Science,* 2012, *336*, 1124.

[70] J. H. Lee, H. B. Lee, and J. D. Andrade, *Progress in Polymer Science,* 1995, *20*, 1043.

[71] J. K. Tessmar, and A. M. Gopferich, *Macromolecular Bioscience,* 2007, *7*, 23.

[72] M. P. Lutolf, J. L. Lauer-Fields, H. G. Schmoekel, A. T. Metters, F. E. Weber, G. B. Fields, and J. A. Hubbell, *Proceedings of the National Academy of Sciences of the United States of America,* 2003, *100*, 5413.

[73] M. P. Lutolf, and J. A. Hubbell, *Nat. Biotechnol.,* 2005, *23*, 47.

[74] M. Ehrbar, S. C. Rizzi, R. G. Schoenmakers, B. S. Miguel, J. A. Hubbell, F. E. Weber, and M. P. Lutolf, *Biomacromolecules,* 2007, *8*, 3000.

[75] M. Ehrbar, S. C. Rizzi, R. Hlushchuk, V. Djonov, A. H. Zisch, J. A. Hubbell, F. E. Weber, and M. P. Lutolf, *Biomaterials,* 2007, *28*, 3856.

[76] K. B. Fonseca, P. L. Granja, and C. C. Barrias, *Progress in Polymer Science,* 2014, *39*, 2010.

[77] A. Sala, P. Hanseler, A. Ranga, M. P. Lutolf, J. Voros, M. Ehrbar, and F. E. Weber, *Integr. Biol. (Camb),* 2011, *3*, 1102.

[78] P. S. Lienemann, Y. R. Devaud, R. Reuten, B. R. Simona, M. Karlsson, W. Weber, M. Koch, M. P. Lutolf, V. Milleret, and M. Ehrbar, *Integr Biol (Camb),* 2015, *7*, 101.

[79] S. Metzger, P. S. Lienemann, C. Ghayor, W. Weber, I. Martin, F. E. Weber, and M. Ehrbar, *Adv Healthc Mater,* 2015, *4*, 550.

[80] U. Blache, S. Metzger, Q. Vallmajo-Martin, I. Martin, V. Djonov, and M. Ehrbar, *Adv Healthc Mater,* 2015.

[81] P. S. Lienemann, M. Karlsson, A. Sala, H. M. Wischhusen, F. E. Weber, R. Zimmermann, W. Weber, M. P. Lutolf, and M. Ehrbar, *Adv Healthc Mater,* 2013, *2*, 292.

[82] K. Pataky, T. Braschler, A. Negro, P. Renaud, M. P. Lutolf, and J. Brugger, *Adv Mater,* 2012, *24*, 391.

[83] M. Lovett, K. Lee, A. Edwards, and D. L. Kaplan, *Tissue Eng Part B Rev,* 2009, *15*, 353.

[84] M. W. Laschke, and M. D. Menger, *Eur Surg Res,* 2012, *48*, 85.

[85] F. A. Auger, L. Gibot, and D. Lacroix, *Annu Rev Biomed Eng,* 2013, *15*, 177.

[86] Z. K. Otrock, R. A. Mahfouz, J. A. Makarem, and A. I. Shamseddine, *Blood Cells Mol Dis,* 2007, *39*, 212.

[87] D. A. Cheresh, and D. G. Stupack, *Oncogene,* 2008, *27*, 6285.

[88] D. R. Senger, C. A. Perruzzi, M. Streit, V. E. Koteliansky, A. R. de Fougerolles, and M. Detmar, *Am J Pathol,* 2002, *160*, 195.

[89] F. Aoudjit, and K. Vuori, *J Cell Biol,* 2001, *152*, 633.

[90] D. R. Senger, and G. E. Davis, *Cold Spring Harb Perspect Biol,* 2011, *3*, a005090.

[91] V. W. van Hinsbergh, A. Collen, and P. Koolwijk, *Ann N Y Acad Sci,* 2001, *936*, 426.

[92] G. E. Davis, and D. R. Senger, *Circ Res,* 2005, *97*, 1093.

[93] L. Lamalice, F. Le Boeuf, and J. Huot, *Circ Res,* 2007, *100*, 782.

[94] S. Kim, M. Harris, and J. A. Varner, *J Biol Chem,* 2000, *275*, 33920.

[95] S. A. Eming, and J. A. Hubbell, *Exp Dermatol,* 2011, *20*, 605.

[96] M. Potente, H. Gerhardt, and P. Carmeliet, *Cell,* 2011, *146*, 873.

[97] M. Dakouane-Giudicelli, N. Alfaidy, and P. de Mazancourt, *Biomed Res Int,* 2014, *2014*, 901941.

[98] B. D. Wilson, M. Ii, K. W. Park, A. Suli, L. K. Sorensen, F. Larrieu-Lahargue, L. D. Urness, W. Suh, J. Asai, G. A. Kock, T. Thorne, M. Silver, K. R. Thomas, C. B. Chien, D. W. Losordo, and D. Y. Li, *Science,* 2006, *313*, 640.

[99] N. Ferrara, H. P. Gerber, and J. LeCouter, *Nat Med,* 2003, *9*, 669.

[100] H. Takahashi, and M. Shibuya, *Clin Sci (Lond),* 2005, *109*, 227.

[101] M. N. Nakatsu, R. C. Sainson, S. Perez-del-Pulgar, J. N. Aoto, M. Aitkenhead, K. L. Taylor, P. M. Carpenter, and C. C. Hughes, *Lab Invest,* 2003, *83*, 1873.

[102] S. H. Wimmer-Kleikamp, P. W. Janes, A. Squire, P. I. Bastiaens, and M. Lackmann, *J Cell Biol,* 2004, *164*, 661.

[103] J. P. Himanen, L. Yermekbayeva, P. W. Janes, J. R. Walker, K. Xu, L. Atapattu, K. R. Rajashankar, A. Mensinga, M. Lackmann, D. B. Nikolov, and S. Dhe-Paganon, *Proc Natl Acad Sci U S A,* 2010, *107*, 10860.

[104] N. Cheng, D. M. Brantley, and J. Chen, *Cytokine Growth Factor Rev,* 2002, *13*, 75.

[105] E. B. Pasquale, *Nat Rev Mol Cell Biol,* 2005, *6*, 462.

[106] S. Kuijper, C. J. Turner, and R. H. Adams, *Trends Cardiovasc Med,* 2007, *17*, 145.

[107] B. Mosch, B. Reissenweber, C. Neuber, and J. Pietzsch, *J Oncol,* 2010, *2010*, 135285.

[108] E. Lejmi, L. Leconte, S. Pedron-Mazoyer, S. Ropert, W. Raoul, S. Lavalette, I. Bouras, J. G. Feron, M. Maitre-Boube, F. Assayag, C. Feumi, M. Alemany, T. X. Jie, T. Merkulova, M. F. Poupon, M. M. Ruchoux, G. Tobelem, F. Sennlaub, and J. Plouet, *Proc Natl Acad Sci U S A,* 2008, *105*, 12491.

[109] E. Lambert, M. M. Coissieux, V. Laudet, and P. Mehlen, *J Biol Chem,* 2012, *287*, 3987.

[110] E. Lejmi, I. Bouras, S. Camelo, M. Roumieux, N. Minet, C. Lere-Dean, T. Merkulova-Rainon, G. Autret, C. Vayssettes, O. Clement, J. Plouet, and L. Leconte, *Vasc Cell,* 2014, *6*, 1.

[111] Y. Han, Y. Shao, T. Liu, Y. L. Qu, W. Li, and Z. Liu, *PLoS One,* 2015, *10*, e0122951.

[112] M. Dakouane-Giudicelli, S. Brouillet, W. Traboulsi, A. Torre, G. Vallat, S. Si Nacer, M. Vallee, J. J. Feige, N. Alfaidy, and P. de Mazancourt, *Placenta,* 2015, *36*, 1260.

[113] M. Nacht, T. B. St Martin, A. Byrne, K. W. Klinger, B. A. Teicher, S. L. Madden, and Y. Jiang, *Exp Cell Res,* 2009, *315*, 784.

[114] W. Tan, and T. A. Desai, *Biomedical Microdevices,* 2003, *5*, 235.

[115] B. Derby, *Science,* 2012, *338*, 921.

[116] K. R. Stevens, M. D. Ungrin, R. E. Schwartz, S. Ng, B. Carvalho, K. S. Christine, R. R. Chaturvedi, C. Y. Li, P. W. Zandstra, C. S. Chen, and S. N. Bhatia, *Nat Commun,* 2013, *4*, 1847.

[117] D. Huh, G. A. Hamilton, and D. E. Ingber, *Trends Cell Biol,* 2011, *21*, 745.

[118] C. C. Lin, and K. S. Anseth, *Pharm Res,* 2009, *26*, 631.

[119] C. A. DeForest, and K. S. Anseth, *Annu Rev Chem Biomol Eng,* 2012, *3*, 421.

[120] K. S. Masters, *Macromol Biosci,* 2011, *11*, 1149.

[121] O. Jeon, C. Powell, L. D. Solorio, M. D. Krebs, and E. Alsberg, *J Control Release,* 2011, *154*, 258.

[122] K. Lee, E. A. Silva, and D. J. Mooney, *J. R. Soc. Interface,* 2011, *8*, 153.

[123] A. K. Silva, C. Richard, M. Bessodes, D. Scherman, and O. W. Merten, *Biomacromolecules,* 2009, *10*, 9.

[124] S. Tada, T. Kitajima, and Y. Ito, *Int J Mol Sci,* 2012, *13*, 6053.

[125] R. G. Wylie, S. Ahsan, Y. Aizawa, K. L. Maxwell, C. M. Morshead, and M. S. Shoichet, *Nat Mater,* 2011, *10*, 799.

[126] M. Ehrbar, R. Schoenmakers, E. H. Christen, M. Fussenegger, and W. Weber, *Nat Mater,* 2008, *7*, 800.

[127] M. M. Kampf, E. H. Christen, M. Ehrbar, M. Daoud-El Baba, G. Charpin-El Hamri, M. Fussenegger, and W. Weber, *Adv Funct Mater,* 2010, *20*, 2534.

[128] R. G. Wylie, and M. S. Shoichet, *Biomacromolecules,* 2011, *12*, 3789.

[129] A. I. Caplan, *J Cell Physiol,* 2007, *213*, 341.

[130] D. Marolt, M. Knezevic, and G. V. Novakovic, *Stem Cell Res Ther,* 2010, *1*, 10.

[131] Y. C. Chen, R. Z. Lin, H. Qi, Y. Yang, H. Bae, J. M. Melero-Martin, and A. Khademhosseini, *Adv Funct Mater,* 2012, *22*, 2027.

[132] O. Tsigkou, I. Pomerantseva, J. A. Spencer, P. A. Redondo, A. R. Hart, E. O'Doherty, Y. Lin, C. C. Friedrich, L. Daheron, C. P. Lin, C. A. Sundback, J. P. Vacanti, and C. Neville, *Proc Natl Acad Sci U S A,* 2010, *107*, 3311.

[133] M. Ehrbar, A. Sala, P. Lienemann, A. Ranga, K. Mosiewicz, A. Bittermann, S. C. Rizzi, F. E. Weber, and M. P. Lutolf, *Biophys. J.,* 2011, *100*, 284.

[134] C. M. Madl, M. Mehta, G. N. Duda, S. C. Heilshorn, and D. J. Mooney, *Biomacromolecules,* 2014, *15*, 445.

[135] N. M. Green, *Adv. Protein Chem.,* 1975, *29*, 85.

[136] S. Cosson, and M. P. Lutolf, *Methods Cell Biol,* 2014, *121*, 91.

[137] R. Ruppert, E. Hoffmann, and W. Sebald, *Eur J Biochem,* 1996, *237*, 295.

[138] H. Uludag, J. Golden, R. Palmer, and J. M. Wozney, *Biotechnol Bioeng,* 1999, *65*, 668.

[139] T. Katagiri, A. Yamaguchi, M. Komaki, E. Abe, N. Takahashi, T. Ikeda, V. Rosen, J. M. Wozney, A. Fujisawa-Sehara, and T. Suda, *J. Cell Biol.,* 1994, *127*, 1755.

[140] J. Hu, and W. Sebald, *Int J Pharm,* 2011, *413*, 140.

[141] S. S. Wong, *Chemistry of Protein Conjugation and Cross-Linking*. CRC Press, Boca Raton, FL, USA, 1991.

[142] P. Ducy, R. Zhang, V. Geoffroy, A. L. Ridall, and G. Karsenty, *Cell,* 1997, *89*, 747.

[143] W. Weber, J. Stelling, M. Rimann, B. Keller, M. Daoud-El Baba, C. C. Weber, D. Aubel, and M. Fussenegger, *Proc Natl Acad Sci U S A,* 2007, *104*, 2643.

[144] N. Humbert, P. Schurmann, A. Zocchi, J. M. Neuhaus, and T. R. Ward, *Methods Mol Biol,* 2008, *418*, 101.

[145] F. E. Weber, G. Eyrich, K. W. Gratz, R. M. Thomas, F. E. Maly, and H. F. Sailer, *Biochem Biophys Res Commun,* 2001, *286*, 554.

[146] O. Frank, M. Heim, M. Jakob, A. Barbero, D. Schafer, I. Bendik, W. Dick, M. Heberer, and I. Martin, *J Cell Biochem,* 2002, *85*, 737.

[147] T. Dvir, B. P. Timko, D. S. Kohane, and R. Langer, *Nat Nanotechnol,* 2011, *6*, 13.

[148] J. K. Mouw, G. Ou, and V. M. Weaver, *Nat Rev Mol Cell Biol,* 2014, *15*, 771.

[149] A. C. Mitchell, P. S. Briquez, J. A. Hubbell, and J. R. Cochran, *Acta Biomater.,* 2015.

[150] G. S. Schultz, and A. Wysocki, *Wound. Rep. Reg.,* 2009, *17*, 153.

[151] C. Streuli, *Curr. Opin. Cell Biol.,* 1999, *11*, 634.

[152] P. Lu, K. Takai, V. M. Weaver, and Z. Werb, *Cold Spring Harb Perspect Biol,* 2011, *3*.

[153] T. E. Cawston, and D. A. Young, *Cell Tissue Res,* 2010, *339*, 221.

[154] C. M. Kirschner, and K. S. Anseth, *Acta Mater.,* 2013, *61*, 931.

[155] C. C. Lin, *RSC Adv.,* 2015, *5*, 39844.

[156] P. S. Lienemann, M. P. Lutolf, and M. Ehrbar, *Adv. Drug Deliv. Rev.,* 2012, *64*, 1078.

[157] H. Nagase, and G. B. Fields, *Biopolymers,* 1996, *40*, 399.

[158] J. Patterson, and J. A. Hubbell, *Biomaterials,* 2011, *32*, 1301.

[159] J. Patterson, and J. A. Hubbell, *Biomaterials,* 2010, *31*, 7836.

[160] A. Papadimitropoulos, E. Piccinini, S. Brachat, A. Braccini, D. Wendt, A. Barbero, C. Jacobi, and I. Martin, *PLoS One,* 2014, *9*, e102359.

[161] H. M. Blau, and A. Banfi, *Nat Med,* 2001, *7*, 532.

[162] M. M. Martino, S. Brkic, E. Bovo, M. Burger, D. J. Schaefer, T. Wolff, L. Gurke, P. S. Briquez, H. M. Larsson, R. Gianni-Barrera, J. A. Hubbell, and A. Banfi, *Front Bioeng Biotechnol,* 2015, *3*, 45.

[163] E. C. Novosel, C. Kleinhans, and P. J. Kluger, *Adv Drug Deliv Rev,* 2011, *63*, 300.

[164] J. L. McBride, and J. C. Ruiz, *Mech Dev,* 1998, *77*, 201.

[165] N. Cheng, D. M. Brantley, H. Liu, Q. Lin, M. Enriquez, N. Gale, G. Yancopoulos, D. P. Cerretti, T. O. Daniel, and J. Chen, *Mol Cancer Res,* 2002, *1*, 2.

[166] D. M. Brantley-Sieders, J. Caughron, D. Hicks, A. Pozzi, J. C. Ruiz, and J. Chen, *J Cell Sci,* 2004, *117*, 2037.

[167] J. P. Himanen, M. J. Chumley, M. Lackmann, C. Li, W. A. Barton, P. D. Jeffrey, C. Vearing, D. Geleick, D. A. Feldheim, A. W. Boyd, M. Henkemeyer, and D. B. Nikolov, *Nat Neurosci,* 2004, *7*, 501.

[168] J. W. Astin, J. Batson, S. Kadir, J. Charlet, R. A. Persad, D. Gillatt, J. D. Oxley, and C. D. Nobes, *Nat Cell Biol,* 2010, *12*, 1194.

[169] T. Kojima, J. H. Chang, and D. T. Azar, *Am J Pathol,* 2007, *170*, 764.

[170] U. Huynh-Do, C. Vindis, H. Liu, D. P. Cerretti, J. T. McGrew, M. Enriquez, J. Chen, and T. O. Daniel, *J Cell Sci,* 2002, *115*, 3073.

[171] J. Borges, F. T. Tegtmeier, N. T. Padron, M. C. Mueller, E. M. Lang, and G. B. Stark, *Tissue Eng,* 2003, *9*, 441.

[172] S. Baiguera, P. Macchiarini, and D. Ribatti, *J Biomed Mater Res B Appl Biomater,* 2012, *100*, 1425.

[173] C. A. Staton, M. W. Reed, and N. J. Brown, *Int J Exp Pathol,* 2009, *90*, 195.

[174] P. Nowak-Sliwinska, T. Segura, and M. L. Iruela-Arispe, *Angiogenesis,* 2014, *17*, 779.

[175] N. Ferrara, *Am J Physiol Cell Physiol,* 2001, *280*, C1358.

[176] O. Baum, F. Suter, B. Gerber, S. A. Tschanz, R. Buergy, F. Blank, R. Hlushchuk, and V. Djonov, *Microcirculation,* 2010, *17*, 447.

[177] R. Hlushchuk, M. Ehrbar, P. Reichmuth, N. Heinimann, B. Styp-Rekowska, R. Escher, O. Baum, P. Lienemann, A. Makanya, E. Keshet, and V. Djonov, *Arterioscler Thromb Vasc Biol,* 2011, *31*, 2836.

[178] F. I. Schneiders, B. Maertens, K. Bose, Y. Li, W. J. Brunken, M. Paulsson, N. Smyth, and M. Koch, *J Biol Chem,* 2007, *282*, 23750.

[179] F. I. Staquicini, E. Dias-Neto, J. Li, E. Y. Snyder, R. L. Sidman, R. Pasqualini, and W. Arap, *Proc Natl Acad Sci U S A,* 2009, *106*, 2903.

[180] M. Ehrbar, V. G. Djonov, C. Schnell, S. A. Tschanz, G. Martiny-Baron, U. Schenk, J. Wood, P. H. Burri, J. A. Hubbell, and A. H. Zisch, *Circ Res,* 2004, *94*, 1124.

[181] L. W. Chow, R. Bitton, M. J. Webber, D. Carvajal, K. R. Shull, A. K. Sharma, and S. I. Stupp, *Biomaterials,* 2011, *32*, 1574.

[182] S. Heinzer, G. Kuhn, T. Krucker, E. Meyer, A. Ulmann-Schuler, M. Stampanoni, M. Gassmann, H. H. Marti, R. Muller, and J. Vogel, *Neuroimage,* 2008, *39*, 1549.

[183] P. Schneider, T. Krucker, E. Meyer, A. Ulmann-Schuler, B. Weber, M. Stampanoni, and R. Muller, *Microsc Res Tech,* 2009, *72*, 690.

[184] R. Auerbach, L. Kubai, D. Knighton, and J. Folkman, *Dev Biol,* 1974, *41*, 391.

[185] S. Blacher, L. Devy, R. Hlushchuk, E. Larger, N. Lamande, P. Burri, P. Corvol, V. Djonov, J. M. Foidart, and A. Noël, *Image Anal Stereol,* 2005, *24*, 169.

[186] V. G. Djonov, A. B. Galli, and P. H. Burri, *Anat Embryol (Berl),* 2000, *202*, 347.

[187] U. Blache, S. Metzger, Q. Vallmajo-Martin, I. Martin, V. Djonov, and M. Ehrbar, *Adv Healthc Mater,* 2016, *5*, 489.

[188] H. Q. Xi, X. S. Wu, B. Wei, and L. Chen, *J Cell Mol Med,* 2012, *16*, 2894.

[189] C. Eveno, J. O. Contreres, P. Hainaud, J. Nemeth, E. Dupuy, and M. Pocard, *Oncol Rep,* 2013, *29*, 73.

[190] C. Eveno, D. Broqueres-You, J. G. Feron, A. Rampanou, A. Tijeras-Raballand, S. Ropert, L. Leconte, B. I. Levy, and M. Pocard, *Am J Pathol,* 2011, *178*, 1861.

Curriculum Vitae

Stéphanie Metzger

Chemin Neuf 41

1897 Les Evouettes

Switzerland

+41(0)78 948 0838

stephanie.metzger@usz.ch

stephanie.metzger@bluewin.ch

Education

2011 – current	**Ph.D. in Bioengineering and Biotechnology** Thesis director: Prof. Jeffrey A. Hubbell, EPFL, Switzerland Thesis co-director: Dr Martin Ehrbar, University Hospital Zürich, Switzerland Position at the Ehrbar Laboratory for Cell and Tissue Engineering, Department of Obstetrics, University Hospital Zürich, Switzerland.
2008 – 2010	**Master of Science in Bioengineering and Biotechnology** Specialization in Bioengineering Ecole Polytechnique Fédérale de Lausanne, Switzerland
2005 – 2008	**Bachelor of Science in Life Science and Technology** Ecole Polytechnique Fédérale de Lausanne, Switzerland
2002 – 2005	**Matura in Mathematics and Natural Sciences** Specialization in Biology and Chemistry Gymnasium Kirchenfeld, Bern, Switzerland

Professional Experience

Aug. 2007 – Feb. 2008	**Research assistant** Laboratory of Molecular Neurobiology and Neuroproteomics, EPFL, Switzerland

List of publications

1. F. Anjum, P. S. Lienemann, **S. Metzger**, J. Biernaskie, M. S. Kallos, and M. Ehrbar, "Enzyme responsive GAG-based natural-synthetic hybrid hydrogel for tunable growth factor delivery and stem cell differentiation", *Biomaterials*, May 2016.

2. U. Blache, **S. Metzger**, Q. Vallmajo-Martin, I. Martin, V. Djonov, and M. Ehrbar, "Dual Role of Mesenchymal Stem Cells Allows for Microvascularized Bone Tissue-Like Environments in PEG Hydrogels", *Advanced Healthcare Materials*, February 2016.

3. P. S. Lienemann, **S. Metzger**, A. Kiveliö, A. Blanc, P. Papageorgiou, A. Astolfo, B. R. Pinzer, P. Cinelli, F. E. Weber, R. Schibli, M. Béhé, and M. Ehrbar, "Longitudinal in vivo evaluation of bone regeneration by combined measurement of multi-pinhole SPECT and micro-CT for tissue engineering", *Scientific Reports*, May 2015.

4. M. Moriyama, **S. Metzger**, A. J. van der Vlies, H. Uyama, M. Ehrbar, and U. Hasegawa, "Antioxidants: Inhibition of Angiogenesis by Antioxidant Micelles", *Advanced Healthcare Materials*, March 2015.

5. **S. Metzger**, P. S. Lienemann, C. Ghayor, W. Weber, I. Martin, F. E. Weber, and M. Ehrbar, "Modular Poly(ethylene glycol) Matrices for the Controlled 3D-Localized Osteogenic Differentiation of Mesenchymal Stem Cells", *Advanced Healthcare Materials*, March 2015.

6. D. C. Hoffmann, S. Willenborg, M. Koch, D. Zwolanek, S. Mueller, A. A. Becker, **S. Metzger**, M. Ehrbar, P. Kurschat, M. Hellmich, J. A. Hubbell, and S. A. Eming, "Proteolytic Processing Regulates Placental Growth Factor Activities", *Journal of Biological Chemistry*, May 2013.

7. K. Müller, R. Engesser, **S. Metzger**, S. Schulz, M. M. Kämpf, M. Busacker, T. Steinberg, P. Tomakidi, M. Ehrbar, F. Nagy, J. Timmer, M. D. Zubriggen, W. Weber, "A red/far-red light-responsive bi-stable toggle switch to control gene expression in mammalian cells", *Nucleic Acids Research*, January 2013.

Submitted manuscripts:

1. **S. Metzger**, U. Blache, P. S. Lienemann, M. Karlsson, F. E. Weber, W. Weber, and M. Ehrbar, "Cell-mediated proteolytic release of growth factors from poly(ethylene) glycol matrices", 2016.

2. R. Reuten, **S Metzger**, Z. Zhou, J. Kaltenberg, K. K. McKee, M. McDougall, T. Bald, K. Pool, T. Tüting, B. Brachvogel, P. Zigrino, J. Stetefeld, V. Djonov, W. Bloch, P. D. Yurchenco, E. Pöschl, M. Ehrbar, and M. Koch, "Netrin-4 regulates functional vascular basement membrane assembly and neo-angiogenic events", 2016.

Manuscripts in preparation

1. P. S. Lienemann, P. Papageorgiou, U. Blache, **S. Metzger**, A. Kiveliö, V. Milleret, Q. Vallmajo-Martin, A. Sala, S. Hohnel, A. Roch, R. Reuten, M. Koch, O. Naveiras, F.E. Weber, W. Weber, M. P. Lutolf, and M. Ehrbar, "Top-down design of a biomimetic cell trap to amplify low-dose BMP-2 treatment for bone regeneration by augmenting homing of endogenous MSCs", 2016.